Autophagy and *Listeria monocytogenes*: the role(s) of cargo receptors

Inaugural Dissertation

submitted to the

Faculty of Medicine

in partial fulfillment of the requirements

for the Ph. D. Degree

of the Faculties of Veterinary Medicine and Medicine

of the Justus Liebig University, Giessen

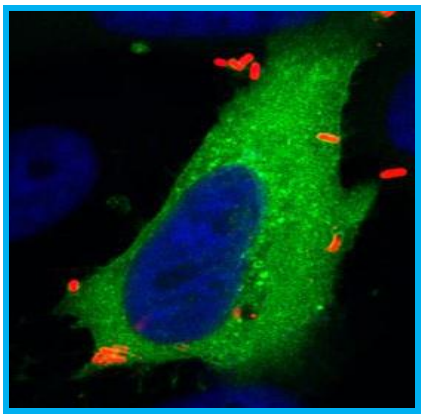

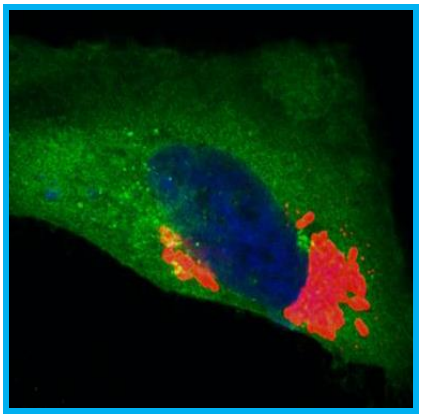

by

Madhu Singh

of

Mumbai, India

Giessen (2014)

From the Institute of Medical Microbiology

Director: Prof. Dr. Trinad Chakraborty

of the Faculty of Medicine of the Justus Liebig University, Giessen

First Supervisor and Committee Member: Prof. Dr. Trinad Chakraborty

Second Supervisor and Committee Member: Prof. Dr. Michael Martin

Date of Doctoral Defense: 30.09.14

Contents

Contents

Contents

Contents

I. Introduction

1.1 *Listeria monocytogenes*

The genus *Listeria* comprises of Gram-positive bacteria of low G + C content, which are facultatively anaerobic, non-spore forming, non-capsulated and motile (Collins *et al.*, 1991; Sallen *et al.*, 1996). Ten species are currently known in the genus *Listeria*: *L. monocytogenes*, *L. ivanovii*, *L. seeligeri*, *L. innocua*, *L. welshimeri*, *L. grayi*, *L. fleischmannii*, *L. marthii*, *L. rocourtiae* and *L. weihenstephanensis*. Two of these species have been shown to be pathogenic for humans and other mammals: *L. monocytogenes* and *L. ivanovii*.

L. monocytogenes, first isolated in 1924 by E.G.D. Murray, R.A. Webb and M.B.R. Swann in Cambridge, England (Murray *et al.,* 1926), is a facultative intracellular pathogen. It is the causative agent of listeriosis. Listeriosis can manifest clinically as gastroenteritis, meningitis and septicemia, and can also result in abortion, fetal death and neonatal infection (Vázquez-Boland *et al.*, 2001). *L. monocytogenes* infects human beings as well as animals (Vázquez-Boland *et al.*, 2001). Among humans, immunocompromised adults, pregnant women, newborns and the elderly are primarily susceptible to *L. monocytogenes* infection (Vázquez-Boland *et al.*, 2001). Infection occurs by the ingestion of contaminated food products like soft cheeses, dairy items, sausages, pâtés, salads, smoked fish and ready-to-eat foodstuffs that are consumed without cooking or re-heating (Farber and Losos, 1988). *L. monocytogenes* is ubiquitously distributed, and can easily adjust to a wide variety of unfavourable conditions like wide temperature ranges, high salt concentrations and extremes of pH (Vázquez-Boland *et al.*, 2001). *L. monocytogenes* also has the unique ability to multiply at refrigeration temperatures, which makes it one of the leading causes of food poisoning. Although the occurrence is low, infection with *L. monocytogenes* is a more likely cause of mortality as a result of food poisoning, as compared to any other bacteria (Ramaswamy *et al.*, 2007). *L. monocytogenes* infects both phagocytic cells like macrophages, and non-phagocytic cells like epithelial cells, endothelial cells, fibroblasts, hepatocytes and neurons (Vázquez-Boland *et al.*, 2001).

I. Introduction

L. monocytogenes has gained importance not just because of being a food safety hazard, but it has also emerged as an invaluable model system for immunological studies and understanding the molecular basis of host cell parasitism (Cossart and Mengaud, 1989).

To achieve efficient infection of the host, *L. monocytogenes* is equipped with several virulence factors. These include:

1. **Listeriolysin O (LLO)**, the hemolysin which mediates phagosomal escape (Geoffroy *et al.*, 1987). LLO was the first virulence factor of *L. monocytogenes* to be identified and sequenced (Geoffroy *et al.*, 1987). It was characterized as a cytolysin belonging to the family of cholesterol-dependent, pore-forming toxins (CDTX) (Geoffroy *et al.*, 1987). This 58 kDa protein is present only in the pathogenic species of the *Listeria* genus. The gene responsible for the production of LLO is *hly*. LLO is functional in a very narrow pH range: 4.5 to 6.5, with the optimum pH being 5.5 (Geoffroy *et al.*, 1987). This is the reason behind the compartment-specific activity of LLO in the acidified phagosome, and negligible activity in the cytosol (pH 7.4). The presence of a PEST-like sequence (peptide sequence rich in proline, glutamic acid, serine and threonine) leads to cytosol-specific degradation of the toxin (Decatur and Portnoy, 2000). A conserved undecapeptide sequence, ECTGLAWEWWR, is present in all CDTXs. This undecapeptide contains a Cys residue, which leads to toxin activation by thiol-reducing compounds and inhibition by thiol-reacting compounds (Alouf and Geoffroy, 1991). The toxin consists of four domains, out of which three domains are responsible for toxin oligomerization and membrane disruption, and the fourth one is involved in membrane binding (Fig. 1.1). LLO forms pores, nearly 35 nm in diameter, in the cell membrane (Vázquez-Boland *et al.*, 2001). This enables *L. monocytogenes* trapped in phagosomal vacuoles to escape out into the cytoplasm.

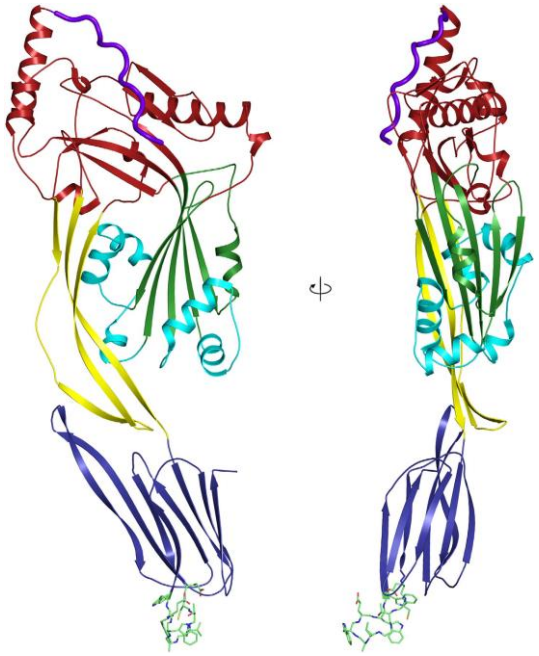

Fig.1.1: The structure of LLO showing its four domains (D). D1 is shown in red, D2 in yellow, D3 in green and D4 in blue (Source: Köster *et al.*, 2014).

2. **Phospholipase A (PlcA) and phospholipase B (PlcB),** which allow bacterial escape from phagosomes (Vázquez-Boland *et al.*, 1992). These are produced by pathogenic *Listeria* species. The phospholipase of *L. monocytogenes* is capable of hydrolyzing phosphatidylcholine, phosphatidylethanolamine, phosphatidylserine, sphingomyelin and phosphatidylinositol, which are present on phagosomal membranes (Geoffroy *et al.*, 1991).

PlcA is a phosphatidylinositol-specific phospholipase, produced by the *plcA* gene. It has a pH optimum between 5.5 and 6.5, which limits its activity to acidified phagocytic vacuoles. PlcB, on the other hand, is a non-specific phospholipase, which is secreted in an inactive form in order to prevent the degradation of bacterial membrane phospholipids. The listerial metalloprotease (Mpl) converts PlcB from its inactive to active form by proteolytic cleavage (Vázquez-Boland *et al.*, 1992).

PlcB is known to mediate efficient escape from both single-membrane (Marquis *et al.*, 1995) and double-membrane phagosomes (Vázquez-Boland *et al.*, 1992), whereas PlcA assists PlcB and LLO to attain optimal escape from single and double membrane phagosomes (Smith *et al.*, 1995).

3. **Internalin A (InlA) and internalin B (InlB)** which allow bacterial internalization into the host cell (Gaillard *et al.*, 1991). Inls are also present in pathogenic *Listeria* species and are encoded by the *inlAB* operon. Inls consist of leucine-rich repeat (LRR) domains, which comprise of a tandem repeat arrangement of an amino acid (aa) sequence with leucine or isoleucine residues at positions 3, 6, 9, 11, 16, 19, and 22 (Kajava, 1998). These LRRs are involved in protein-protein interactions.

InlA consists of 800 aa, which include a signal peptide, 15 LRR units, an LPXTG motif which attaches InlA to the bacterial surface, and a hydrophobic membrane spanning region. InlA interacts with the host cell receptor E-cadherin to mediate bacterial entry in the cell. On the other hand, InlB consists of 7 LRR units, and a region of tandemly arranged repeats for its attachment to the bacterial surface. It lacks the LPXTG motif and the hydrophobic tail (Vázquez-Boland *et al.*, 2001). InlA mediates bacterial entry in E-cadherin-expressing cells, whereas InlB mediates entry in other cell types like epithelial and endothelial cells (Dramsi *et al.*, 1997; Greiffenberg *et al.*, 1998).

4. **ActA**, the surface protein which enables the recruitment of the host-cell actin machinery to permit bacterial movement in the cytosol and cell-to-cell spread (Kocks *et al.*, 1992). The ActA protein, a product of the *actA* gene, is responsible for the intracellular movement of *L. monocytogenes* (Kocks *et al.*, 1992). The secreted form of the protein consists of 639 aa, whereas the mature form is 610 aa long. The mature form further comprises of three main domains (Fig. 1.2):

a) The N-terminal domain, which is rich in cationic residues and regulates actin assembly, filament elongation and interaction with F-actin.
b) The central domain, which contains proline-rich repeats and is crucial for binding the actin-associated proteins: vasodilator-stimulated phosphoprotein (VASP) and murine Enabled protein (Mena).
c) The C-terminal domain, which consists of a hydrophobic region for the attachment of the protein to the surface of the bacterium.

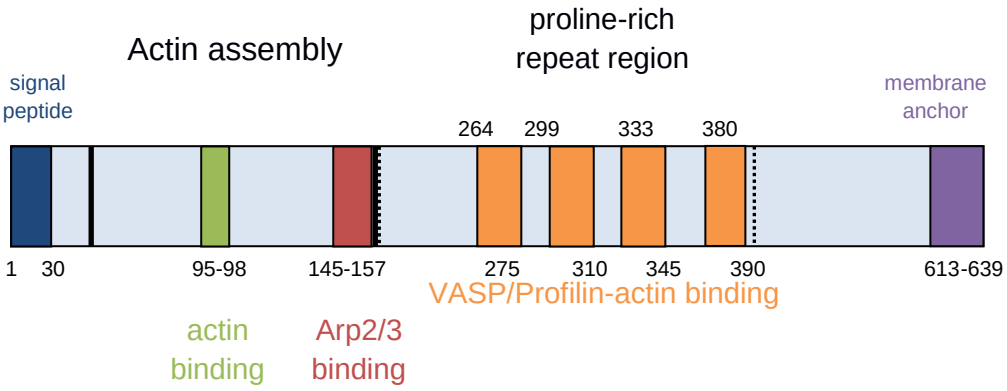

Fig. 1.2: The structure of ActA protein. (adapted from Vázquez-Boland *et al.*, 2001; Yoshikawa *et al.*, 2009).

The Arp2/3 complex, which comprises of actin-related proteins Arp2 and Arp3, constitutes an essential component of the actin assembly unit on *L. monocytogenes*. Host cell components VASP and Mena establish a connection between the host cell cytoskeleton and intracellular *L. monocytogenes* through binding with ActA and profilin/actin complexes. The driving force behind the intracellular movement of *L. monocytogenes* is the deposition of actin only at one pole of the bacterium, thereby propelling it forward (Dabiri *et al.*, 1990).

The genes *hly*, *mpl*, *plcA*, *plcB* and *actA* are organized in a 9-kb chromosomal island known as the *Listeria* pathogenicity island 1 (LIPI-1). They are tightly regulated by a master regulator, i.e. positive regulatory factor A (PrfA) which controls their expression. The *inlA* and *inlB* genes are present on a separate operon called the *inlAB* operon, which is partially regulated by PrfA (Vázquez-Boland *et al.*, 2001). While the *hly*, *plcA*, *plcB*, *actA* and *mpl* genes are only expressed intracellularly, the *inl* genes are also expressed extracellularly (Bubert *et al.*, 1999; Vázquez-Boland *et al.*, 2001).

The following diagram summarizes the virulence factors involved in the intracellular life cycle of *L. monocytogenes* (Fig. 1.3).

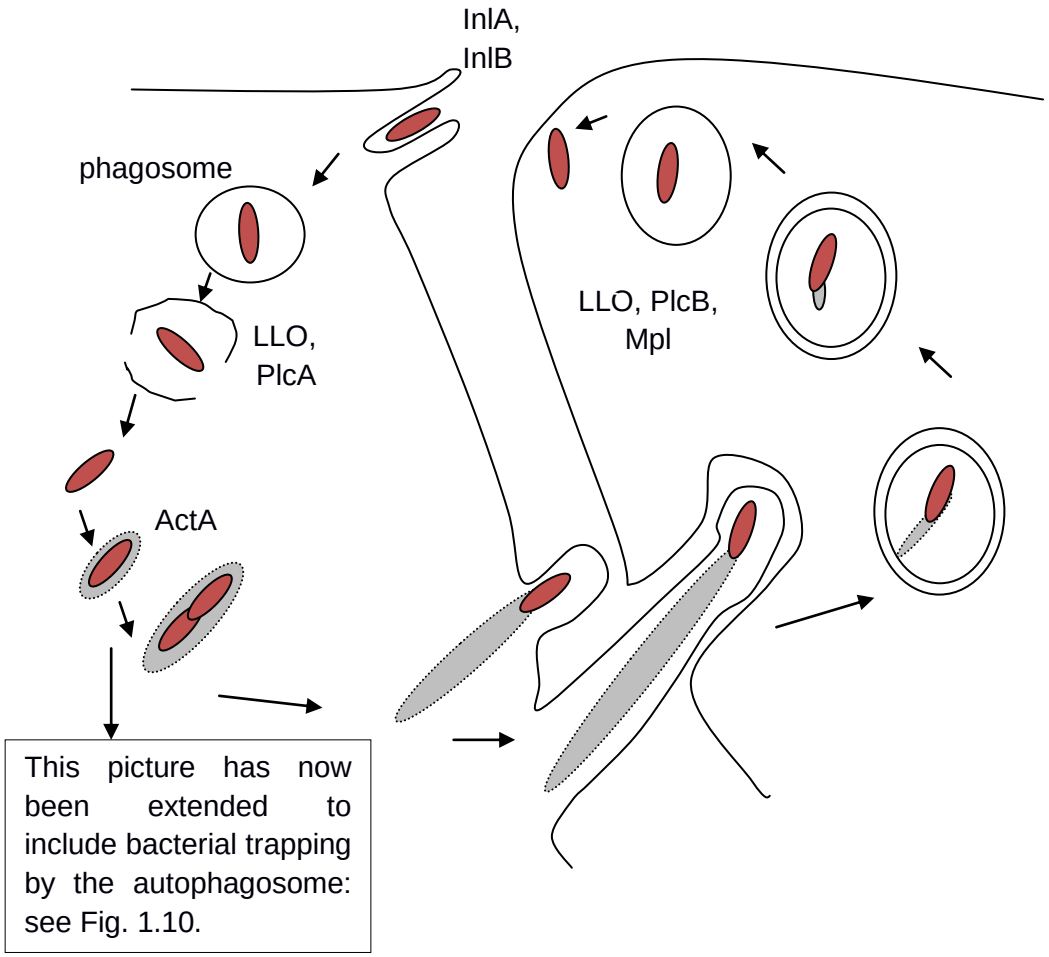

Fig. 1.3: Intracellular life cycle of *L. monocytogenes*. *L. monocytogenes* enters the host cell by induced phagocytosis, and is enclosed within a phagocytic vacuole. LLO and PlcA mediate *L. monocytogenes*' escape from the phagosome into the cytoplasm, where the bacterium replicates and recruits the host cell actin machinery for actin-based motility. Pseudopods are formed and neighbouring cells phagocytose the pseudopods, leading to the formation of a double-membrane secondary phagosome. LLO, PlcB and metalloprotease (Mpl) help in the escape from this secondary phagosome and the cycle continues. (adapted from Vázquez-Boland *et al.*, 2001).

L. monocytogenes has evolved numerous strategies to cross and escape various intracellular membranes. It escapes from the single-membrane phagosome by means of the pore-forming toxin LLO. It has recently been reported that a certain population of intracellular *L. monocytogenes* trapped in the single-membrane phagosome expresses low levels of LLO and continues to grow within this compartment. These phagosomes, termed spacious *Listeria*-containing phagosomes (SLAPs), enable *L. monocytogenes* to establish persistent infection in the host (Birmingham *et al.*, 2008). After coming out free in the cytoplasm, *L. monocytogenes*

expresses ActA protein on its surface, which, by its interaction with the host-cell actin machinery, disguises the bacterium as a host-cell organelle and, thereby prevents its ubiquitination and subsequent degradation by autophagy (Yoshikawa *et al.*, 2009; discussed further in section 1.3). Further, with the help of LLO and PlcB, *L. monocytogenes* is again able to escape out of the double-membrane secondary phagosome, which encloses it as it enters the neighbouring cell. These features make *L. monocytogenes* an excellent tool to study the types of membrane barriers employed by the cell to combat infection, and also to study the mechanisms bacteria have evolved to escape these barriers. Hence, the simplified picture depicted in Fig. 1.3 has become more complex over the years, and provides a starting point for new studies on the interaction of *L. monocytogenes* with host cell defense mechanisms.

1.2 Autophagy

The term autophagy was coined by Belgian biochemist Christian de Duve (de Reuck and Cameron, 1963; Klionsky, 2008). It comprises of the Greek words “auto” meaning self and “phagy” meaning eating. Autophagy can be defined as the cloistering of cellular organelles, protein aggregates or pathogens in a double-membrane vesicle, known as the autophagosome, which are then targeted to lysosomes for degradation by hydrolytic enzymes (Klionsky, 2008). It is an important cellular process involved in cell growth, development, starvation, stress and infection (Burman and Ktistakis, 2010).

Autophagy can be induced following a variety of conditions, like amino acid starvation, low cellular energy levels, endoplasmic reticulum (ER) stress, oxidative stress, withdrawal of growth factors, hypoxia, damage to cellular organelles and pathogen infection (Burman and Ktistakis, 2010).

Autophagy is an indispensable part of cellular homeostasis, and defects in autophagy are associated with many diseases, including neurodegenerative diseases, diabetes, cardiomyopathy, tumorigenesis, fatty liver, and Crohn’s disease (Burman and Ktistakis, 2010).

Several genes and proteins mediate autophagy, and those most relevant to this thesis are represented in a tabular form in Table 1.2.1.

Table1.2.1: Some of the core autophagy related genes present in mammals

Mammals	Yeasts	Function
ATG 12 conjugation		
ATG (autophagy related gene)12	ATG12	Modifier, conjugates with ATG5
ATG5	ATG5	Target of ATG12 localizing to isolated membranes
ATG16L1, L2	ATG16	Determines the site of LC3 conjugation
ATG7	ATG7	E1-like enzyme for ATG12 and LC3/ATG8 conjugation
ATG10	ATG10	E2-like enzyme for ATG12 conjugation
LC3/ATG8 conjugation		
MAP1LC3B/LC3B (Microtubule-associated proteins 1A/1B light chain 3B)	ATG8	Modifier conjugating with phosphatidylethanolamine and localizing to autophagosomes
GABARAP (Gamma-aminobutyric acid receptor-associated protein)	ATG8	Modifier, $GABA_A$-receptor associating protein
ATG7	ATG7	E1-like enzyme for ATG12 and ATG8/LC3 conjugation
ATG3	ATG3	E2-like enzyme for ATG12 and ATG8/LC3 conjugation

Adapted from Tanida, 2011.

The hallmark of autophagy is the conversion of the microtubule-associated protein light chain 3 (LC3) from its inactive to active form, i.e. LC3-I to LC3-II. After the synthesis of LC3, it is cleaved at the COOH terminal to yield the cytosolic LC3-I form. LC3-I is converted to LC3-II, which is the membrane-bound form of the protein. Upon the induction of autophagy, ATG5 and ATG7

induce the lipidation of LC3 by conjugating it with phosphatidylethanolamine, wherein LC3-I is converted into LC3-II. Thus, the ratio of LC3-II to LC3-I increases. This active LC3-II associates with the autophagosomal membrane and recruits the substrate to the autophagosome for its degradation (Fig. 1.4). LC3-II is present on the autophagosomal membrane from the start of the process till the very end and, is, therefore, considered a very good marker for autophagy (Klionsky *et al.*, 2008).

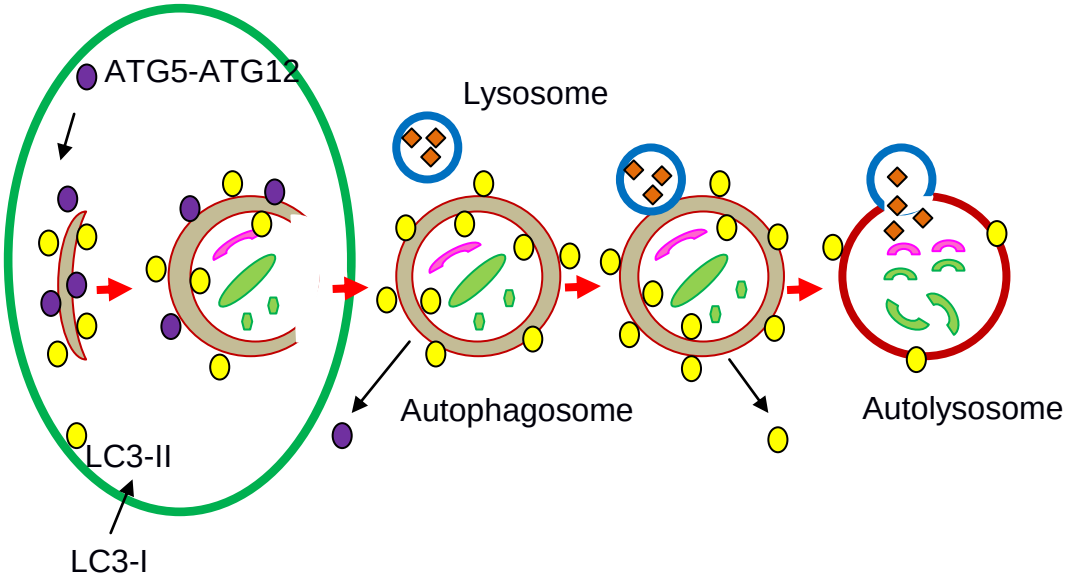

Fig.1.4: A diagram depicting the stages in autophagy. The work in this thesis addresses the association of *L. monocytogenes* to the autophagosomal membrane (green encircled part). ATG: autophagy related gene; LC3: microtubule-associated protein 1 light chain 3.

1.2.1 Selective autophagy

Selective autophagy is a recently recognized mechanism in the field of autophagy. It is characterized by the presence of molecules known as “autophagy adaptors” or “cargo receptors”, which specifically and selectively recognize target molecules and deliver them to the autophagosome (Johansen and Lamark, 2011). Selective autophagy can be harnessed to degrade misfolded proteins, protein aggregates and whole organelles like peroxisomes and mitochondria, and can also eliminate pathogenic bacteria from cells (Johansen and Lamark, 2011; Rogov *et al.*, 2014).

Cargo receptors recognize pathogenic bacteria as prospective cargo due to the presence of poly-ubiquitin signals on them. Bacteria can be directly ubiquitinated, or membrane remnants associated with them can be ubiquitinated (Fujita *et al.*, 2013). It is also known that ubiquitin chains of different linkage types are associated with bacteria, namely, K48 chains which pertain to proteasomal degradation, and K63 chains which are related with autophagy and endocytic trafficking (van Wijk *et al.*, 2012). Autophagy cargo receptors bind to these chains and deliver bacteria for their degradation.

To date, five autophagy cargo receptors are known, and they are discussed in the following sections.

1.2.1.1 Sequestosome 1 (SQSTM1)

SQSTM1, or p62, has the distinction of being the first cargo receptor to be recognized (Bjørkøy *et al.*, 2005). It is a member of the protein kinase C (PKC) family of proteins, a family of protein kinase enzymes which are involved in controlling the function of other proteins through the phosphorylation of hydroxyl groups of serine and threonine, and regulate several signal transduction cascades.

SQSTM1 is a 62 kDa, 440 aa long protein. At its N-terminus, it has a Phox and Bem1p (PB1) domain which is critical for its interaction with the 26S proteasome. It also functions to polymerize SQSTM1 and binds to other proteins containing PB1 domains (*viz.* NBR1). A ZZ type zinc finger domain is present after the PB1 domain. A PEST region containing putative phosphorylation sites, and a COOH-terminal ubiquitin-binding domain (UBD) follow after. The UBD region is responsible for its non-covalent binding to ubiquitin (Geetha and Wooten, 2002). The recently discovered LC3-interacting region (LIR) interacts with LC3 and GABARAP (Fig. 1.5; Gal *et al.*, 2009). Thus, SQSTM1 binds to ubiquitinated cargo *via* its UBD and delivers it for autophagic degradation *via* its interaction with LC3/GABARAP.

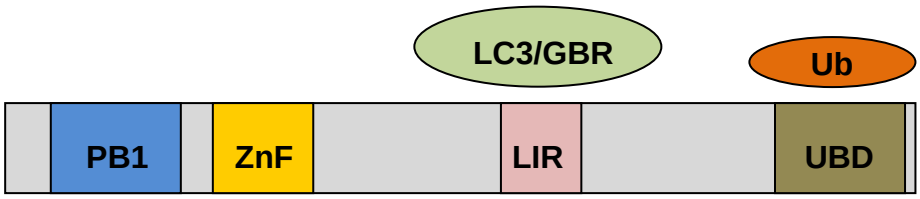

Fig.1.5: The structure of SQSTM1, showing its various domains. PB1: Phox and Bem1p domain; ZnF: zinc finger; LC3: microtubule associated protein 1 light chain 3; LIR: LC3-interacting region; GBR: GABARAP; Ub: ubiquitin; UBD: ubiquitin-binding domain. (adapted from Boyle and Randow, 2013).

SQSTM1 was first identified as a component of protein aggregates found in various neurodegenerative diseases, *viz.* Lewy bodies in Parkinson's disease and neurofibrillary tangles in Alzheimer's disease, to name a few (Zatloukal *et al.*, 2002). Bjørkøy *et al.* (2005) reported that SQSTM1 may play a role in linking ubiquitinated protein aggregates to the autophagosomal machinery *via* LC3. Hence, SQSTM1 protects the cytosol from the deleterious consequences of misfolded proteins. SQSTM1 has been associated with bacterial autophagy (xenophagy) as well, delivering ubiquitinated *Listeria* (Yoshikawa *et al.*, 2009), *Salmonella* (Zheng *et al.*, 2009), *Mycobacteria* (Seto *et al.*, 2012), *Burkholderia* (Al-Khodor *et al.*, 2014), *Legionella* (Khweek *et al.*, 2013) and *Shigella* (Dupont *et al.*, 2009) to the autophagosome by its interaction with LC3. Therefore, it can be concluded from these findings that cellular homeostasis is tightly regulated by SQSTM1, as it mediates the autophagy of ubiquitinated cargo.

1.2.1.2 Optineurin (OPTN)

The 67 kDa autophagy adaptor protein OPTN was first isolated by Li *et al.* (1998) in a yeast two-hybrid screen when they were looking for interacting partners of the E3-14.7 kDa protein (E3-14.7K) present in human adenoviruses, in order to understand the mechanism by which E3-14.7K inhibits the functions of TNF-α. Thus, OPTN was initially christened 14.7K-interacting protein-2 or FIP-2 after being identified as a binding partner of E3-

14.7K. It was later on renamed OPTN, which stands for “optic neuropathy inducing“ protein, after it was found to be associated with normal tension glaucoma, a subtype of primary open-angle glaucoma (Rezaie *et al.*, 2002).

The *optn* gene in humans is present on chromosome 10 and is 37kb in size. It encodes four transcripts that differ in their 5‘ untranslated region. The OPTN protein is 577 aa long, and consists of three coiled-coil domains, one zinc finger domain, one UBD and a LIR (Fig. 1.6). The UBD is essential for its inhibitory function, subcellular localization and interaction with tank binding kinase 1 (TBK1) (Wild *et al.*, 2011).

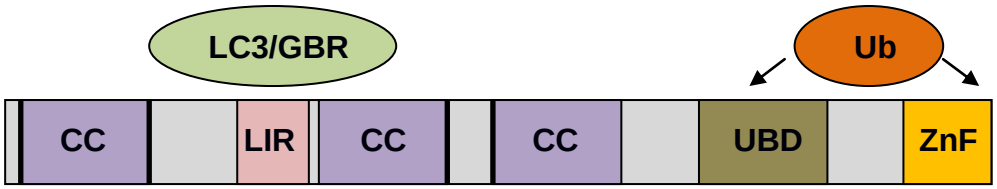

Fig.1.6: The structure of OPTN. CC: coiled-coil; ZnF: zinc finger; LC3: microtubule-associated protein 1 light chain 3; LIR: LC3-interacting region; GBR: GABARAP; Ub: ubiquitin; UBD: ubiquitin-binding domain. (adapted from Boyle and Randow, 2013).

OPTN has been shown to be present in dystrophic neuritis and neurofibrillary tangles in Alzheimer’s disease (Ying and Yue, 2012) and glial cytoplasmic inclusions in multiple system atrophy (Osawa *et al.*, 2011).

OPTN is expressed in the perinuclear region of the cytoplasm and the trans-Golgi network in the Golgi apparatus (Ying and Yue, 2012). OPTN plays important roles in various cellular processes, like the maintenance of the Golgi complex, membrane trafficking, exocytosis as well as Golgi ribbon formation (Sahlender *et al.*, 2005).

It is known that OPTN is induced during viral infections, as well as tumor necrosis factor (TNF) and interferon treatments (Sahlender *et al.*, 2005).

Wild *et al.* (2011) have recently published that phosphorylation of OPTN by TBK1 restricts the intracellular growth of *Salmonella enterica* serovar Typhimurium (*S.* Typhimurium), a bacterium which replicates in *Salmonella*-containing vacuoles (SCVs). The phosphorylation of OPTN by TBK1 results

in enhanced LC3 binding to the autophagic cargo. So far, this is the only study which reports that OPTN regulates bacterial growth during infection.

1.2.1.3 Neighbor of BRCA1 gene 1 (NBR1)

NBR1 was identified by Kirkin *et al.* (2009) as an autophagy adaptor, and they have shown that it localizes to ubiquitin-positive inclusions in liver dysfunction patients. They have also reported that siRNA-mediated knockdown of NBR1 led to the ablation of ubiquitin-positive SQSTM1 bodies after puromycin treatment of cells (which induced the formation of aggresome-like inducible structures), thus indicating the interdependence of NBR1 on SQSTM1.

Despite being twice as large as SQSTM1, NBR1 (966 aa) has a domain architecture similar to that of SQSTM1. It consists of a PB1 domain at the N-terminal, followed by a zinc finger, two coiled-coil domains and a domain that interacts with ubiquitin (UBD) at its C-terminal. Deletion mapping analysis has revealed two LIRs in NBR1, one between aa 727-738, and the second one between aa 542-636, both of which are capable of ATG8 interaction, although it is the former which mainly interacts with ATG8-like proteins (Fig.1.7; Kirkin *et al.*, 2009).

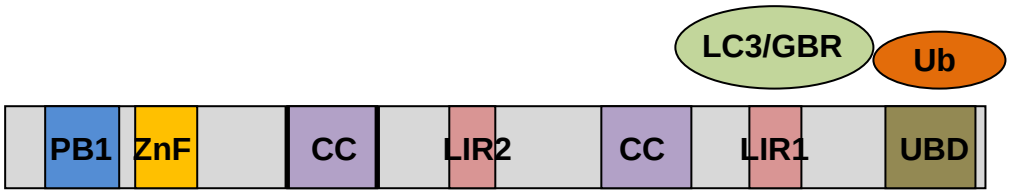

Fig.1.7: NBR1 protein structure, with its functional domains. ZnF: zinc finger; CC: coiled-coil; PB1: Phox and Bem1p domain; LC3: microtubule-associated protein 1 light chain 3; LIR: LC3-interacting region; GBR: GABARAP; Ub: ubiquitin; UBD: ubiquitin-binding domain (adapted from Kirkin *et al.*, 2009).

The level of NBR1 is regulated by autophagy, as it is continuously degraded by autophagy (Lamark *et al.*, 2009). It interacts and forms an oligomeric complex with SQSTM1, and is localized to SQSTM1 bodies formed in *atg5*$^{-/-}$

mouse embryonic fibroblasts (MEFs) or as aggresome-like inducible structures formed after puromycin treatment (Kirkin *et al.*, 2009). Nevertheless, NBR1 can also function independent of SQSTM1, as exemplified by siRNA-mediated studies (Kirkin *et al.*, 2009).

There are two reports which highlight the role of NBR1 in xenophagy. NBR1 is recruited to cytosolic *Shigella flexneri,* and its depletion reduces the recruitment of SQSTM1 and nuclear dot protein 52 (NDP52) to *S. flexneri* (Mostowy *et al.*, 2011). NBR1 has also been shown to be recruited to ubiquitinated *Francisella tularensis* (Chong *et al.*, 2012). Interestingly, a major proportion of the ubiquitinated SQSTM1-positive population of *F. tularensis* also recruits NBR1, which is a proof of the co-operative activity of SQSTM1 and NBR1 in the promotion of autophagic targeting of ubiquitinated cargo (Chong *et al.*, 2012).

1.2.1.4 Nuclear dot protein 52 (NDP52)

NDP52 or CALCOCO2 was first identified as a component of nuclear promyelocytic leukemia bodies. Thurston *et al.* (2009) recognized its role in immunity. They not only identified NDP52 as an adaptor for the recruitment of LC3 to ubiquitinated *S.* Typhimurium and induction of autophagy, but also elaborated on its role as an ubiquitin-sensing receptor for TBK1. They showed that NDP52 binds TBK1 *via* an interaction with additional adaptor proteins nucleosome assembly protein 1 (Nap1) and similar to Nap1 TBK1 adaptor (Sintbad).

The NDP52 protein is 460 aa long, and comprises of two zinc finger domains which bind ubiquitin, one coiled-coil domain, a skeletal muscle and kidney enriched inositol phosphate carboxyl homology (SKICH) domain and a LIR (Fig. 1.8; Thurston *et al.*, 2009).

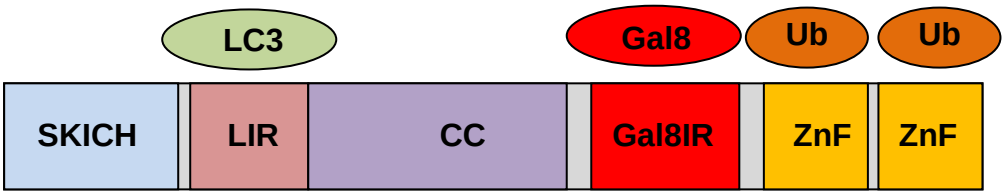

Fig.1.8: NDP52 domain structure. LC3: microtubule-associated protein 1 light chain 3; LIR: LC3-interacting region; CC: coiled-coil; Gal8: Galectin 8; Gal8IR: Galectin-8-interacting region; SKICH: skeletal muscle and kidney enriched inositol phosphate carboxyl homology; Ub: ubiquitin; ZnF: zinc finger. (adapted from Boyle and Randow, 2013).

NDP52 has been shown to play a vital role in facilitating the autophagy of *L. monocytogenes* (Mostowy *et al.*, 2011), *S. flexneri* (Mostowy *et al.*, 2011), *Streptococcus pyogenes* and *S.* Typhimurium (Ivanov and Roy, 2009). It has been reported to restrict the growth of *S.* Typhimurium and *S. pyogenes* (Thurston *et al.*, 2009). NDP52 is recruited to ubiquitinated *S. flexneri*, and this recruitment is dependent on SQSTM1 recruitment, i.e. less NDP52 is recruited to *S. flexneri* in SQSTM1-depleted cells and *vice versa*. On the other hand, the recruitment of NDP52 to *L. monocytogenes* is independent of SQSTM1, as is evident by the recruitment of NDP52 to *L. monocytogenes* in SQSTM1-depleted cells (Mostowy *et al.*, 2011). Ubiquitinated *S.* Typhimurium binds to host proteins Nap1 and Sintbad, which are upstream regulators of TBK1 (Thurston *et al.*, 2009). Despite the presence of ubiquitin-binding regions in Nap1 and Sintbad, they did not observe direct binding between ubiquitin and Nap1/Sintbad. It was found that NDP52 was the missing link between ubiquitinated *S.* Typhimurium, and Nap1 and Sintbad. The zinc finger domain of NDP52 binds ubiquitin, and the SKICH domain binds Nap1/Sintbad. It was subsequently discovered that NDP52 binds ubiquitinated *S.* Typhimurium and the number of intracellular *S.* Typhimurium increases in NDP52-depleted cells. Thus, NDP52 restricts the intracellular replication of *S.* Typhimurium, and also of *S. pyogenes*.

1.2.1.5 TAX1 binding protein 1 (TAX1BP1)

TAX1BP1 is the most recently identified autophagy cargo receptor (Newman *et al.*, 2012). It was independently identified as a binding partner of TNF receptor-associated factor 6 (TRAF6) (Newman *et al*., 2012), T-lymphotropic

virus Type I (HTLV-I) TAX1 and A20 (De Valck *et al.*, 1999). It is localized in the cytoplasm, Golgi complex, nucleus as well as in the plasma membrane (Verstrepen *et al.*, 2011).

TAX1BP1 is a paralog of NDP52, which is evident by the homology of its N terminal region with NDP52. The two cargo receptors have similar structural domains. TAX1BP1 consists of a LIR, two zinc fingers which bind to ubiquitin, one SKICH domain, and three coiled-coil domains (Fig. 1.9; Deretic *et al.*, 2013).

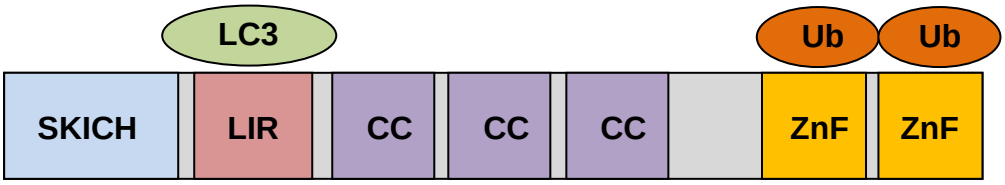

Fig.1.9: TAX1BP1 protein structure. LC3: microtubule-associated protein 1 light chain 3; LIR: LC3-interacting region; CC: coiled-coil; SKICH: skeletal muscle and kidney-enriched inositol phosphate carboxyl homology; Ub: ubiquitin; ZnF: zinc finger. (adapted from Deretic *et al.*, 2013).

Currently, there is just one report by Newman *et al.* (2012), which highlights the role of TAX1BP1 as an autophagy cargo receptor protein. They have shown that TAX1BP1 is recruited to basal autophagosomes in A549 cells, and that ubiquitin-like proteins of the LC3/GABARAP family bind to TAX1BP1. TBK1 has also been reported to bind to TAX1BP1.

1.3 Autophagy and *L. monocytogenes*

Numerous reports highlight the induction of autophagy by *L. monocytogenes* infection. The first evidence of autophagy induction during infection with *L. monocytogenes* was provided by Py *et al.* (2007), who demonstrated that the expression of LLO by *L. monocytogenes* activates autophagy, as infection with a LLO mutant resulted in decreased ratios of LC3-II/LC3-I in MEFs in comparison to infection with wild-type *L. monocytogenes*. They also showed that PlcA and PlcB are not essential for autophagy induction. Another study

performed in *Drosophila* has reported that the pathogen recognition receptor (PRR) peptidoglycan recognition protein LE (PGRP-LE) recognizes diaminopimelic acid-type peptidoglycans present on *L. monocytogenes*, and this is essential for the induction of autophagy during infection with *L. monocytogenes* (Yano *et al.*, 2008). The induction of autophagy by PGRP-LE restricts the intracellular growth of *L. monocytogenes* in hemocytes. A further study performed by the same group identified a novel antibacterial gene in *Drosophila*, designated as *Listericin*, which is expressed in response to *L. monocytogenes* infection in a PGRP-LE-dependent manner. The expression of *Listericin* leads to the growth inhibition of *L. monocytogenes* (Goto *et al.*, 2010). The involvement of other PRRs has also been demonstrated in the activation of autophagy following *L. monocytogenes* infection (Anand *et al.*, 2011). They have reported that Toll-like receptor 2 and Nod-like receptors 1 and 2, acting *via* the downstream extracellular signal-regulated kinases, are involved in the activation of the autophagic response during infection with *L. monocytogenes*. A recent study mentions that LLO-dependent phagosomal lysis during *L. monocytogenes* infection triggers amino acid starvation, leading to autophagy induction (Tattoli *et al.*, 2013). Thus, these reports have shown that induction of autophagy during *L. monocytogenes* infection is an essential event in controlling infection.

Just as the host cells have employed various signaling mechanisms to control *L. monocytogenes* infection, *L. monocytogenes* has developed certain strategies to evade autophagic recognition. It has been proposed by Yoshikawa *et al.* (2009) that the ActA protein, which is ubiquitously distributed on the surface of *L. monocytogenes*, forms an actin core motility machinery by employing one VASP tetramer containing four profilin units, one Arp2/3 complex and actin filaments. This actin machinery forms an actin tail at one end of the bacterium, which is responsible for its movement from one cell to the other. Through the recruitment of host cell actin machinery components by ActA, *L. monocytogenes* disguises itself as a host cell organelle and is not heavily ubiquitinated when it is in the cytosol, thereby successfully evading autophagy. On the other hand, *L. monocytogenes*

which lacks ActA (LmΔ*actA*) is unable to form an actin tail to propel its movement to neighbouring cells, and subsequently, is heavily ubiquitinated in the cytosol. The autophagy cargo receptor SQSTM1 binds to ubiquitinated LmΔ*actA* and delivers it to the autophagosome for degradation (Yoshikawa *et al.*, 2009; Fig. 1.10).

Another study has reported that in the absence of ActA, InlK present in *L. monocytogenes* interacts with the major vault protein (MVP) to decorate its surface with MVP, (in a manner similar to that of actin complex recruitment by ActA), and evades autophagy (Dortet *et al.*, 2011). Based upon the expression of ActA and InlK, these authors have outlined four possibilities: (1) when *L. monocytogenes* co-expresses ActA and InlK: InlK recruits MVP to the surface of the bacterium. InlK is then replaced by ActA and actin replaces MVP to disguise the bacterium and prevents ubiquitination, recognition by autophagy adaptor (SQSTM1) and LC3 recruitment, (2) when ActA is expressed, but InlK is absent: *L. monocytogenes* recruits VASP and the Arp2/3 complex and polymerizes actin, which is sufficient to prevent ubiquitination, autophagy adaptor recognition and LC3 recruitment, (3) in the absence of ActA, InlK recruits MVP and protects *L. monocytogenes* from ubiquitination, autophagy adaptor recognition and LC3 recruitment, and (4) when neither ActA nor InlK is expressed: *L. monocytogenes* is ubiquitinated and autophagy adaptor and LC3 are recruited, leading to its autophagic degradation. However, these results were obtained when InlK was overexpressed in cells, because InlK is neither expressed in *L. monocytogenes* grown in BHI medium, nor in cells infected with *L. monocytogenes* grown in BHI medium. Thus, it may be possible that out of ActA and InlK, ActA plays a major role in the evasion of autophagy by *L. monocytogenes*. Nevertheless, *L. monocytogenes* has evolved different strategies to evade degradation by autophagy (Fig. 1.10).

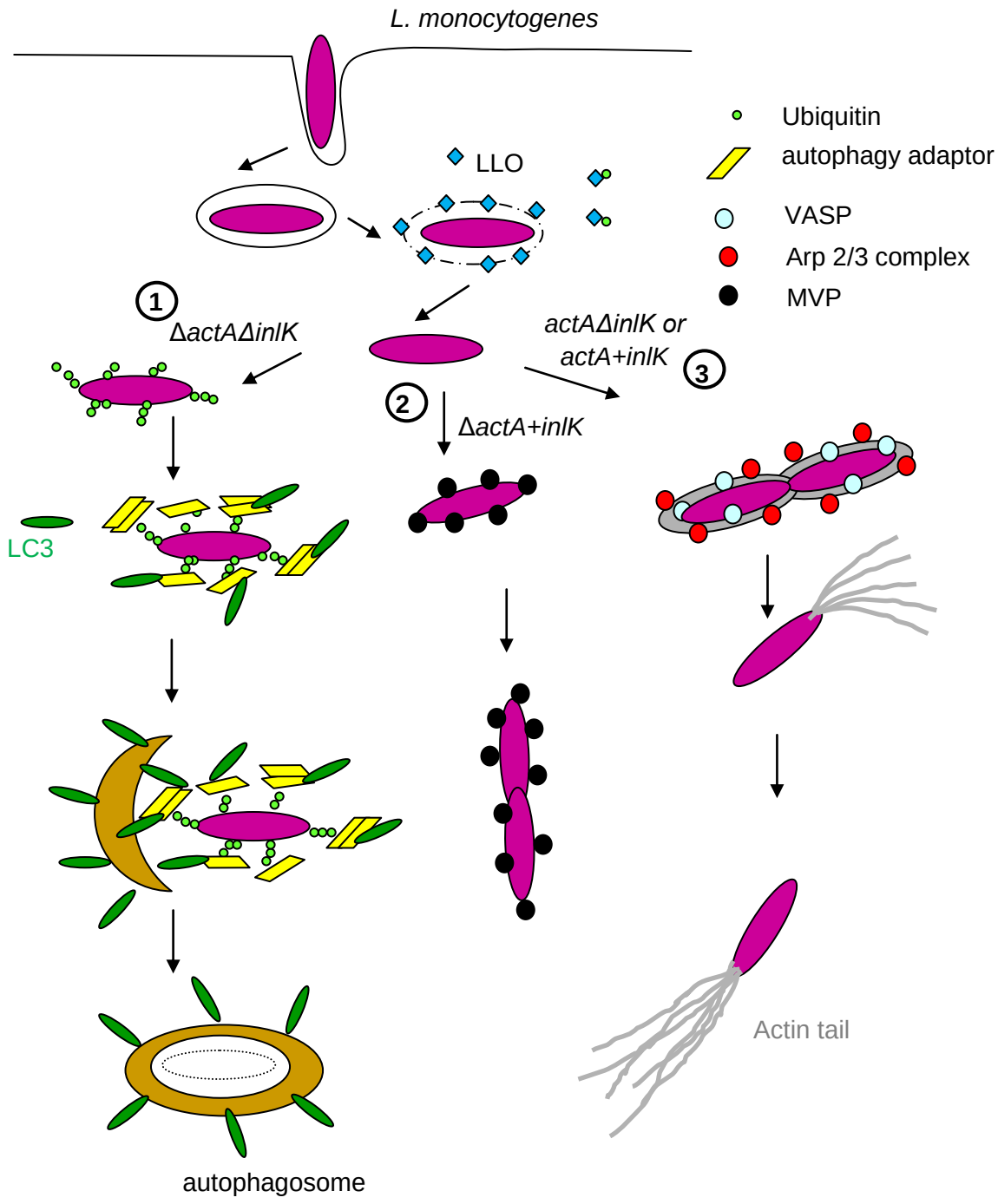

Fig. 1.10: ActA- and InlK-mediated evasion of autophagy by *L. monocytogenes*. Intracellular *L. monocytogenes* express ActA which enables bacterial movement in the cytosol by means of actin polymerization, and by recruiting VASP and Arp 2/3, ActA enables the bacterium to escape autophagy. Moreover, the recruitment of MVP *via* InlK also protects *L. monocytogenes* from autophagy. (1) The bacteria devoid of ActA or InlK are ubiquitinated, followed by autophagy adaptor binding and LC3 recruitment, and are subsequently captured in an autophagosomal compartment. (2) In the absence of ActA, InlK protects *L. monocytogenes* against autophagy recognition *via* MVP recruitment. (3) When both ActA and InlK are expressed, or only ActA is expressed, *L. monocytogenes* escapes autophagy (adapted from Yoshikawa *et al.*, 2009; Dortet *et al.*, 2011).

1.4 Objective of the study

Autophagy is an important cellular defense mechanism against infections, and autophagic control of bacterial replication promotes bacterial clearance during infections. Selective autophagy, mediated by autophagy cargo receptors, has been shown to restrict the growth of intracellular pathogens (Johansen and Lamarck, 2011). It is well-known that *L. monocytogenes* infection induces autophagy, and to avoid autophagy, *L. monocytogenes* has devised multiple strategies to evade autophagic recognition (Birmingham *et al.*, 2007; Yoshikawa *et al.*, 2009; Dortet *et al.*, 2011). *L. monocytogenes*, which lacks ActA, undergoes ubiquitination when it is free in the host cell cytoplasm (Yoshikawa *et al.*, 2009). SQSTM1 is recruited to ubiquitinated *L. monocytogenes* and delivers it to the autophagosome *via* its interaction with LC3 (Yoshikawa *et al.*, 2009). Like SQSTM1, NDP52 is also recruited to ubiquitinated *L. monocytogenes* which mediates its autophagy (Mostowy *et al.*, 2011). Thus, until now, only these two autophagy cargo receptors have been reported to mediate the autophagy of *L. monocytogenes*.

Previous studies in our laboratory have shown that the addition of LLO to eukaryotic cells up-regulates the expression of the *optn* gene (Ghai, 2006). OPTN is a member of the family of autophagy cargo receptors, and has so far not been implicated in the autophagy of *L. monocytogenes*. There is mounting evidence which suggests an interdependence and cooperation between the functionalities of different autophagy cargo receptors, for example, the decrease in the recruitment of NDP52 and SQSTM1 to cytosolic *Shigella* in NBR1-depleted cells (Mostowy *et al.*, 2011), and the cooperation of SQSTM1 and NDP52 to facilitate efficient autophagy of *S.* Typhimurium (Cemma *et al.*, 2011). Additionally, it has been suggested that different autophagy cargo receptors may engage distinct signaling molecules or pathways for the selective degradation of pathogens (Mostowy *et al.*, 2011). Therefore, the study of different autophagy cargo receptors in the autophagy-mediated growth restriction of *L. monocytogenes* is of relevance and very much warranted.

SQSTM1, NDP52 and OPTN are recruited to ubiquitinated *S.* Typhimurium, which is then delivered to the autophagosome (Zheng *et al.*, 2009; Thurston *et al.*, 2009; Wild *et al.*, 2011). Because both *L. monocytogenes* and *S.* Typhimurium are facultative intracellular pathogens, it was hypothesized that SQSTM1, OPTN and NDP52 may be involved in the autophagy-mediated growth restriction of *L. monocytogenes*. Additionally, due to the fact that NBR1 has been shown to be associated with the autophagy of *S. flexneri* and *F. tularensis*, and because TAX1BP1 is a paralog of NDP52, it was considered expedient to examine if they (NBR1and TAX1BP1) too play a role in the autophagy of *L. monocytogenes*.

Because bacteria are known to differ in their ability to evade autophagy, it was further hypothesized that autophagy cargo receptors and autophagy markers may play some role(s) in their differential growth restriction by autophagy. Towards this end, in the studies reported herein, it was intended to use two different strains of *L. monocytogenes*: wild-type Lm EGD-e, which is motile in cytosol and displays all phenotypes of autophagy evasion explained in Fig. 1.3 and 1.10, and LmΔ*actA2* (a mutant of Lm EGD-e which lacks the critical regions required for actin-based motility: the Arp2/3 complex-binding region, the VASP region and the actin-binding region), which is non-motile in cytosol and is unable to evade autophagy. Thus, Lm EGD-e and LmΔ*actA2* reflect two ends of a spectrum, and are expected to serve as the best tools to investigate the differences in their growth restriction.

With this in the back-drop, the objective of this dissertation was to determine the role(s) of all the five known autophagy adaptors (SQSTM1, OPTN, NBR1, NDP52 and TAX1BP1) in the *in vitro*:

- autophagy of *L. monocytogenes*.
- differential growth restriction of Lm EGD-e and LmΔ*actA2*.

II. Materials and methods

General note

For sterilization, all the glassware and plastic-ware (microcentrifuge tubes, 1.5 ml; pipette tips etc.) were either heat-sterilized (180°C, 4h) or autoclaved (121°C, 20 min), respectively. The media and solutions were prepared by using water from water purification systems (U > 18MΩ; mQH_2O). The bacterial media and various solutions for culture applications were autoclaved. All the concentrations for media and solutions are given as final concentrations.

2.1 Equipment

Table 2.1 List of all the equipment used

Item	Manufacturer
Analytical balance	Mettler; Giessen, Germany
	Kern; Baligen, Germany
Autoclave	Getinge; Getinge, Sweden
CO_2-incubator	Labotect; Göttingen, Germany
Confocal microscope	Leica; Solms, Germany
Cell-counting chamber	Brand; Wertheim, Germany
Centrifuges	Eppendorf 5415D; Hamburg, Germany
	Heraeus Biofuge 15; Thermo Scientific, Waltham, MA, USA
	Heraeus Megafuge 1.0R; Thermo Scientific, Waltham, MA, USA
	Merck Galaxy Mini; Darmstadt, Germany

Item	Manufacturer
Electro-blotting apparatus	Construction of the institute
Electrophoresis apparatus (agarose gel electrophoresis)	Construction of the institute
Electrophoresis apparatus (SDS-PAGE)	Biometra; Göttingen, Germany
Electroporator	Bio-Rad; Hercules, CA, USA
Film developer for Western blots (Curix 60)	Agfa Healthcare; Mortsel, Belgium
Freezer (-20°C)	Bosch; Stuttgart, Germany
	Liebherr; Bulle, Switzerland
Freezer (-80°C)	Heraeus; Thermo Scientific, Waltham, MA; USA
Fridge (4°C)	Bosch; Stuttgart, Germany
	Electrolux; Stockholm, Sweden
	Liebherr; Bulle, Switzerland
Freezing chamber for eukaryotic cells	Nalgene Sigma Aldrich; St. Louis, MO, USA
Gel doc (imaging) system	Bio-Rad; Hercules, CA, USA
Hypercassette for film development	Amersham Biosciences; Little Chalfont, Buckinghamshire, UK
Ice machine	Ziegra; Isernhagen, Germany
Incubator	Heraeus; Thermo Scientific, Waltham, MA, USA

Item	Manufacturer
Light microscope	Hund; Wetzlar, Germany
Magnetic stirrer	IKA; Staufen, Germany
Microwave oven	AEG; Luton, Berdfordshire, UK
Microliter pipettes	Gilson; Middleton, WI, USA
	Biohit; Helsinki, Finland
	Eppendorf; Hamburg, Germany
Multi-channel pipette	Biozym; Hessisch Oldendorf, Germany
NanoDrop Spectrophotometer	Thermo Scientific; Waltham, MA, USA
pH-Meter	Knick; Berlin, Germany
Plate reader (Phomo)	Autobio labtec; Zhengzhou, China
Plate shaker	IKA; Staufen, Germany
Pipetboy (pipet controller)	Integra Biosciences; Zizers, Switzerland
Shaking-incubator	Infors; Basel, Switzerland
Sterile-work bench	Heraeus; Handu, Germany
	Nuaire; Plymouth, MN, USA
Thermomixer	Eppendorf; Hamburg, Germany
Vortex mixer	VWR; Radnor, PA, USA
	IKA; Staufen, Germany

Item	Manufacturer
Vortex mixer	Scientific Industries; Bohemia, NY, USA
Water bath	Grant; Shepreth, Cambridgeshire, UK
Water purification system	Millipore; Billerica, MA, USA

2.2 Consumables

Table 2.2: List of all the consumables used

Item	Manufacturer
96-well plates U-bottom	Greiner; Frickenhausen, Germany
Cell scraper	Greiner; Frickenhausen, Germany
Cryovials	Sarstedt; Nümbrecht, Germany
Cover slips	R. Langenbrinck; Emmendingen, Germany
Cuvettes	Ratiolab; Dreieich, Germany
Disposable pipettes	Greiner Bio-One; Frickenhausen, Germany
Disposable scalpels	Feather; Osaka, Japan
Disposable syringes	Braun; Melsungen, Germany
ECL films	Amersham Biosciences; Little Chalfont, Buckinghamshire, UK
Electroporation cuvettes	Invitrogen, Thermo Fischer; Waltham, MA, USA
Examination gloves	Ansell; Richmond, VIC, Australia

Item	Manufacturer
Films for 96-well plates	Thermo Scientific; Waltham, MA, USA
Glass slides	R. Langenbrinck; Emmendingen, Germany
Glassware	Schott; Mainz, Germany
Inoculating loops	Nunc Sigma Aldrich; St. Louis, MO, USA
Microcentrifuge tubes, 1.5 ml	Eppendorf; Hamburg, Germany
Multiwell tissue culture plates	Becton Dickinson; Franklin Lakes, NJ, USA
Paper towels (lintless)	Kimberly Clark; Irwing, TX, USA
Parafilm	Pechiney Plastic Packaging; Chicago, IL, USA
Petri dishes (13.5 cm)	Greiner; Frickenhausen, Germany
Pipette tips	Greiner; Frickenhausen, Germany
Pipette tips (with filter)	Nerbe Plus; Winsen/Luke, Germany
Plastic tubes 50 ml, 15 ml	Greiner Bio-One; Frickenhausen, Germany
PVDF membrane	Roche; Basel, Switzerland
Tissue culture dishes	Becton Dickinson; Franklin Lakes, NJ, USA
Whatman 3MM Chr chromatography paper	Thermo Scientific; Waltham, MA, USA

2.3 Antibodies

Table 2.3: List of all the antibodies used; WB: Western blot, IF: immunofluorescence

Antibody	Dilution	Incubation	Diluent	Source	React-ivity	Manufa-cturer
Alexa Fluor 488	1:1000	2h	IF buffer	-	Rabbit	*CST
Alexa Fluor 647	1:1000	2h	IF buffer	-	Mouse	*CST
Alexa Fluor 647	1:1000	2h	IF buffer	-	Rabbit	*CST
Anti-β-actin	1:5000	Overnight	BSA	Rabbit	Human, mouse, rat	*CST
Anti-goat IgG (HRP)	1:2000	1h	Milk	Donkey	Goat	**SCB
Anti-Lm (M108)	Undiluted	overnight	-	Mouse	Lm surface antigen	Product of the institute
Anti-MAP LC3 β	1:200	2h	Milk	Goat	Human, mouse, rat	**SCB
Anti-NBR1	1:1000 (WB) 1:100 (IF)	overnight	Milk (WB) IF buffer (IF)	Rabbit	Human, mouse, rat	Proteintech, Chicago, IL, USA
Anti-NDP52	1:1000 (WB) 1:200 (IF)	overnight	Milk (WB) IF buffer (IF)	Rabbit	Human	Abcam, Cambridge, UK

Antibody	Dilution	Incubation	Diluent	Source	React-ivity	Manufa-cturer
Anti-OPTN	1:1000 (WB) 1:100 (IF)	overnight	Milk (WB) IF buffer (IF)	Rabbit	Human, mouse, rat	Proteintech, Chicago, IL, USA
Anti-pSer177 OPTN	1:500	overnight	Milk	Rabbit	Human, mouse	Provided by Wild *et al.* (2011)
Anti-rabbit IgG (HRP)	1:2000	1h	Milk	Goat	Rabbit	**SCB
Anti-SQSTM1	1:1000 (WB) 1:100 (IF)	overnight	Milk (WB) IF buffer (IF)	Rabbit	Human, mouse, rat	Proteintech, Chicago, IL, USA
Anti-TAX1BP1	1:200 (WB) 1:50 (IF)	2h	Milk (WB) IF buffer (IF)	Rabbit	Human, mouse, rat	**SCB

*CST: Cell Signalling Technology; Danvers, MA, USA
**SCB: Santa Cruz Biotechnology; Dallas, TX, USA

2.4 Chemicals

Table 2.4: List of all the chemicals used

Chemical	Supplier
1 kb plus DNA ladder	Thermo Scientific; Waltham, MA, USA
6-amino-N-hexanoic acid	Sigma Aldrich; St. Louis, MO, USA
Agar	Sigma Aldrich; St. Louis, MO, USA

Chemical	Supplier
Agarose	Sigma Aldrich; St. Louis, MO, USA
Ammonium peroxidisulphate (APS)	Merck; Darmstadt, Germany
Ampicillin	Sigma Aldrich; St. Louis, MO, USA
β-mercaptoethanol	Sigma Aldrich; St. Louis, MO, USA
Bicinchoninic acid (BCA)	Sigma Aldrich; St. Louis, MO, USA
Bovine serum albumin (BSA)	Sigma Aldrich; St. Louis, MO, USA
Brain heart infusion (BHI)	Sigma Aldrich; St. Louis, MO, USA
Bromophenol blue	Serva; Heidelberg, Germany
BX-795	Merck Millipore; Billerica, MA, USA
CHAPS cell lysis buffer	Protein Simple; Santa Clara, CA, USA
Cell wash buffer (for CHAPS lysis)	Protein Simple; Santa Clara, CA, USA
Copper(II) sulphate solution	Sigma Aldrich; St. Louis, MO, USA
Dimethyl sulphoxide (DMSO)	Merck; Darmstadt, Germany
Dithiothreitol (DTT)	Serva; Heidelberg, Germany
DMEM medium	Invitrogen, Thermo Fischer; Waltham, MA, USA
ECL detection system	Thermo Fischer; Waltham, MA, USA
EDTA	Merck; Darmstadt, Germany
Ethanol	Sigma Aldrich; St. Louis, MO, USA

Chemical	Supplier
Ethidium bromide	Roth; Karlsruhe, Germany
Fetal bovine serum (FBS)	PAA Laboratories; Cölbe, Germany
Ficoll	Pharmacia biotech, GE Healthcare Life Sciences; Freiburg, Germany
Film developer solution for Western blots (Unimatic D)	Calbe Chemie; Calbe, Germany
Film fixer solution for Western blots (Unimatic F)	Calbe Chemie; Calbe, Germany
Formaldehyde	Merck; Darmstadt, Germany
Formic acid	Sigma Aldrich; St. Louis, MO, USA
Gentamicin	Invitrogen, Thermo Fischer; Waltham, MA, USA
Glucose	Merck; Darmstadt, Germany
Glycerol	Merck; Darmstadt, Germany
Glycine	Roth; Karlsruhe, Germany
Hanks´ balanced salt solution (HBSS)	Biochrom AG; Berlin, Germany
HiPerfect Transfection Reagent	Qiagen; Hilden, Germany
HEPES	Serva; Heidelberg, Germany
Hydrochloric acid	Merck; Darmstadt, Germany
Isopropanol	Sigma Aldrich; St. Louis, MO, USA
Kanamycin	Sigma Aldrich; St. Louis, MO, USA

Chemical	Supplier
Lipofectamine 2000	Thermo Fischer; Waltham, MA, USA
Methanol	Sigma Aldrich; St. Louis, MO, USA
Midi plasmid isolation kit	Qiagen; Hilden, Germany
MTT	Calbiochem, Merck Millipore; Billerica, MA, USA
Opti-MEM I medium	Invitrogen, Thermo Fischer; Waltham, MA, USA
Page ruler plus pre-stained protein ladder	Fermentas, Thermo Scientific; Waltham, MA, USA
PBS	Biochrom AG; Berlin, Germany
PMSF	Sigma Aldrich; St. Louis, MO, USA
Polyacrylamide	Roth; Karlsruhe, Germany
Potassium chloride	Merck; Darmstadt, Germany
Potassium hydrogen phosphate	Merck; Darmstadt, Germany
ProLong Gold Antifade with 4',6-diamidino-2-phenylindole (DAPI)	Invitrogen, Thermo Fischer; Waltham, MA, USA
Protease inhibitor cocktail III	Calbiochem, Merck Millipore; Billerica, MA, USA
Re-Blot Plus stripping solution	Millipore; Billerica, MA, USA
RNase-free water	Thermo Fischer; Waltham, MA, USA
Skimmed milk powder	Sigma Aldrich; St. Louis, MO, USA

Chemical	Supplier
Sodium chloride	Roth; Karlsruhe, Germany
Sodium deoxycholate	Merck; Darmstadt, Germany
SDS	Sigma Aldrich; St. Louis, MO, USA
Sodium hydrogen phosphate	Merck; Darmstadt, Germany
Sodium hydroxide	Merck; Darmstadt, Germany
TEMED	Roth; Karlsruhe, Germany
Tris	Roth; Karlsruhe, Germany
Triton X-100	Serva; Heidelberg, Germany
Trypsin/EDTA	PAA Laboratories; Cölbe, Germany
Tryptone	Becton Dickinson; Franklin Lakes, NJ, USA
Tween-20	Serva; Heidelberg, Germany
Yeast extract	Becton Dickinson; Franklin Lakes, NJ, USA

2.5 Buffers and solutions

The following buffers and solutions were used.

Antibiotic stock solutions	Ampicillin: 100 mg/ml in mQ water Kanamycin: 100 mg/ml in mQ water
1x TBS with Tween-20	10 mM tris-HCl (pH 8) 150 mM NaCl 0.1% (v/v) Tween-20

	dissolved in double distilled water
10x SDS-PAGE running buffer	250 mM tris 1.92 M glycine 1% (w/v) SDS dissolved in double distilled water
5x SDS-PAGE sample buffer	62.5 mM tris-HCl (pH 6.8) 2% (w/v) SDS 20% (v/v) gycerol 5% (v/v) β-mercaptoethanol 0.125 % (w/v) bromophenol blue dissolved in double distilled water
Blotting solution I	30 mM tris 10% (v/v) methanol dissolved in double distilled water
Blotting solution II	25 mM tris 10% (v/v) methanol dissolved in double distilled water
Blotting solution III	40 mM 6-amino-N-hexanoic acid 10% (v/v) methanol dissolved in double distilled water
RIPA cell lysis buffer	50 mM tris-HCl (pH 7.4) 150 mM NaCl 1 mM EDTA 1% (v/v) triton X-100 1% (w/v) sodium deoxycholate 0.1% (w/v) SDS 1 mM PMSF [#] 1:80 protease inhibitor cocktail III [#] [#] to be added just before use
10x PBS	27 mM KCl 1.4 M NaCl 81 mM Na_2HPO_4 15 mM KH_2PO_4 dissolved in double distilled water pH set to 7.4
Immunofluorescence buffer	0.3% triton X-100 (v/v) 1% BSA 1x PBS

5X sample buffer (agarose gel electrophoresis)	25% (w/v) ficoll type 400 0.25% (w/v) bromophenol blue in 1X TE buffer
1X TE buffer	10mM tris-HCl (pH 8) 1 mM EDTA

2.6 Bacterial culture

Table 2.6.1: Bacterial strains used in this study

Strain	Characteristic	Reference
Escherichia coli Top 10	Derivative of *E. coli* laboratory strain MG1655	Invitrogen, Thermo Fischer; Waltham, MA, USA
Listeria monocytogenes EGD-e serotype 1/2a	Wild-type *L. monocytogenes* strain	Glaser *et al.*, 2001
Listeria monocytogenes EGDΔ*actA2*	Mutant Lm EGD-e lacking amino acids 20-602, incapable of actin-based motility	Chakraborty *et al.*, 1995
Listeria monocytogenes EGDΔ*actA16*	Mutant Lm EGD-e lacking the Arp2/3 complex-binding region, capable of actin-based motility	Yoshikawa *et al.*, 2009
Listeria monocytogenes EGDΔ*actA21*	Mutant Lm EGD-e lacking the actin-binding region, the Arp2/3 complex-binding region and the VASP-binding region, incapable of actin-based motility	Yoshikawa *et al.*, 2009
Salmonella enterica serovar Typhimurium	Wild-type *S.* Typhimurium strain	ATCC 14028

The bacterial handling was done under a Biosafety cabinet (Class II A2, BSL-2) using sterile media, solutions and equipment.

2.6.2 Bacterial media

BHI medium	3.7% (w/v) BHI
LB medium	10 g tryptone 5 g yeast extract 10 g NaCl 1L double distilled water
SOB medium	0.5% (w/v) yeast extract 2% (w/v) tryptone 10 mM NaCl 2.5 mM KCl Double distilled water
BHI agar	BHI medium 1.5% (w/v) agar
LB agar	LB medium 1.5% (w/v) agar

2.6.3 Propagation of bacteria

Overnight cultures of *L. monocytogenes* were prepared by inoculating 10 ml BHI medium with one bacterial colony, followed by overnight incubation at 37°C in an orbital shaker (180 rpm) incubator.

Overnight cultures of *S.* Typhimurium and *E. coli* were prepared by inoculating 10 ml LB medium with one colony of bacteria, followed by overnight incubation at 37°C at 180 rpm.

The bacteria were prepared for short-term storage by plating out a suitable volume of an overnight culture on BHI or LB agar plates, followed by overnight incubation at 37°C. Long-term storage cultures were prepared by mixing 750 µl of an overnight culture with 750 µl of 60% (v/v) glycerol in BHI/LB medium in a cryovial. These cultures can be stored at -80°C for up to 3–4 years.

2.6.4 Infection with bacteria

For *L. monocytogenes* infections, overnight cultures were diluted 1:50 in BHI medium and cultured to an OD_{600} of 0.2–0.4. An adequate culture volume was centrifuged at 13000 rpm for 1 min at RT, washed twice with sterilized HBSS, resuspended in medium containing 0.5% FBS and used for infection. Unless stated otherwise, a multiplicity-of-infection (MOI; cell: bacteria) of 1:10 was used for infection. For the elimination of extracellular bacteria, the cells were incubated with DMEM containing 10% FBS and 50 µg/ml gentamicin.

For infections with *S.* Typhimurium, an overnight culture was diluted 1:33 in LB medium and cultured to an OD_{600} of 1–1.2. An appropriate volume of culture was centrifuged (13000 rpm; 1 min; RT), washed (x2; sterilized PBS) and resuspended (medium containing 0.5% FBS). The cells were infected at a MOI of 1:100. The extracellular bacteria were eliminated by adding DMEM with 10% FBS and 200 µg/ml gentamicin.

2.7 Cell culture

HeLa cells (human cervical adenocarcinoma cells) were used in this study. The cells were handled in a sterile environment under a laminar flow hood. Sterile buffers, media, solutions, glassware, reaction vessels and consumables were used throughout.

2.7.1 Media and solutions (described as mentioned by the manufacturer)

DMEM: Dulbecco's Modified Eagle medium containing Earle's Salts, 1g/l D-glucose, L-glutamine and pyruvate.

Hank's balanced salt solution (HBSS): without Ca^{2+}, Mg^{2+} and phenol red.

Opti-MEM I: Reduced serum Eagle's minimum essential medium with HEPES, sodium bicarbonate, hypoxanthine, thymidine, sodium pyruvate, L-glutamine, trace elements and growth factors.

FBS: 100% foetal bovine serum, inactivated at 56°C for 30 min.

Trypsin/EDTA: 1x trypsin/EDTA; 0.05% / 0.02% (w/v) in PBS; without Ca^{2+} and Mg^{2+}.

PBS: 1x PBS; without Ca^{2+} and Mg^{2+}.

Freeze-down medium: 90% FBS, 10% DMSO.

2.7.2 Culture of HeLa cells

HeLa cells were maintained in 10 cm plates containing DMEM with 10% FBS at 37°C in a humidified atmosphere. They were split every alternate day or whenever they attained 80–90% confluency. For this, they were washed once with HBSS and trypsinized until detachment from the plate. DMEM with 10% FBS was added to stop the enzymatic action of trypsin, and the cells were then transferred into new cell culture dishes containing the fresh medium.

2.7.3 Storage of HeLa cells

The cells were trypsinized and centrifuged at 1200 rpm for 2 min at RT. The cell pellet was resuspended in the freeze-down medium and transferred to cryovials. The cryovials were cooled-down in a freezing container filled with isopropanol at a cooling rate of 1°C per min; they were then stored at -80°C.

To recover frozen HeLa cells, they were thawed at 37°C and transferred to 10 cm cell culture dishes containing 9 ml of fresh medium with 10% FBS. When the cells had attached to the bottom of the dishes, their medium was changed and the cells were incubated at 37°C until they were 80–90% confluent.

2.7.4 Cell plating for transfections

HeLa cells were plated 16–18h prior to DNA transfections, and 5–10 min before siRNA transfections. The cells were trypsinized as mentioned in the section 2.7.2, and resuspended in the fresh medium. For DNA transfections, $1.4x10^5$ cells were plated in 24-well plates, and for siRNA transfections, 1.6–

$1.7x10^5$ cells were plated in 12-well plates. The cells were then incubated at 37°C. In case of DNA transfections, the cells were washed five-times with HBSS and the medium was changed to DMEM without FBS prior to transfection.

2.7.5 Cell preparation for infection assays

HeLa cells were plated at a concentration of $6x10^5$ cells per well in 2 ml of the medium in 6-well plates, 18–20h prior to infection, as described in section 2.7.4. On the day of infection, the cells were washed once with HBSS and the fresh medium was added. The cells were then incubated at 37°C for 2h. Later, the cells were washed three-times with HBSS and the medium was changed to DMEM containing 0.5% FBS. The cells were then ready to be infected.

2.8 Transfection of cells

HeLa cells were transfected either with DNA or siRNA. The protocols are described below.

2.8.1 DNA transfection

The plasmid DNA (4.75 µg/well for a 6-well plate and 0.95 µg/well for a 24-well plate; Table 2.8.1) was diluted in Opti-MEM I medium. Lipofectamine 2000 (15 µl for a 6-well plate and 3 µl for a 24-well plate) was also diluted in Opti-MEM I medium and incubated for 5 min at RT. Equal volumes of the plasmid DNA and Lipofectamine 2000 dilutions were combined and incubated for 20 min at RT. The plasmid DNA-Lipofectamine 2000 complexes were added to the cells (300 µl for a 6-well plate and 100 µl for a 24-well plate) and incubated at 37°C for 4h. After 4h, fresh DMEM containing 10% FBS was added and the cells were incubated for 24h until infection.

Table 2.8.1: Plasmids used in this study

Plasmid	Characteristic	Source
pcDNA3.1(+)/HA-OPTN	Plasmid expressing wild-type HA-tagged OPTN	Wild *et al.* (2011)
pcDNA3.1-TBK1-myc-His_6	Plasmid expressing wild-type Myc-His_6–tagged mouse TBK1	Wild *et al.* (2011)
pcDNA3.1-TBK1-myc-His_6 KM	Plasmid expressing Myc-His_6-tagged mouse TBK1, K38 mutated to arginine; kinase-binding deficient	Wild *et al.* (2011)
pEGFP-C1-OPTN	Plasmid expressing GFP-tagged OPTN	Wild *et al.* (2011)
pEGFP-C1-OPTN E478G	Plasmid expressing GFP-tagged OPTN with E478 mutated to glycine	Wild *et al.* (2011)
pEGFP-C1-OPTN F178A	Plasmid expressing GFP-tagged OPTN with F178 mutated to alanine	Wild *et al.* (2011)
pRK5	Empty vector	BD Biosciences; Heidelberg, Germany

2.8.2 siRNA transfection

1.6–1.7x10^5 HeLa cells per well (12-well plate) were plated in DMEM containing 10% FBS, shortly before transfection and incubated at 37°C. The siRNA and the HiPerFect reagent were diluted in DMEM (Table 2.8.2) and incubated for 5 min at RT to allow the formation of transfection complexes. The transfection complexes were added drop-wise to the cells and incubated at 37°C for 48h. siRNA transfections were performed by Dr. Helena Pillich. The knockdown was validated by Western blotting of lysed cells.

Table 2.8.2: siRNAs used in this study

siRNA	siRNA conc. (nM)	HiPerFect volume (µl)	Catalogue number	Manufacturer
OPTN	10	3	SI00132020	Qiagen
NDP52	5	1.5	SI04325755	Qiagen
NBR1	5	1.5	SI03035186	Qiagen
SQSTM1	10	3	SI03089023	Qiagen
TAX1BP1	10	1.5	SI02781268	Qiagen
MAP1LC3B	5	1.5	SI02655597	Qiagen
ATG5L	20	3	SI02655310	Qiagen
Negative control	same as target gene	same as target gene	1022076	Qiagen
Positive control	5	3	1027298	Qiagen

2.9 Propagation of plasmids

Plasmids obtained from respective sources were propagated for long-term usage as described below.

2.9.1 Preparation of electrocompetent *E. coli*

An overnight culture of *E. coli* Top 10 was diluted 1:50 in LB medium and cultured to an OD_{600} of 0.5–0.6. The culture was centrifuged at 5000 rpm for 8 min at 4°C. The pellet was resuspended in 50 ml of cold 10% glycerol and centrifuged again at 5000 rpm for 8 min at 4°C. After such washing with cold 10% glycerol twice, the pellet was finally resuspended in 500 µl of cold 10% glycerol and stored in aliquots of 50 µl at -80°C.

2.9.2 Transformation of *E. coli* by electroporation

An aliquot of electrocompetent *E. coli* Top 10 was mixed with 500 ng of plasmid DNA, the mixture transferred to a pre-cooled electroporation cuvette (0.1 cm, Invitrogen) and electroporation was performed at 1.8 kV, 200 Ω and 25µF. The transformed bacteria were immediately transferred to 500 µl of SOB medium and incubated at 180 rpm, 37°C for 1h. The transformed bacteria were plated on LB plates containing the appropriate antibiotic and incubated at 37°C, overnight.

2.9.3 Plasmid isolation from *E. coli*

Plasmids were isolated using the Midi plasmid isolation kit (Qiagen, Hilden, Germany). An overnight culture of transformed *E. coli* (containing the appropriate antibiotic) was centrifuged at 6000 rpm for 15 min at 4°C to harvest bacterial cells. The pellet was resuspended in 6 ml of P1 buffer (resuspension buffer) containing RNase, mixed vigorously with 6 ml of P2 buffer (lysis buffer) and incubated for 5 min at RT. After this, 6 ml of P3 buffer (neutralization buffer) was added to the lysate, mixed thoroughly and centrifuged at 6000 rpm for 10 min at RT. The lysate was poured into the barrel of the QIA filter cartridge and incubated for 10 min at RT in order to remove proteins and genomic DNA. The lysate was then filtered through a HiSpeed column (containing an anion-exchange resin) equilibrated with 4 ml of QBT buffer (equilibration buffer). The HiSpeed column was washed with 20 ml of QC buffer (wash buffer) to remove contaminants and the flow through was discarded. Plasmid DNA was eluted with 5 ml of QF buffer (elution buffer), precipitated with 3.5 ml of isopropanol and incubated for 5 min at RT. Plasmid DNA was centrifuged at 6000 rpm for 30 min at 4°C, washed twice with 2 ml ethanol, air-dried for 5–10 min and re-dissolved in 50 µl of mQ water. It was then stored at -20°C.

2.9.4 Measurement of plasmid DNA concentration

The measuring point of the NanoDrop spectrophotometer was cleaned with RNase free water and 1.2 µl of mQ water was used to make a blank

measurement. The measuring point was cleaned again, 1.2 µl of plasmid DNA was loaded and its concentration was measured.

2.9.5 Agarose gel electrophoresis of plasmid DNA

The quality of the isolated plasmid DNA was assessed by agarose gel electrophoresis. Agarose gel (0.8%) was prepared by dissolving agarose in 1X TE buffer; it was boiled for 2 min with shaking at intervals, cooled to 60°C and poured in the gel tray. A plastic comb was inserted to enable the formation of sample wells and the gel was allowed to polymerize at RT. The comb was removed and the gel tray was placed in an electrophoresis tank filled with 1X TE buffer. The plasmid DNA samples were diluted in water and sample buffer was added to them. They were cooled on ice and loaded into the sample wells of the agarose gel. Electrophoresis was performed at 80V, 150 mA for 30–40 min. The agarose gel was stained with ethidium bromide for 2–3 min and de-stained in TE buffer for 1 min. It was then visualized using the gel-doc imaging system (Bio-Rad, Hercules, CA, USA).

2.10 Determination of bacterial numbers

Both intracellular and extracellular bacteria were plated as described below.

2.10.1 Intracellular bacteria

At specific time-points following infection, HeLa cells were washed thrice with PBS in order to remove any residual gentamicin, and lysed with 1 ml of cold water containing 0.2% Triton X-100 for 20 min at RT. Cell lysis was observed by light microscopy and serial dilutions of bacteria (in PBS) were plated on BHI (*L. monocytogenes*) or LB (*S.* Typhimurium) agar plates. The plates were then incubated at 37°C for 18–24h.

2.10.2 Extracellular bacteria

An adequate volume of bacteria used for infection was added in DMEM and incubated for 1h at 37°C in 5%CO_2-air atmosphere. After 1h, the bacteria

were serially diluted in PBS, and plated on BHI agar plates. The plates were then incubated at 37°C for 18–24h.

2.11 Preparation of HeLa cell lysates

2.11.1 Cell lysis

Following infection, HeLa cells were scraped in the medium, transferred to microcentrifuge tubes, and centrifuged at 700 rcf for 2 min at 4°C. The cell pellet was washed twice with ice cold PBS (RIPA) or cell wash buffer (CHAPS) and resuspended in RIPA or CHAPS (Protein simple) cell lysis buffer. The cells were lysed at 300 rpm for 30 min at 4°C on a thermomixer. The lysates were centrifuged at 16000 rcf for 10 min at 4°C, and the supernatant was stored at -20°C (RIPA) or -80°C (CHAPS).

2.11.2 Determination of protein concentration

The bicinchoninic acid (BCA) assay (Sigma Aldrich, St. Louis, MO, USA) was employed to measure the total protein content in the cell lysates. A standard curve was constructed using BSA as a standard. The lysates were diluted in RIPA or CHAPS, and 6.25 µl of the diluted lysates were transferred to a 96-well plate. BCA solution was combined with copper (II) sulphate solution at a 1:50 ratio and 50 µl from this mixture were added to the BSA standard and diluted lysates, incubated at 37°C for 30 min and the absorbance was measured at 562 nm using a plate reader (Phomo, Autobio labtec, Zhengzhou, China).

2.12 Measurement of cell viability

MTT [3-(4,5-dimethylthiazol-2-yl)-2,5-diphenyltetrazolium bromide] assay was used to determine the viability of cells following infection. MTT solution was prepared by adding 5 mg MTT to 1 ml of PBS. This MTT solution was further diluted 1:10 in DMEM containing 10% FBS and 50 µg/ml gentamicin. After 4h

of infection, the cells were washed with PBS and incubated with either 500 µl (24-well plate) or 1 ml (12-well plate) of the diluted MTT solution at 37°C in 5% CO_2-air atmosphere for 2h. Afterwards, MTT solution was removed and stopping solution, consisting of 5% formic acid in isopropanol, was added to the cells. The plate was incubated on a plate shaker for 1 min at RT. The solution (100 µl) from each well was added in triplicates to a 96-well plate and absorbance was measured at 562 nm.

2.13 Separation of proteins by SDS-PAGE

Sodium dodecyl sulfate polyacrylamide gel electrophoresis (SDS-PAGE) is a technique which is employed to separate proteins based on their ability to move in an electrical field, which is a function of the length of their polypeptide chains or of their molecular weight. SDS, an anionic detergent, is used which coats the proteins, proportional to their molecular weight and, confers the same negative electrical charge across all proteins in the sample and thereby removes secondary and tertiary protein structures.

The Laemmli gel system used in SDS-PAGE consists of tris-glycine gels comprised of two gels (Laemmli, 1970). The first is the stacking gel to focus the proteins into sharp bands at the beginning of the electrophoretic run and the second is the resolving gel where different acrylamide gel percentages are used to separate the proteins based on their molecular weight. A discontinuous buffer system is used for electrophoresis.

The resolving gel was prepared as per Table 2.13, poured between two glass plates and allowed to polymerize at RT. A small volume (400–500 µl) of 70% ethanol was also poured above the resolving gel to produce a smooth, completely level surface on top of the gel, so that bands were straight and uniform. After the resolving gel was polymerized, the ethanol was drained and the stacking gel (Table 2.13) was poured on top of it. A plastic comb was inserted to enable the formation of sample wells and the gel was allowed to polymerize at RT. Later, the comb was removed and the gel cassette was

placed in the electrophoresis chamber filled with 1x SDS running buffer. The samples were denatured in SDS sample buffer at 99°C for 5 min, cooled on ice, centrifuged at 16000 rcf for 1 min at RT and loaded in the sample wells of the gel. Electrophoresis was performed at 125 V till the samples crossed the stacking gel, and thereafter at 150 V.

Table 2.13: Composition of resolving and stacking gels (values are for one gel; 1 mm thick)

Components	10% resolving gel	17% resolving gel	5.7% stacking gel
ddH_2O	2.72 ml	1.52 ml	1.8 ml
Tris HCl (pH 8.8; 1.5 M)	1.67 ml	1.67 ml	-
Tris HCl (pH 6.8; 0.5 M)	-	-	835 µl
Polyacrylamide 30%	2.15 ml	3.9 ml	635 µl
SDS 10%	66.65 µl	66.65 µl	33.35 µl
TEMED*	3.34 µl	5 µl	1.15 µl
APS 10%*	50 µl	50 µl	33.35 µl

* to be added immediately before use

2.14 Western blotting

Western blotting is an analytical method that involves the immobilization of proteins on a membrane, followed by their detection using monoclonal or polyclonal antibodies (Towbin *et al.*, 1979).

Fifteen sheets of filter paper (Whatman-3MM) and the PVDF transfer membrane were cut according to the size of the gel. Six sheets of filter paper were moistened in blotting solution I and III, and three sheets were

moistened in blotting solution II. The PVDF membrane was activated in methanol for 2–3 s and then immersed in water for 1–2 min, followed by moistening in blotting solution II. The SDS-PAGE gel was also immersed in blotting solution II. A blotting sandwich was then assembled in the transfer chamber as follows: the six sheets of filter paper immersed in blotting solution I were placed on the anode side of the transfer chamber. On top of this, the three sheets immersed in blotting solution II were placed, followed by the activated PVDF membrane. The SDS-PAGE gel was placed on top of the PVDF membrane. Finally, the six sheets of filter paper immersed in blotting solution III were placed on top of it. Bubbles were removed by rolling a glass pipette over the transfer sandwich. The transfer apparatus was closed by placing the cathode lid over the transfer sandwich. The transfer was performed at the rate of 1 mA/cm^2 for 1.5h. After the transfer was complete, the pre-stained protein ladder bands were marked on the PVDF membrane using a pen.

The PVDF membrane was blocked with 5% non-fat dry milk in TBS-T (TBS with 0.1% Tween-20) for 1h at RT or overnight at 4°C. It was incubated with the primary antibody (Table 2.3) diluted either in 5% non-fat dry milk in TBS-T or 5% BSA in TBS-T, overnight at 4°C or for 2h at RT. The membrane was then washed thrice with TBS-T and incubated with the secondary IgG-horseradish peroxidase-conjugated antibody (Table 2.3) for 1h at RT.

Enhanced chemiluminescence (ECL) method was used for the development of blots. It consists of a stable peroxide solution and an enhanced luminol solution. When equal volumes of the two components are mixed together and incubated with a blot on which HRP-conjugated antibodies are bound, the chemical reaction produces light that can be detected by the film. The membrane was incubated with the ECL mixture for 1 min and was placed between the two transparent foils of a hypercassette. In the dark, the hyperfilm was placed on the transparent foils in the hypercassette, incubated for varying periods of time and developed.

Membranes were stripped using Millipore Re-Blot Plus Strong Antibody Stripping Solution (diluted 1:10 in water) for 15 min at RT, washed with TBS-T, blocked using 5% non-fat dry milk in TBS-T and a second immune and substrate reaction was performed.

2.15 Immunofluorescence

At the indicated times following infection, the medium of the cells on coverslips was aspirated and they were washed three-times with PBS. The cells were fixed using 3.7% formaldehyde in PBS for 10 min at RT. Fixed cells could be stored in PBS at 4°C.

The cells fixed on coverslips were incubated with immunofluorescence buffer for 1h at RT, and were then placed in an incubation chamber consisting of parafilm placed on moist blotting paper. The cells were incubated with primary antibody (diluted in immunofluorescence buffer as per Table 2.3) at 4°C, overnight. The following day, the coverslips were washed three-times with the immunofluorescence buffer to remove the excess primary antibody. Alexa Fluor-conjugated secondary antibody was diluted to a 1:1000 concentration in immunofluorescence buffer, added to the cells in the same manner as the primary antibody and incubated for 2h at 37°C. The coverslips were washed three-times with immunofluorescence buffer and dried of excess liquid. They were mounted on glass slides using ProLong Gold Antifade containing DAPI with the cells facing down. DAPI is a fluorescent stain which binds to A-T rich regions in DNA and is, therefore, used to label nuclei. Slides were stored in the dark at 4°C and imaged by confocal microscopy (Leica microsystems, Wetzlar, Germany). Quantification was done by counting the number of bacteria which co-localized with the target molecule.

2.16 Statistical analysis

The data are shown as mean +/- standard deviation (SD) from at least three independent experiments. The statistical analysis toolkit included in the Microsoft Office Excel 2010 software package was used to test variances between experimental groups and run the *t*-test. The 2-tailed, unpaired *t*-test was used to check for significant differences between the groups.

III. Results

3.1 Depletion of LC3 and ATG5 results in increased intracellular growth of Lm EGD-e and LmΔ*actA2*

It is known that a small percentage of cytosolic wild-type *L. monocytogenes* is trapped in the autophagosome, but a greater percentage is able to escape autophagy, as the ActA protein helps disguise the bacterium as a host cell organelle due to the accumulation of the actin core motility machinery on its surface. LmΔ*actA2* is a mutant of the wild type EGD-e strain, which lacks the critical regions required for actin-based motility (aa 20–602), namely the Arp2/3 complex-binding region, the vasodilator-stimulating phosphoprotein (VASP) binding domain and the actin binding region and is, therefore, unable to evade autophagy (Yoshikawa *et al.*, 2009).

To investigate if the intracellular growth of Lm EGD-e and LmΔ*actA2* is affected when the autophagy machinery itself is compromised, the autophagy markers LC3 and ATG5 were knocked down in HeLa cells using siRNA and the cells were infected with Lm EGD-e and LmΔ*actA2* for 4h. The knockdown of LC3 and ATG5 was confirmed by Western blotting (Fig. 3.1 a and Fig. 3.2 a, respectively; the established knockdown of LC3 and ATG5 of one experiment each is shown). Infection of LC3 siRNA-transfected HeLa cells with Lm EGD-e and LmΔ*actA2* led to an increase in the intracellular growth of both these bacteria, as compared to infection of control siRNA-transfected cells (Fig. 3.1 b). An increase was also observed in the intracellular growth of both Lm EGD-e and LmΔ*actA2*, in ATG5-depleted cells, as compared to non-depleted cells (Fig. 3.2 b). Moreover, there was no significant difference between the intracellular numbers of Lm EGD-e and LmΔ*actA2* in control siRNA-treated cells (Fig. 3.1 b and 3.2 b). In order to rule out the possibility that the above difference in bacterial numbers could have been caused by cell death resulting from the infection of siRNA-transfected cells, MTT assay was performed to measure the viability of HeLa cells after transfection and infection, in comparison to the viability of transfected, but uninfected cells. As shown in Fig. 3.1 c and 3.2 c, 85–95% viability was seen in all groups of transfected and infected cells.

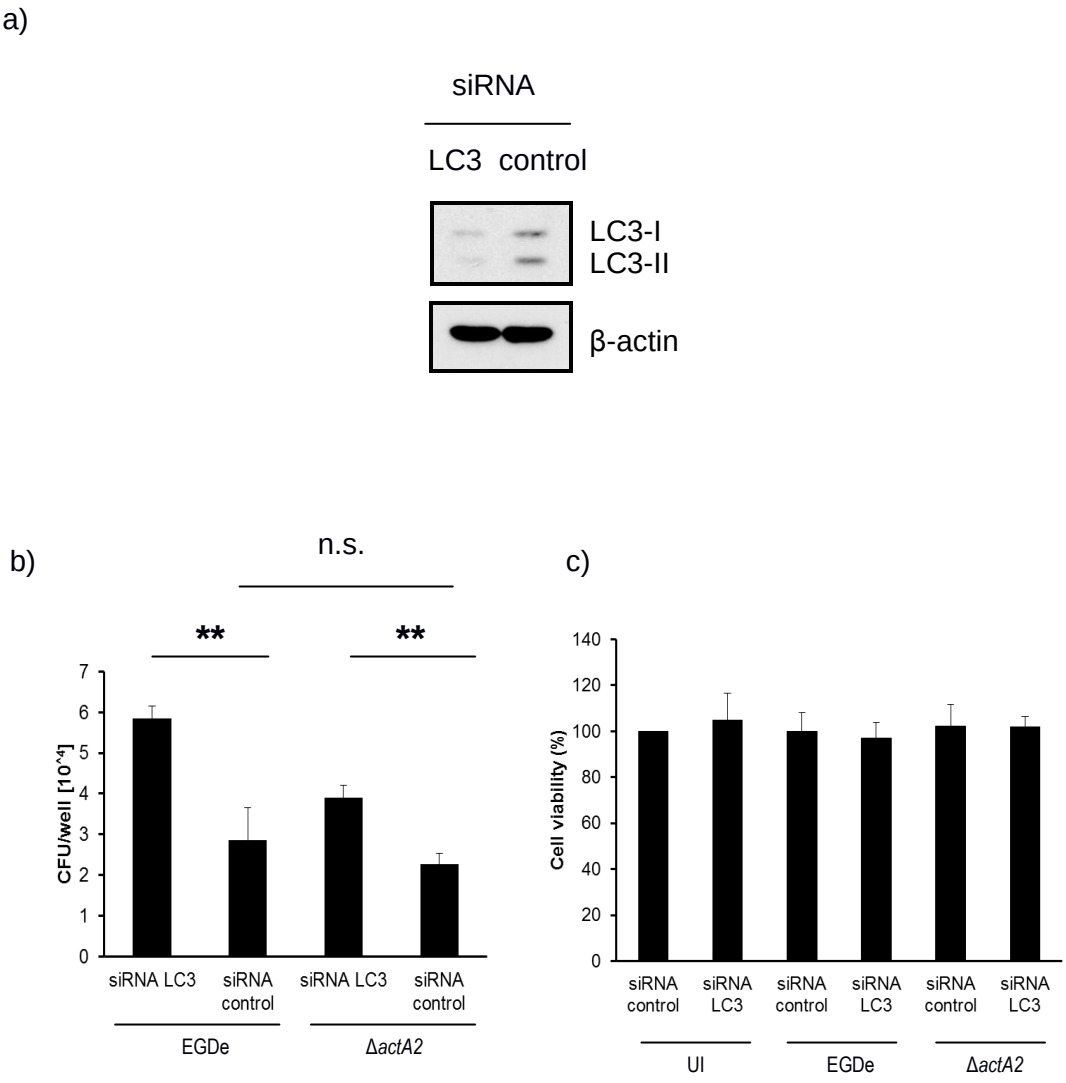

Fig. 3.1: Depletion of LC3 increases the intracellular growth of Lm EGD-e and Lm*ΔactA2*. a) Western blotting of HeLa cells transfected with LC3 and control siRNA, showing LC3 knockdown. β-actin was used as a loading control. **b)** HeLa cells were transfected with LC3 siRNA and infected with Lm EGD-e and Lm*ΔactA2* for 4h. Gentamicin (50 µg/ml) was added 1h p. i. to eliminate the extracellular bacteria. The intracellular bacteria were plated. The results are expressed as CFU per well. Each bar represents the mean value + SD of three independent experiments performed in triplicates (** $p < 0.01$; n.s.: not significant). **c)** LC3 was knocked down in HeLa cells and they were infected with Lm EGD-e and Lm*ΔactA2* for 4h. Gentamicin (50 µg/ml) was added 1h p. i. to eliminate the extracellular bacteria. The cells were incubated with MTT solution for 2h. The reaction was stopped by adding isopropanol containing 5% formic acid and the cell viability was measured by absorbance at 562 nm. The results are expressed as percent cell viability. Each bar represents the mean value + SD of three independent experiments performed in triplicates. UI: uninfected cells.

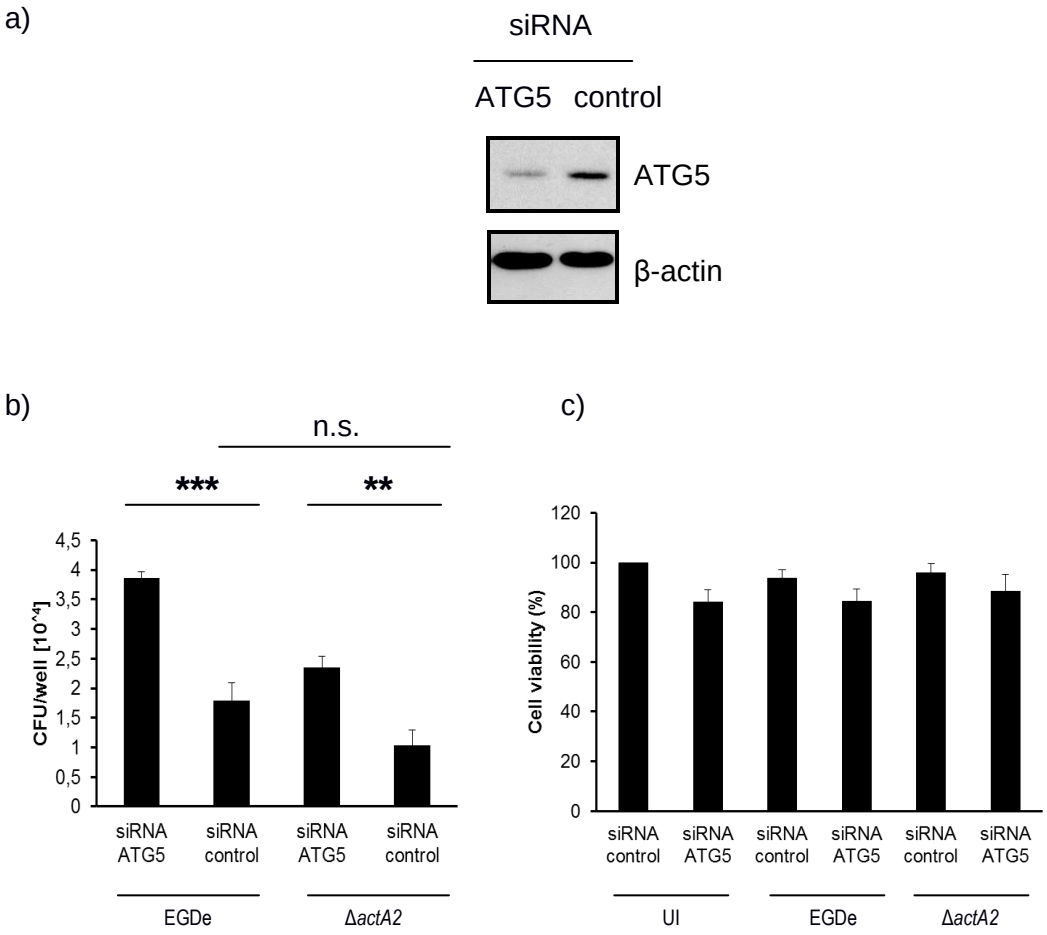

Fig. 3.2: Depletion of ATG5 increases the intracellular growth of Lm EGD-e and LmΔ*actA2*. a) Western blotting of HeLa cells transfected with ATG5 and control siRNA, showing ATG5 knockdown. β-actin was used as a loading control. **b)** HeLa cells were transfected with ATG5 siRNA and infected with Lm EGD-e and LmΔ*actA2* for 4h. Gentamicin (50 µg/ml) was added 1h p. i. to eliminate the extracellular bacteria. The intracellular bacteria were plated. The results are expressed as CFU per well. Each bar represents the mean value + SD of three independent experiments performed in triplicates (** $p < 0.01$; *** $p < 0.001$; n.s.: not significant). **c)** ATG5 was knocked down in HeLa cells and they were infected with Lm EGD-e and LmΔ*actA2* for 4h. Gentamicin (50 µg/ml) was added 1h p. i. to eliminate the extracellular bacteria. The cells were incubated with MTT solution for 2h. The reaction was stopped by adding isopropanol containing 5% formic acid and cell viability was measured by absorbance at 562 nm. The results are expressed as percent cell viability. Each bar represents the mean value + SD of three independent experiments performed in triplicates. UI: uninfected cells.

3.2 SQSTM1 is an autophagy adaptor for *L. monocytogenes*

SQSTM1, commonly known as p62, was the first autophagy adaptor to be identified. It has been published that SQSTM1 is recruited to ubiquitinated LmΔ*actA2*, which delivers it to the autophagosome for its degradation

(Yoshikawa *et al.*, 2009). The following experiments were performed to elaborate these previous findings.

3.2.1 SQSTM1 is recruited to Lm EGD-e and LmΔ*actA2*

It has been shown in MDCK (Madine-Darby canine kidney) cells that SQSTM1 co-localizes with LmΔ*actA2* (Yoshikawa *et al.*, 2009). To establish the protocol for HeLa cells, they were infected with Lm EGD-e and LmΔ*actA2* for 4h, and immunofluorescence analysis was done to analyse the co-localization of SQSTM1 with both these bacterial strains. As shown in Fig. 3.2.1, both Lm EGD-e and LmΔ*actA2* co-localized with SQSTM1. Moreover, because LmΔ*actA2* are non-motile, they clumped together in the cytosol, whereas Lm EGD-e, which are capable of intracellular movement, did not form clumps. Additionally, it could also be seen that despite the fact that LmΔ*actA2* are known to be heavily ubiquitinated, only a part of the LmΔ*actA2* population was associated with SQSTM1.

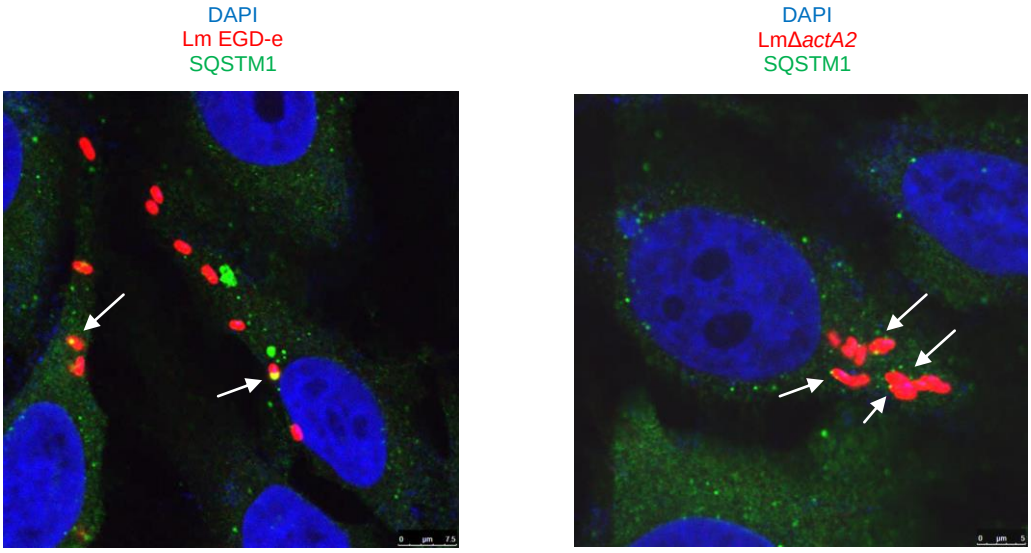

Fig. 3.2.1: SQSTM1 is recruited to Lm EGD-e and LmΔ*actA2*. HeLa cells were infected with Lm EGD-e and LmΔ*actA2* for 4h. Gentamicin (50 µg/ml) was added 1h p.i. to eliminate the extracellular bacteria. The cells were fixed, permeabilized and stained with anti-SQSTM1 (green) and anti-Lm (red). Nuclei were stained with DAPI (blue). Arrows indicate co-localization of Lm with SQSTM1.

3.2.2 The depletion of SQSTM1 results in increased intracellular growth of Lm EGD-e, but decreased growth of Lm**Δ*actA2***

Yoshikawa *et al.* (2009) have demonstrated that the rate of the intracellular survival of Lm**Δ***actA2* is equal to that of Lm EGD-e in *sqstm1*$^{-/-}$ MEFs. To see if this is also the case in HeLa cells, they were depleted of SQSTM1 using siRNA. The knockdown of SQSTM1 was confirmed by Western blotting of the siRNA lysates (Fig 3.2.2 a; the established knockdown of SQSTM1 of one experiment is shown). Infection of SQSTM1 siRNA-transfected HeLa cells with Lm EGD-e resulted in an increase (2-fold) in the intracellular bacterial growth in comparison to infection of control siRNA-transfected HeLa cells. Surprisingly, a decline (1.9-fold) in the intracellular growth of Lm**Δ***actA2* (although not significant), was observed in SQSTM1-depleted cells, as compared to non-depleted cells. Also, no significant difference could be observed between the intracellular numbers of Lm EGD-e and Lm**Δ***actA2* in control siRNA-treated cells (Fig. 3.2.2 b). It could be possible that the infection of siRNA-transfected cells could have led to cell death, resulting in the above findings. Therefore, as control, MTT assay was performed to measure the viability of HeLa cells after transfection and infection, in comparison to the viability of transfected, but uninfected cells. As shown in Fig. 3.2.2 c, the above findings were not a result of the loss of cell viability.

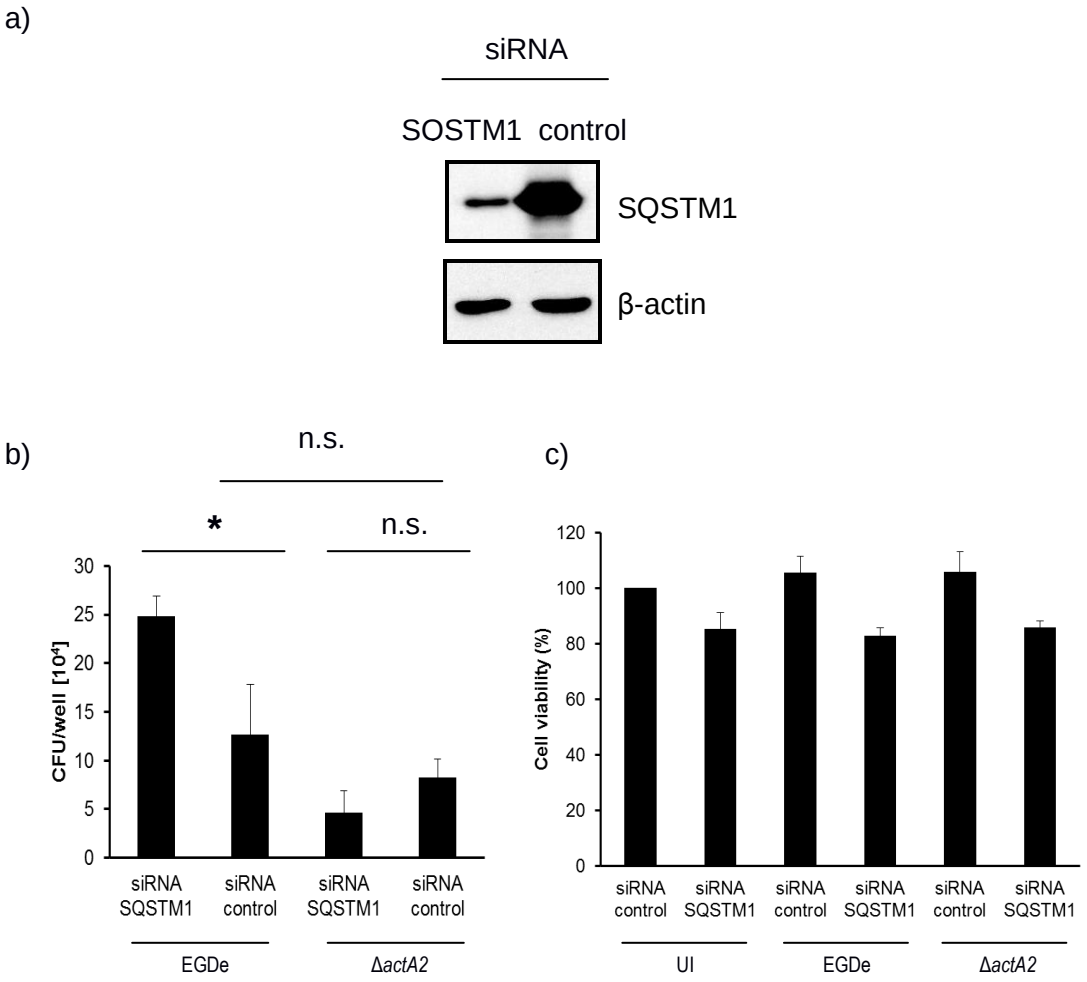

Fig. 3.2.2: The depletion of SQSTM1 increases the intracellular growth of Lm EGD-e but decreases that of Lm*ΔactA2*. a) Western blotting of HeLa cells transfected with SQSTM1 and control siRNA, showing SQSTM1 knockdown. β-actin was used as a loading control. **b)** SQSTM1 was knocked down in HeLa cells and they were infected with Lm EGD-e and Lm*ΔactA2* for 4h. Gentamicin (50 µg/ml) was added 1h p.i. to eliminate the extracellular bacteria. The intracellular bacteria were plated. The results are expressed as CFU per well. Each bar represents the mean value + SD of at least three independent experiments performed in triplicates (* $p < 0.05$; n.s.: not significant). **c)** SQSTM1 was knocked down in HeLa cells and they were infected with Lm EGD-e and Lm*ΔactA2* for 4h. Gentamicin (50 µg/ml) was added 1h p.i. to eliminate the extracellular bacteria. The cells were incubated with MTT solution for 2h. The reaction was stopped by adding isopropanol containing 5% formic acid and cell viability was measured by absorbance at 562 nm. The results are expressed as percentage cell viability. Each bar represents the mean value + SD of at least three independent experiments performed in triplicates. UI: uninfected cells.

3.2.3 SQSTM1 knockdown leads to decreased intracellular growth of LmΔ*actA2*, LmΔ*actA16* and LmΔ*actA21*

Because a decrease in the intracellular growth of LmΔ*actA2* after SQSTM1 depletion was observed, the following experiment was performed to find out if differently ubiquitinated LmΔ*actA* strains also show the same results. For this, two ActA mutants were selected: i) LmΔ*actA16*, which is motile (but relatively less motile than Lm EGD-e) and lacks the Arp2/3 complex binding region and, ii) LmΔ*actA21*, which is non-motile and lacks the actin binding region, the Arp2/3 complex binding region and the VASP binding region (Fig 3.2.3 and Table 3.2.3; Yoshikawa *et al.*, 2009). Thus, out of all the four strains, Lm EGD-e is the least ubiquitinated, followed by LmΔ*actA16*, and finally LmΔ*actA2* and LmΔ*actA21* are the most ubiquitinated (Yoshikawa *et al.*, 2009).

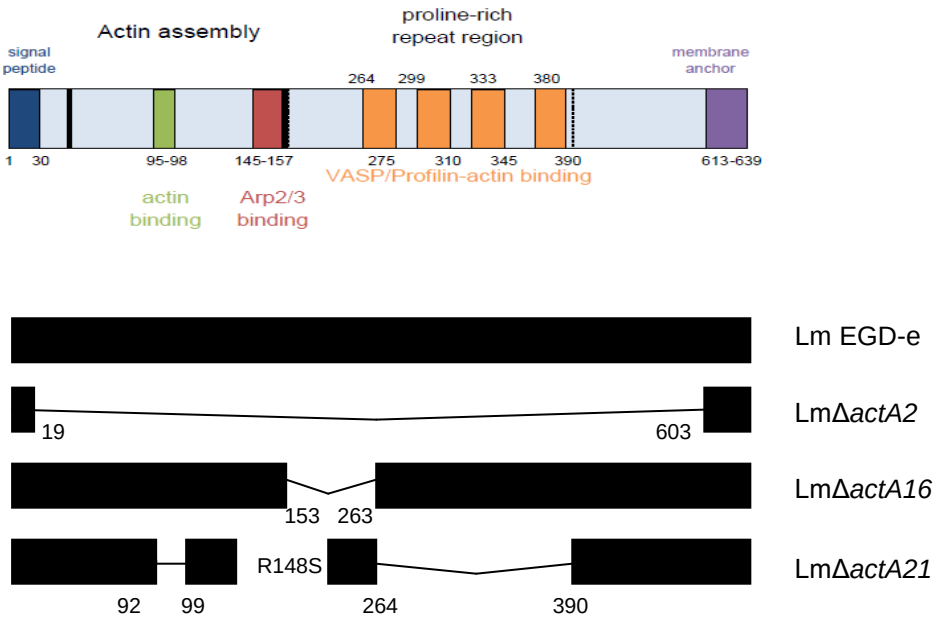

Fig. 3.2.3: Structure of Lm EGD-e, LmΔ*actA2*, LmΔ*actA16* and LmΔ*actA21* actin domains, showing amino acid deletions and substitutions (adapted from Yoshikawa *et al.*, 2009)**.**

Table 3.2.3: Characteristics of the different Lm strains used (adapted from Yoshikawa *et al.*, 2009)

Strain	Motility	Arp 2/3	VASP	Ubiquitination	C-terminal
Lm EGD-e	++	+	+	+	+
LmΔ*actA2*	-	-	-	+++	-
LmΔ*actA16*	+	-	+	++	+
LmΔ*actA21*	-	-	-	+++	+

The HeLa cells depleted of SQSTM1 were infected with Lm EGD-e, LmΔ*actA2*, LmΔ*actA16* and LmΔ*actA21* for 4h. Again, an increase (1.6-fold) in the intracellular Lm EGD-e was observed in HeLa cells transfected with SQSTM1 siRNA, as compared to those transfected with control siRNA (Fig. 3.2.4). On the other hand, a decline in the intracellular growth of LmΔ*actA2* (1.8-fold), LmΔ*actA16* (1.4-fold) and LmΔ*actA21* (1.6-fold) was observed in SQSTM1-depleted cells, as compared to non-depleted cells (Fig. 3.2.4). This decline in the intracellular growth in SQSTM1-depleted cells was significant in the case of LmΔ*actA2* ($p < 0.05$) and LmΔ*actA21* ($p < 0.05$), but not for LmΔ*actA16*. Again, as observed previously, the intracellular numbers of Lm EGD-e, *LmΔactA2* and LmΔ*actA16* in control siRNA-treated cells were similar. However, an unexpectedly high number of intracellular LmΔ*actA21* was observed in both SQSTM1 siRNA-transfected (15*10^5 cfu per well) and non-transfected cells (35*10^5 cfu per well).

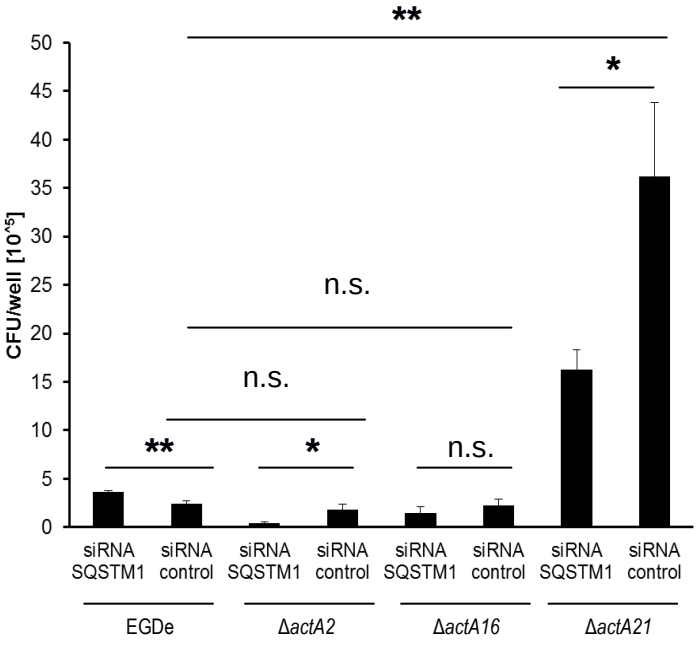

Fig. 3.2.4: The knockdown of SQSTM1 decreases the intracellular growth of LmΔ*actA2*, LmΔ*actA16* and LmΔ*actA21*. HeLa cells were transfected with SQSTM1 siRNA and were infected with Lm EGD-e, LmΔ*actA2*, LmΔ*actA16* and LmΔ*actA21* for 4h. Gentamicin (50 µg/ml) was added 1h p. i. to eliminate the extracellular bacteria. The intracellular bacteria were plated out. The results are expressed as CFU per well. Each bar represents the mean value + SD of at least three independent experiments performed in triplicates (* $p < 0.05$; ** $p < 0.01$; n.s.: not significant).

3.3 NDP52 is an autophagy cargo receptor for *L. monocytogenes*

NDP52 has been associated with the autophagy of *S.* Typhimurium (Thurston *et al.*, 2009), *S. flexneri* (Mostowy *et al.*, 2011) and *L. monocytogenes* (Mostowy *et al.*, 2011). The following experiments were performed to build upon these findings related to *L. monocytogenes* and NDP52.

3.3.1 NDP52 is recruited to Lm EGD-e and LmΔ*actA2*

Prior to determining the role of NDP52 in the autophagy of *L. monocytogenes*, it was essential to observe the recruitment of NDP52 to intracellular *L. monocytogenes*. For this, HeLa cells were infected with Lm EGD-e and LmΔ*actA2* for 4h, and subjected to immunofluorescence microscopy. NDP52 co-localized to both Lm EGD-e and LmΔ*actA2*, which confirmed that it is recruited to both these strains (Fig. 3.3.1). As seen before, LmΔ*actA2* clumped together in the cytosol, whereas Lm EGD-e, did not. Moreover, only a part of the Lm EGD-e and LmΔ*actA2* population was associated with NDP52.

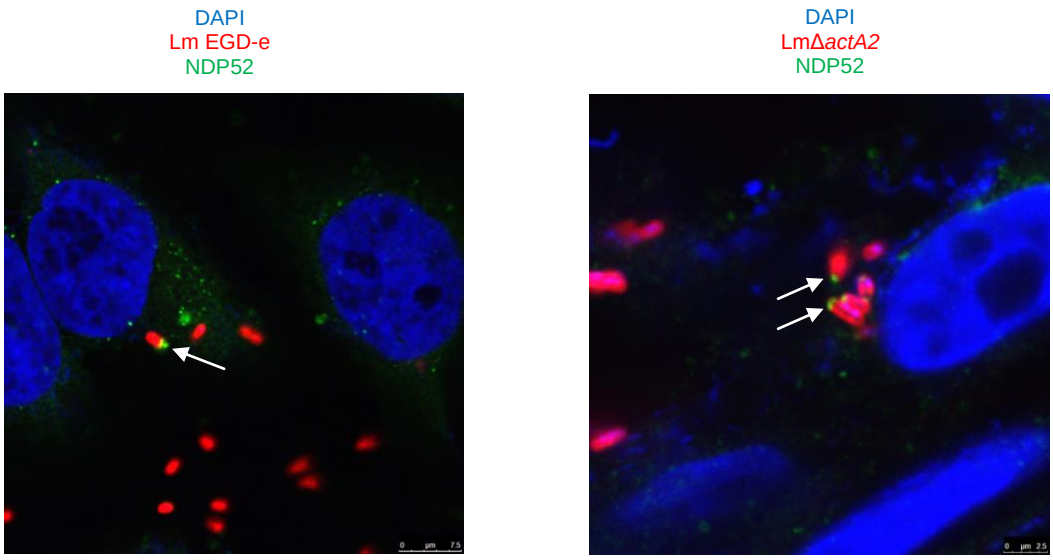

Fig. 3.3.1: NDP52 is recruited to Lm EGD-e and LmΔ*actA2*. HeLa cells were infected with Lm EGD-e and LmΔ*actA2* for 4h. Gentamicin (50 µg/ml) was added 1h p. i. to eliminate the extracellular bacteria. The cells were fixed, permeabilized and stained with anti-NDP52 (green) and anti-Lm (red). The nuclei were stained with DAPI (blue). Arrows indicate co-localization of Lm with NDP52.

3.3.2 The loss of NDP52 promotes the intracellular growth of Lm EGD-e but not that of Lm**Δ*actA2***

HeLa cells were transfected with NDP52 and control siRNA for 48h and infected with Lm EGD-e and Lm*ΔactA2* for 4h. NDP52 knockdown was confirmed by Western blotting (Fig. 3.3.2 a; the established knockdown of NDP52 of one experiment is shown). Infection of NDP52-depleted HeLa cells with Lm EGD-e resulted in an increase (1.4-fold) in the intracellular bacterial growth in comparison to infection of non-depleted HeLa cells (Fig. 3.3.2 b). In contrast, no difference was observed in the intracellular growth of Lm*ΔactA2* in HeLa cells transfected with NDP52 siRNA as compared to those transfected with control siRNA. Additionally, no significant difference could be observed between the intracellular numbers of Lm EGD-e and Lm*ΔactA2* in control siRNA-treated cells (Fig. 3.3.2 b). In order to rule out the possibility that the above observed difference in bacterial numbers could have been caused by cell death resulting from the infection of siRNA-transfected cells, MTT assay was performed to measure the viability of HeLa cells after transfection and infection, in comparison to the viability of transfected, but uninfected cells. As shown in Fig. 3.3.2 c, over 90% viability was seen in all groups of transfected and infected cells.

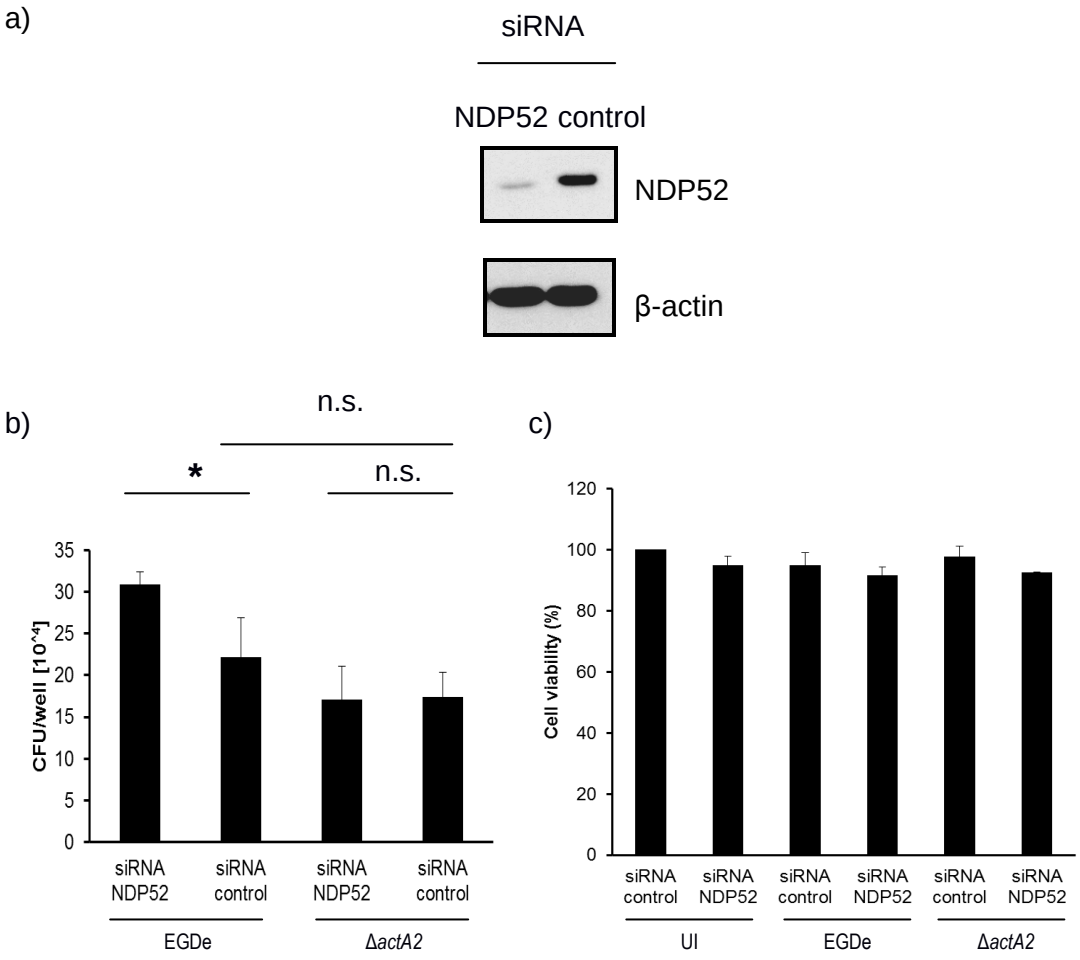

Fig. 3.3.2: NDP52 depletion increases the intracellular growth of Lm EGD-e but not that of LmΔ*actA2*. a) Western blotting of HeLa cells transfected with NDP52 and control siRNA, showing NDP52 knockdown. β-actin was used as a loading control. **b)** HeLa cells were transfected with NDP52 siRNA and infected with Lm EGD-e and LmΔ*actA2* for 4h. Gentamicin (50 µg/ml) was added 1h p. i. to eliminate the extracellular bacteria. The intracellular bacteria were plated. The results are expressed as CFU per well. Each bar represents the mean value + SD of at least three independent experiments performed in triplicates (* $p < 0.05$; n.s.: not significant). **c)** NDP52 was knocked down in HeLa cells and they were infected with Lm EGD-e and LmΔ*actA2* for 4h. Gentamicin (50 µg/ml) was added 1h p. i. to eliminate the extracellular bacteria. The cells were incubated with MTT solution for 2h. The reaction was stopped by adding isopropanol containing 5% formic acid and cell viability was measured by absorbance at 562 nm. The results are expressed as percent cell viability. Each bar represents the mean value + SD of at least three independent experiments performed in triplicates. UI: uninfected cells.

3.4 OPTN is an autophagy adaptor for *L. monocytogenes*

OPTN is a recent addition to the family of autophagy cargo receptors (Wild *et al.*, 2011). It has been reported that the phosphorylation of OPTN leads to growth restriction of *S.* Typhimurium in infected cells (Wild *et al.*, 2011). To date, apparently, there is no study on the interaction of *L. monocytogenes* with OPTN. The following experiments were aimed to investigate the role of OPTN during *L. monocytogenes* infection.

3.4.1 OPTN is phosphorylated by TBK1

TBK1 is a serine/threonine kinase which acts as an integrator of multiple signals induced by receptor-mediated pathogen detection. Wild *et al.* (2011) have reported that OPTN interacts with TBK1 *via* its ubiquitin binding domain and is phosphorylated by TBK1. To repeat this finding in our experimental settings, HeLa cells were transfected with plasmids expressing OPTN, OPTN and wild-type TBK1, or OPTN and a mutant of TBK1 with an ineffective kinase (TBK1 KM) for 24h. OPTN phosphorylation was analyzed by Western blotting. Transfection with OPTN resulted in OPTN expression, but only background phosphorylation (Fig. 3.4.1). Cells transfected with both OPTN and TBK1 showed increased OPTN phosphorylation. This was abrogated when mutated TBK1 (TBK1 KM) was co-transfected with OPTN (Fig. 3.4.1).

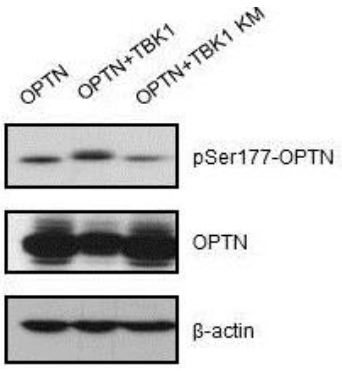

Fig.3.4.1: OPTN is phosphorylated by TBK1. HeLa cells were transfected with plasmids expressing wild-type OPTN (pcDNA3.1(+)/HA-OPTN), wild-type OPTN (pcDNA3.1(+)/HA-OPTN) and wild-type TBK1 (pcDNA3.1-TBK1-myc-His_6) or wild-type OPTN (pcDNA3.1(+)/HA-OPTN) and TBK1 kinase mutant (pcDNA3.1-TBK1-myc-His_6 KM). Cell lysates were analyzed using anti-phospho-OPTN (pSer177-OPTN) and anti-OPTN (total). β-actin was used as a loading control. The image represents three independent experiments.

3.4.2 Autophagy is induced during infection with *S.* Typhimurium, and OPTN depletion leads to the increased intracellular growth of *S.* Typhimurium

S. Typhimurium invades host cells and resides and replicates within SCVs (Jo *et al.*, 2013). A certain population of these intracellular *S.* Typhimurium becomes a target for xenophagy, after their escape from SCVs into the cytosol (Birmingham *et al.*, 2006; Jo *et al.*, 2013). It is well known that these *S.* Typhimurium are also associated with LC3 (Birmingham *et al.*, 2006; von Muhlinen *et al.*, 2012; Jo *et al.*, 2013). To establish the protocol, the induction of autophagy was monitored following *S.* Typhimurium infection. HeLa cells were infected with *S.* Typhimurium for 6h and 8h, and the extracellular bacteria were eliminated by gentamicin treatment 30 min p. i. As positive control, the cells were treated with 20 µM rapamycin, which is a potent inducer of autophagy, and with an equal amount of DMSO as negative control. LC3 conversion was observed by Western blotting. An increase in the ratio of LC3-II to LC3-I was observed at 6h and 8h p. i., which signified that infection with *S.* Typhimurium leads to the induction of autophagy (Fig. 3.4.2). Additionally, treatment of the cells with rapamycin also showed an increase in the ratio of LC3-II to LC3-I, as compared to the cells treated with DMSO.

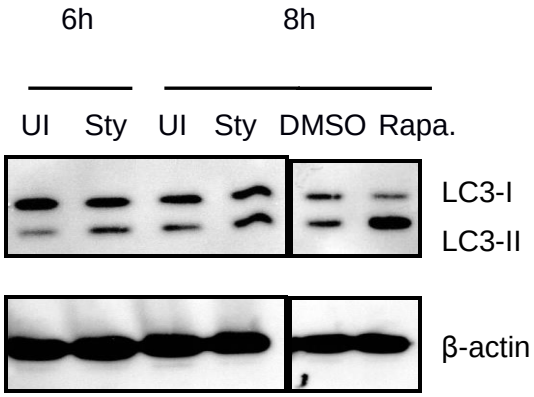

Fig. 3.4.2: *S.* Typhimurium infection induces autophagy in HeLa cells. HeLa cells were infected with *S.* Typhimurium (Sty) for 6h and 8h. Gentamicin (200 µg/ml) was added 30 min p.i. to kill the extracellular bacteria. As positive control, the cells were treated with 20 µM rapamycin (Rapa.) for 8h. The cells were treated with an equal amount of DMSO as negative control, because rapamycin was diluted in DMSO. The cells were lysed and immunoblotting was performed using anti-LC3. β-actin was used as a loading control. The image is a representative of three independent experiments. UI: uninfected cells.

It has been recently reported by Wild *et al.* (2011) that siRNA- or shRNA-mediated knockdown of OPTN in HeLa cells results in increased proliferation of *S.* Typhimurium. Prior to conducting similar experiments with *L. monocytogenes*, it was thought expedient to repeat the experiment of Wild *et al.* (2011) to establish and standardize the protocol. For this, HeLa cells were transfected with siRNA against OPTN for 48h. After 48h, the transfected cells were infected with *S.* Typhimurium 14028, another wild-type strain, for 6h and 8h, the time-points at which autophagy induction was observed. The knockdown of OPTN was confirmed by Western blotting of the siRNA lysates (Fig 3.4.3 a; the established knockdown of OPTN of one experiment is shown). A 2-fold increase in the intracellular growth of *S.* Typhimurium at 6h p.i. was observed in OPTN-depleted cells, in comparison to those treated with control siRNA (Fig. 3.4.3 b). However, the increase in the intracellular growth of *S.* Typhimurium at 8h p.i. in cells transfected with OPTN siRNA was not significant as compared to that in cells transfected with control siRNA.

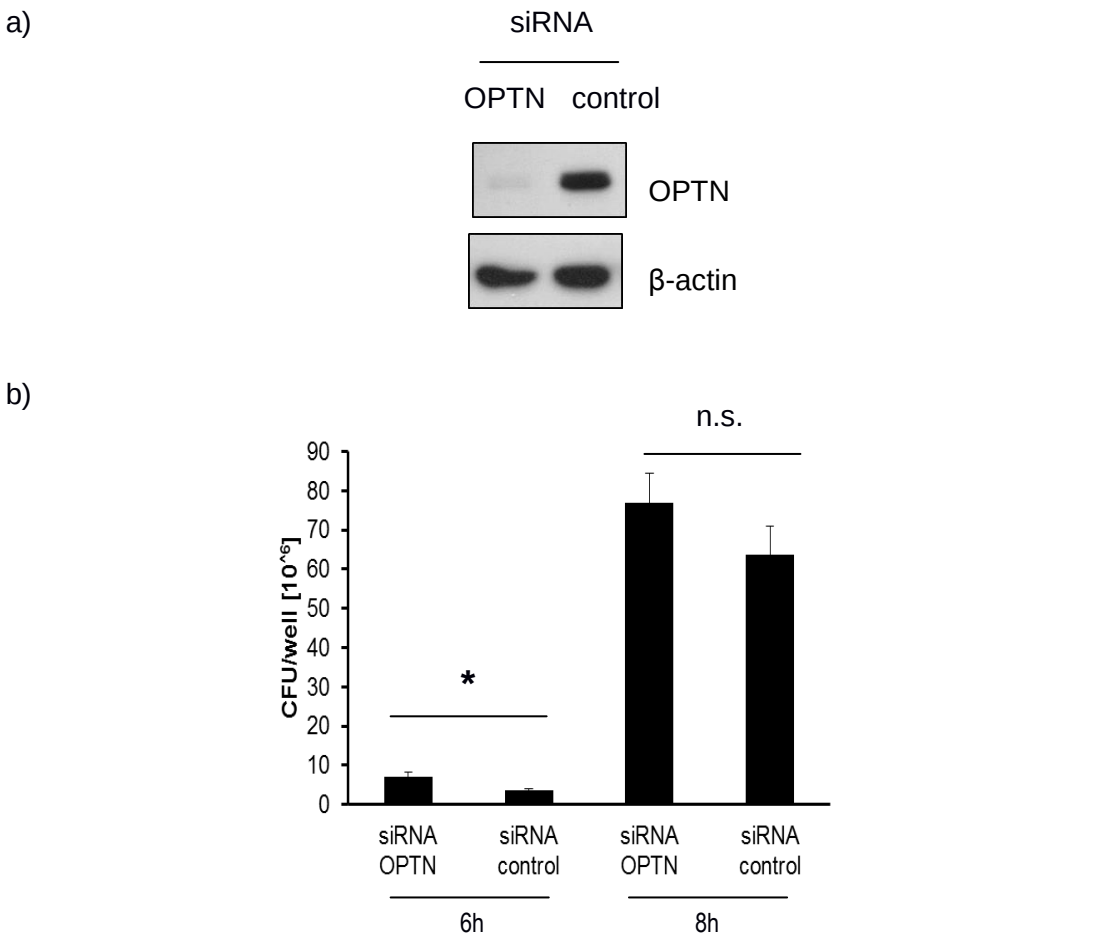

Fig. 3.4.3: OPTN knockdown results in increased intracellular growth of *S.* Typhimurium. a) Western blotting of HeLa cells transfected with OPTN and control siRNA, showing knockdown of OPTN. β-actin was used as a loading control. **b)** OPTN was knocked down in HeLa cells and they were infected with *S.* Typhimurium for 6h and 8h. Gentamicin (200 µg/ml) was added 30 min p.i. to kill the extracellular bacteria. The intracellular bacteria were plated on LB agar plates and the CFUs were counted. The results are expressed as CFU per well, each bar represents the mean value + SD of at least three independent experiments performed in triplicates (* $p < 0.05$; n.s.: not significant).

3.4.3 OPTN is phosphorylated during *L. monocytogenes* infection

L. monocytogenes and *S.* Typhimurium are both facultative intracellular pathogens, and during infection, are targeted by autophagy (Jo *et al.*, 2013). A small population of cytosolic *S.* Typhimurium or *L. monocytogenes* is ubiquitinated and delivered to the proteasome for their degradation (Jo *et al.*, 2013 ; Mostowy *et al.*, 2011). Another population of ubiquitinated *S.* Typhimurium and *L. monocytogenes* is recruited by the autophagy adaptors SQSTM1 and NDP52, and allocated to the autophagosomal machinery (Mostowy *et al.*, 2011). Because OPTN has recently been recognized as an

autophagy adaptor for *S.* Typhimurium (Wild *et al.*, 2011), it was hypothesized that it may also be an autophagy adaptor for *L. monocytogenes*.

To see if OPTN is phosphorylated during *L. monocytogenes* infection, HeLa cells were infected with Lm EGD-e for 4h, and the phosphorylation of OPTN was analyzed by Western blotting using an anti-pSer177 OPTN antibody. As shown in Fig. 3.4.4, OPTN was phosphorylated during *L. monocytogenes* infection.

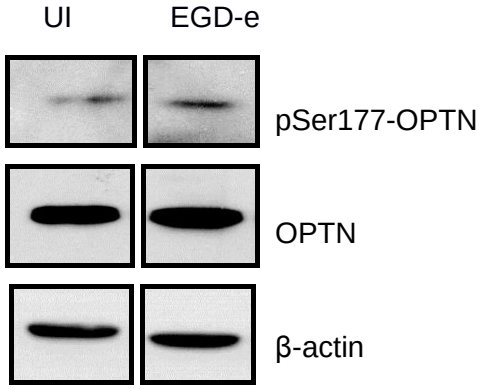

Fig. 3.4.4: OPTN is phosphorylated during *L. monocytogenes* infection in HeLa cells. HeLa cells were infected with Lm EGD-e for 4h. Gentamicin (50 µg/ml) was added 1h p.i. to kill the extracellular bacteria. The cells were lysed and immunoblotting was performed using anti-phospho-OPTN (pSer177-OPTN) and anti-OPTN (total). β-actin was used as a loading control. UI: uninfected cells. The image is a representative of three independent experiments.

3.4.4 OPTN is essential for the delivery of *L. monocytogenes* to the autophagosome

To investigate the relevance of OPTN phosphorylation during *L. monocytogenes* infection, HeLa cells were transfected with OPTN siRNA and infected with Lm EGD-e for 2h and 4h. When the intracellular bacteria were plated, an increase was observed in the intracellular growth of Lm EGD-e at 2h (not significant) and 4h p.i. (significant; $p < 0.001$) in cells treated with OPTN siRNA, as compared to that in cells treated with control siRNA (Fig. 3.4.5). These results demonstrate that OPTN led to the restriction of the intracellular growth of *L. monocytogenes*.

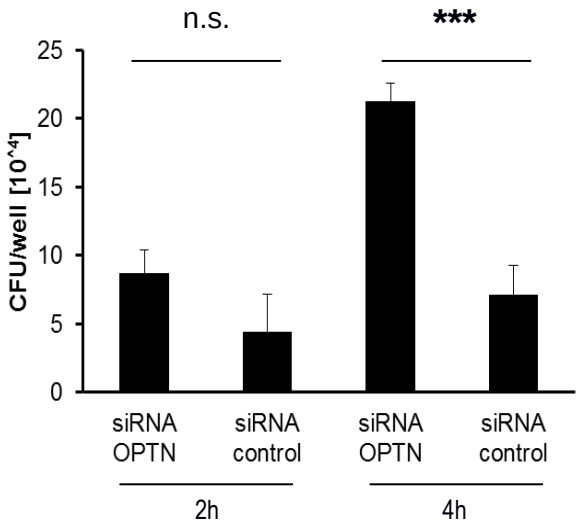

Fig. 3.4.5: OPTN depletion increases the intracellular growth of *L. monocytogenes*. OPTN was knocked down in HeLa cells and they were then infected with Lm EGD-e for 4h. Gentamicin (50 µg/ml) was added 1h p. i. to eliminate the extracellular bacteria. The intracellular bacteria were plated on BHI agar plates and the CFUs were counted. The results are expressed as CFU per well. Each bar represents the mean value + SD of at least three independent experiments performed in triplicates (*** $p < 0.001$; n.s.: not significant).

Previous studies with OPTN have reported that TBK1 phosphorylates OPTN at Ser177, which leads to enhanced LC3 binding to ubiquitinated cytosolic *Salmonella* (Wild *et al.*, 2011). Moreover, TBK1-mediated OPTN phosphorylation also leads to the autophagic degradation of protein aggregates (Korac *et al.*, 2013). This observation prompted the investigation to observe if the TBK1-mediated phosphorylation of OPTN restricts the intracellular growth of *L. monocytogenes*. OPTN and TBK1 were overexpressed by co-transfecting HeLa cells with plasmids expressing OPTN and wild-type TBK1 or OPTN and a mutant of TBK1 with an ineffective kinase (TBK1 KM) for 24h. As control, another set of cells was transfected with a plasmid containing an empty vector (pRK5). These cells were then infected with Lm EGD-e for 4h. As shown in Fig. 3.4.6 a, OPTN was phosphorylated in the cells transfected with wild-type TBK1, whereas the TBK1 mutant was unable to phosphorylate OPTN. As a result, when HeLa cells were expressing OPTN, but TBK1 was not functional and OPTN was, therefore, not phosphorylated, *L. monocytogenes* showed a similar intracellular survival in these cells as that in HeLa cells expressing the empty

vector (Fig. 3.4.6 b). However, when OPTN was phosphorylated by TBK1, the intracellular growth of *L. monocytogenes* was restricted, which indicated that TBK1-mediated phosphorylation of OPTN is essential for restricting the growth of *L. monocytogenes* (Fig. 3.4.6 b). MTT assay was performed to verify that these results were not a consequence of the loss of cell viability (Fig. 3.4.6 c).

BX-795 ($C_{23}H_{26}IN_7O_2S$) is a well-known, potent, ATP-competitive and reversible inhibitor of TBK1, which acts by blocking its phosphorylation. When HeLa cells treated with different concentrations of BX-795 were infected with Lm EGD-e for 4h, an increase (1.5-fold) in the intracellular growth of *L. monocytogenes* was observed (Fig. 3.4.7 a). However, treatment with 5 µM of BX-795 led to a decrease in the number of intracellular bacteria, which was a result of the loss of cell viability (Fig. 3.4.7 b). Additionally, bacteria (without cells) were treated with BX-795 and plated to confirm that the aforementioned observation was not due to bacterial death caused by BX-795 treatment (Fig. 3.4.7 c).

The last two results not only validate the hypothesis that OPTN plays a vital role to restrict the intracellular growth of *L. monocytogenes* but also reveal that TBK1-mediated OPTN phosphorylation is essential for restricting the intracellular growth of *L. monocytogenes* during infection.

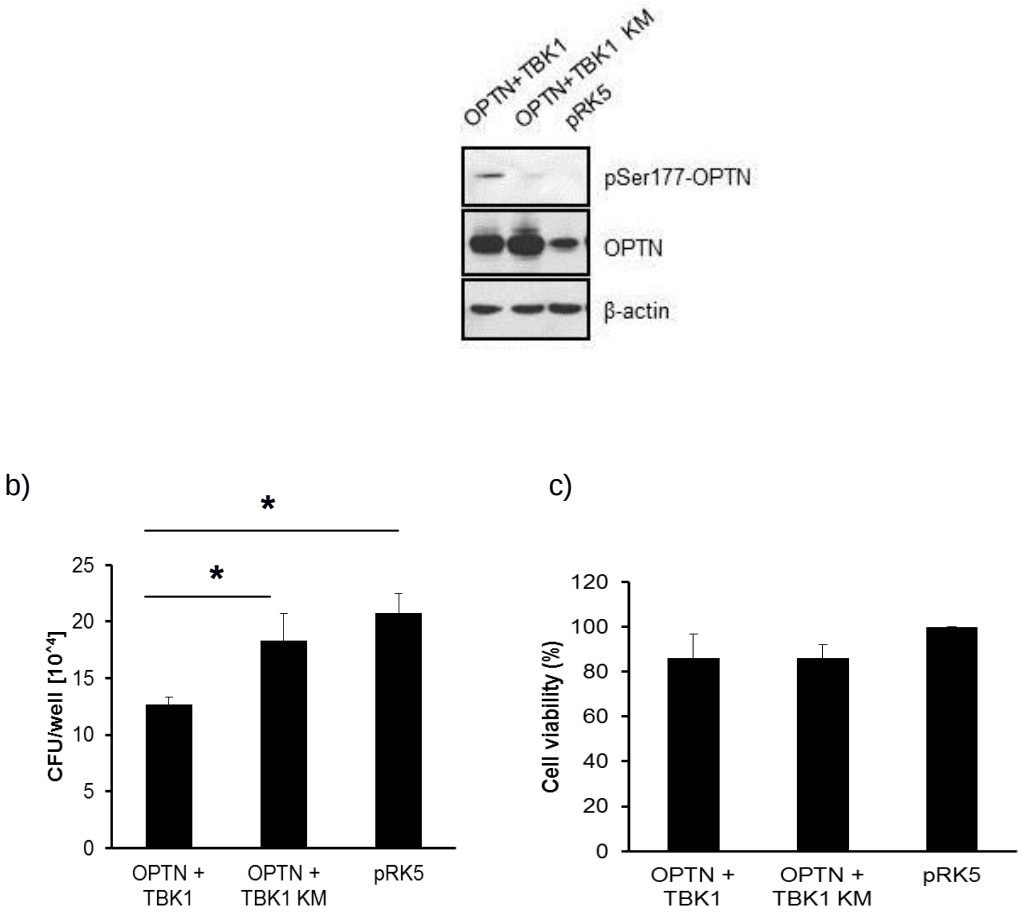

Fig. 3.4.6: The phosphorylation of OPTN by TBK1 decreases the intracellular growth of *L. monocytogenes*. a) HeLa cells were transfected with plasmids expressing wild-type OPTN (pcDNA3.1(+)/HA-OPTN) and wild-type TBK1 (pcDNA3.1-TBK1-myc-His_6) or wild-type OPTN (pcDNA3.1(+)/HA-OPTN) and TBK1 kinase mutant (pcDNA3.1-TBK1-myc-His_6 KM). As control, they were transfected with pRK5 (empty vector). The cell lysates were analyzed using anti-phospho-OPTN (pSer177-OPTN) and anti-OPTN (total). β-actin was used as a loading control. **b)** HeLa cells were transfected with plasmids expressing wild-type OPTN (pcDNA3.1(+)/HA-OPTN) and wild-type TBK1 (pcDNA3.1-TBK1-myc-His_6) or wild-type OPTN (pcDNA3.1(+)/HA-OPTN) and TBK1 kinase mutant (pcDNA3.1-TBK1-myc-His_6 KM). As control, cells were transfected with pRK5 (empty vector). They were then infected with Lm EGD-e for 4h. Gentamicin (50 µg/ml) was added 1h p. i. to eliminate the extracellular bacteria. The intracellular bacteria were plated. The results are expressed as CFU per well. Each bar represents the mean value + SD of three independent experiments performed in triplicates (* $p < 0.05$). **c)** HeLa cells were transfected with OPTN (pcDNA3.1(+)/HA-OPTN) and wild-type TBK1 (pcDNA3.1-TBK1-myc-His_6), wild-type OPTN (pcDNA3.1(+)/HA-OPTN) and TBK1 kinase mutant (pcDNA3.1-TBK1-myc-His_6 KM), or pRK5, and they were then infected with Lm EGD-e for 4h. Gentamicin (50 µg/ml) was added 1h p. i. to eliminate the extracellular bacteria. The cells were incubated with MTT solution for 2h. The reaction was stopped by adding isopropanol containing 5% formic acid and the cell viability was measured by absorbance at 562 nm. The results are expressed as percent cell viability. Each bar represents the mean value + SD of three independent experiments performed in triplicates.

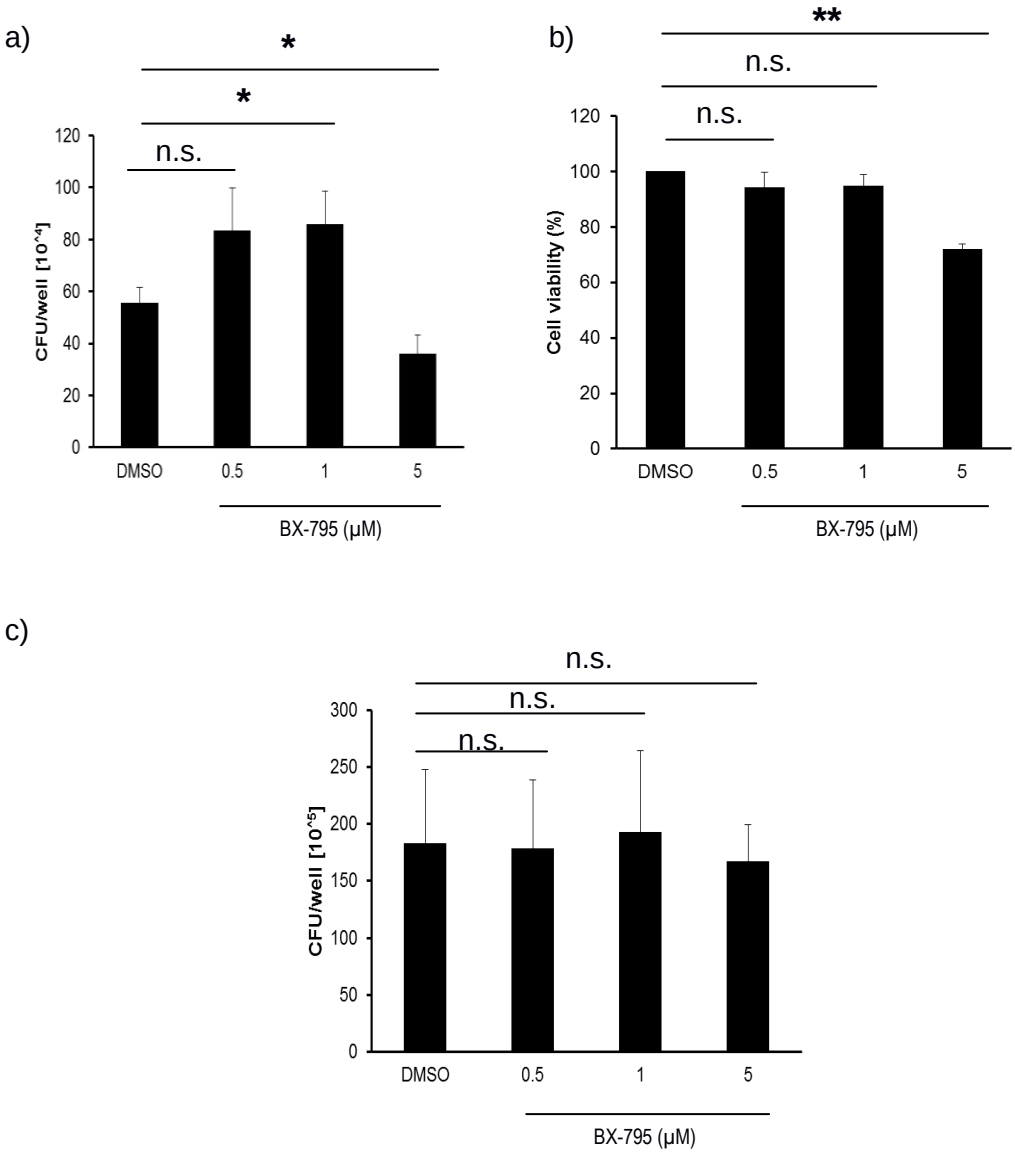

Fig. 3.4.7: The inhibition of TBK1 increases the intracellular growth of *L. monocytogenes*. a) HeLa cells were pre-treated with the indicated concentrations of BX-795 or an equal amount of DMSO (negative control) for 1h and then infected with Lm EGD-e for 4h. Gentamicin (50 µg/ml) and BX-795 were added 1h p.i. and the intracellular bacteria were plated. The results are expressed as CFU per well. Each bar represents the mean value + SD of at least three independent experiments performed in triplicates (* $p < 0.05$; n.s.: not significant). **b)** HeLa cells were pre-treated with the indicated concentrations of BX-795 for 1h and infected with Lm EGD-e for 4h. Gentamicin (50 µg/ml) and BX-795 were added 1h p.i. The cells were incubated with MTT solution for 2h. The reaction was stopped by adding isopropanol containing 5% formic acid and cell viability was measured by absorbance at 562 nm. The results are expressed as percent cell viability. Each bar represents the mean value + SD of three independent experiments performed in triplicates (** $p < 0.01$; n.s.: not significant). **c)** Lm EGD-e was added to the cell culture media (without cells) and BX-795 was added after 1h at the indicated concentrations. The bacteria were plated. The results are expressed as CFU per well. Each bar represents the mean value + SD of three independent experiments performed in triplicates (n.s.: not significant).

3.4.5 The loss of OPTN results in reduced LC3 levels after *L. monocytogenes* infection

OPTN has a conserved LC3-interacting motif at its N-terminal region (Wild *et al.*, 2011). OPTN also localizes to LC3-positive vesicles, bacteria and protein aggregates upon autophagy induction (Wild *et al.*, 2011; Korac *et al.*, 2013). This observation was the basis for the next set of experiments to determine if LC3 levels were altered after *L. monocytogenes* infection of OPTN-depleted cells. OPTN-depleted HeLa cells were infected with Lm EGD-e for 4h, and LC3 levels were analyzed by immunoblotting. Another set of non-transfected HeLa cells were treated with 20 µM rapamycin (positive control for autophagy induction) and an equal amount of DMSO (negative control) for 4h. In accordance with literature, infection with *L. monocytogenes* induced the conversion of LC3-I to LC3-II, as observed by the increase in the LC3-II to LC3-I ratio after *L. monocytogenes* infection in cells transfected with control siRNA (Fig. 3.4.8). On the other hand, a decline in the ratio of the levels of LC3-II to LC3-I was seen in OPTN-depleted cells after *L. monocytogenes* infection, as compared to non-depleted cells after infection (Fig. 3.4.8). Moreover, treatment of cells with rapamycin also induced an increase in the ratio of LC3-II to LC3-I, as compared to cells treated with DMSO (Fig. 3.4.8).

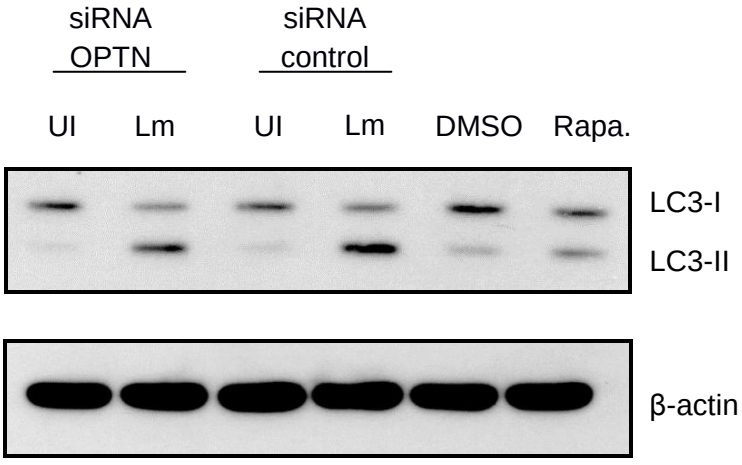

Fig. 3.4.8: OPTN knockdown decreases the ratio of LC3-II to LC3-I after *L. monocytogenes* infection. OPTN was knocked down in HeLa cells and they were infected with Lm EGD-e for 4h. As control, the cells were treated with 20 µM rapamycin (Rapa.; positive control) and an equal amount of DMSO (negative control) for 4h. The cell lysates were analyzed by immunoblotting using anti-LC3. β-actin was used as a loading control. The image represents three independent experiments. UI: uninfected cells.

3.4.6 OPTN knockdown does not affect the intracellular growth of Lm*Δ*actA2*

It is known that Lm*Δ*actA2* induces more conversion of LC3-I to LC3-II and co-localizes more with LC3, as compared to Lm EGD-e (Yoshikawa *et al.*, 2009). Having this in mind, it was imperative to investigate if the intracellular growth of Lm*Δ*actA2* is greater than that of Lm EGD-e after OPTN knockdown.

HeLa cells were transfected with OPTN siRNA and infected with Lm EGD-e and Lm*Δ*actA2* for 4h. Infection of OPTN siRNA-transfected HeLa cells with Lm EGD-e resulted in an increase (2.2-fold) in the intracellular bacterial growth in comparison to infection of control siRNA-transfected HeLa cells, as observed previously (Fig. 3.4.9 a). However, OPTN depletion had no effect on the intracellular growth of Lm*Δ*actA2*, as compared to non-depleted cells (Fig. 3.4.9 a). Moreover, no significant difference could be observed between the intracellular numbers of Lm EGD-e and Lm*Δ*actA2* in control siRNA-treated cells (Fig. 3.4.9 a). As control, MTT assay was performed to measure the viability of HeLa cells after transfection and infection, in comparison to the viability of transfected, but uninfected cells. As shown in Fig. 3.4.9 b, these results were not a consequence of the loss of cell viability.

To determine if the above results were caused by a low MOI, the same experiment was repeated by infecting OPTN siRNA-transfected HeLa cells with Lm EGD-e and Lm*Δ*actA2* at a higher MOI (1:100), and still there was no difference in the intracellular growth of Lm*Δ*actA2* in OPTN-depleted cells, as compared to that in non-depleted cells (Fig. 3.4.9 c).

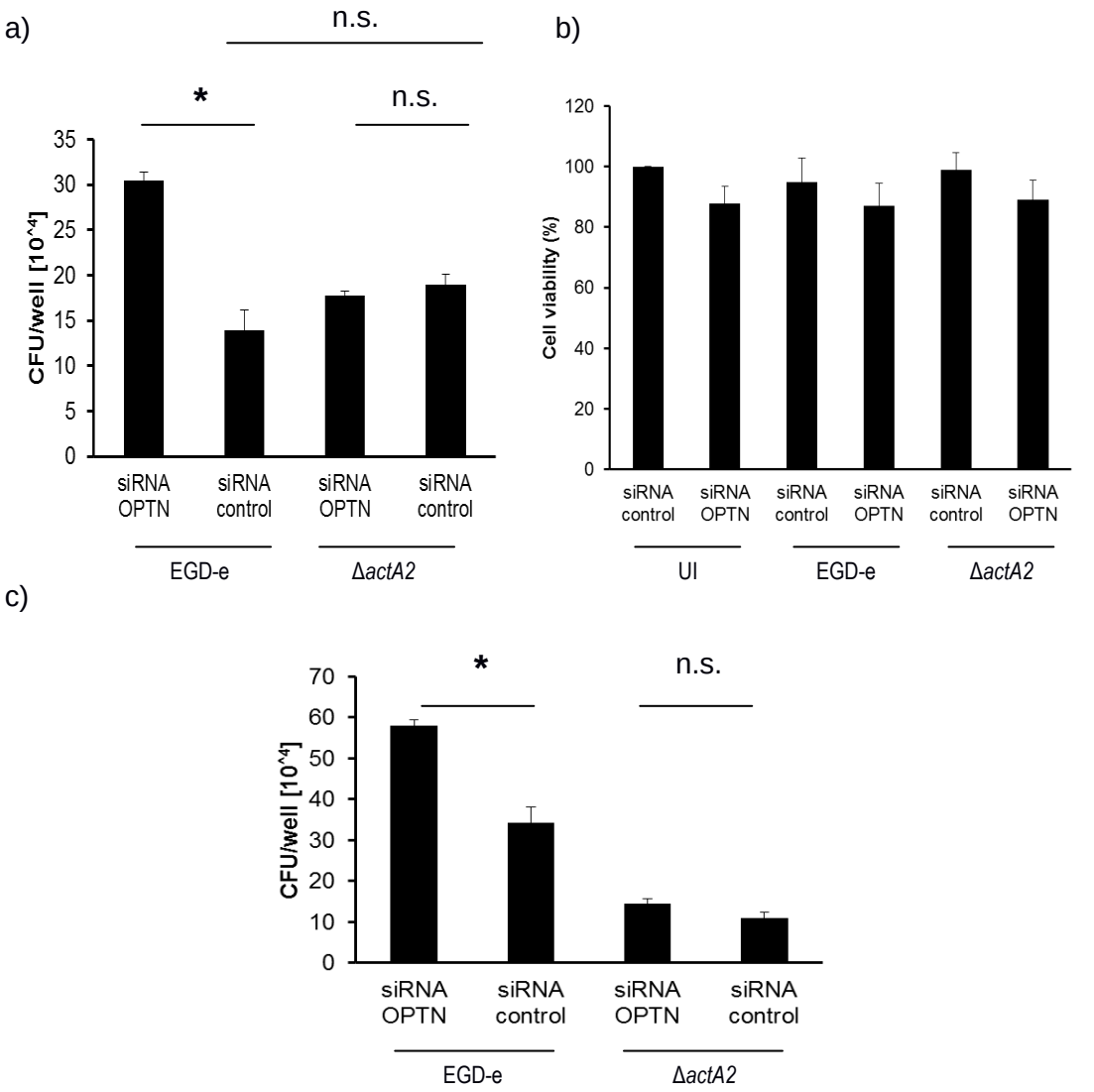

Fig. 3.4.9: The depletion of OPTN does not affect the intracellular growth of Lm*ΔactA2*. a) OPTN was knocked down in HeLa cells and they were infected with Lm EGD-e and Lm*ΔactA2* (MOI, 1:10) for 4h. Gentamicin (50 µg/ml) was added 1h p. i. to eliminate the extracellular bacteria. The intracellular bacteria were plated. The results are expressed as CFU per well. Each bar represents the mean value + SD of at least three independent experiments performed in triplicates (* $p < 0.05$; n.s.: not significant). **b)** OPTN was knocked down in HeLa cells and they were infected with Lm EGD-e and Lm*ΔactA2* for 4h. Gentamicin (50 µg/ml) was added 1h p. i. to eliminate the extracellular bacteria. The cells were incubated with MTT solution for 2h. The reaction was stopped by adding isopropanol containing 5% formic acid and cell viability was measured by absorbance at 562 nm. The results are expressed as percent cell viability. Each bar represents the mean value + SD of at least three independent experiments performed in triplicates. UI: uninfected cells. **c)** OPTN was knocked down in HeLa cells and they were infected with Lm EGD-e and Lm*ΔactA2* (MOI, 1:100) for 4h. Gentamicin (50 µg/ml) was added 1h p. i. to eliminate the extracellular bacteria. The intracellular bacteria were plated. The results are expressed as CFU per well. Each bar represents the mean value + SD of at least three independent experiments performed in triplicates (* $p < 0.05$; n.s.: not significant).

3.4.7 OPTN knockdown does not affect the intracellular growth of Lm**Δ*actA16*** and Lm**Δ*actA21***

No significant change was seen in the intracellular number of LmΔ*actA2* after OPTN depletion, even at a higher MOI. As done previously in the case of SQSTM1, the ActA mutants LmΔ*actA16* and LmΔ*actA21* were employed (Lm EGD-e is the least ubiquitinated, followed by LmΔ*actA16*, and finally LmΔ*actA2* and LmΔ*actA21* are the most ubiquitinated) to investigate if differently ubiquitinated Lm*actA* strains also show the same results.

HeLa cells were transfected with OPTN siRNA and infected with Lm EGD-e, LmΔ*actA2*, LmΔ*actA16* and LmΔ*actA21* for 4h. The plating of intracellular bacteria revealed no significant changes in the intracellular growth of LmΔ*actA2*, LmΔ*actA16* and LmΔ*actA21* in cells transfected with OPTN siRNA, as compared to that in cells transfected with control siRNA. As observed previously, the intracellular numbers of Lm EGD-e, *LmΔactA2* and LmΔ*actA16* in control siRNA-treated cells were similar (Fig. 3.4.10). However, unexpectedly high intracellular numbers of LmΔ*actA21* were observed in both OPTN siRNA (38*10^5 cfu per well) and control siRNA (36*10^5 cfu per well) treated cells.

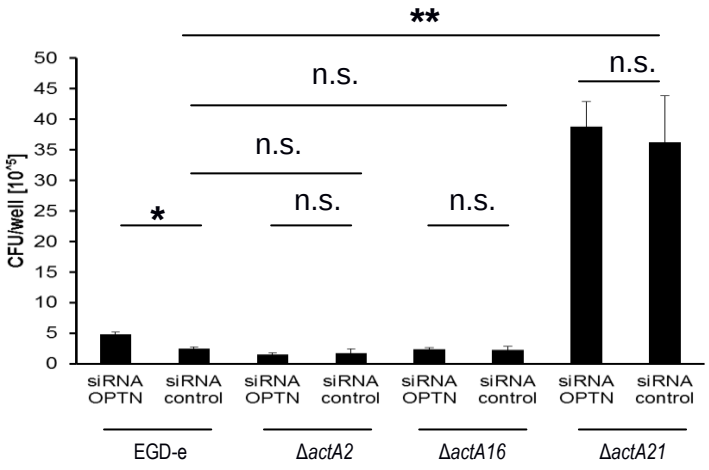

Fig. 3.4.10: The knockdown of OPTN does not affect the intracellular growth of LmΔ***actA2*****, Lm**Δ***actA16*** **and Lm**Δ***actA21*****.** HeLa cells were transfected with OPTN siRNA and were infected with Lm EGD-e, LmΔ*actA2*, LmΔ*actA16* and LmΔ*actA21* for 4h. Gentamicin (50 µg/ml) was added 1h p. i. to eliminate the extracellular bacteria. The intracellular bacteria were plated. The results are expressed as CFU per well. Each bar represents the mean value + SD of three independent experiments performed in triplicates (* $p < 0.05$; ** $p < 0.01$; n.s.: not significant).

3.4.8 OPTN co-localizes with *L. monocytogenes* and requires the LIR and UBD domains for this co-localization

Wild *et al.* (2011) have shown that OPTN is recruited to ubiquitinated cytosolic *S.* Typhimurium *via* its UBD, and it delivers *S.* Typhimurium to the autophagosome by the interaction of its LIR with LC3 present on the autophagosomal membrane. To test if this is also the case with *L. monocytogenes*, HeLa cells were transfected with GFP-OPTN, GFP-OPTN E478G (an ubiquitin-binding-deficient OPTN mutant) or GFP-OPTN F178A (a LC3-binding-deficient OPTN mutant). The transfected cells were then infected with Lm EGD-e and Lm*Δactα2* for 4h. Immunofluorescence analysis was used to observe the co-localization of bacteria with OPTN. As shown in Fig. 3.4.11 a, a majority of intracellular Lm EGD-e and Lm*Δactα2* co-localized with GFP-OPTN, which showed that OPTN is recruited to both these strains. Moreover, fewer bacteria co-localized with GFP-OPTN E478G and GFP-OPTN F178A, which implies that both the LIR and UBD domains are required for OPTN recruitment to Lm EGD-e and Lm*Δactα2* (Fig.3.4.11 a). The percentage of Lm EGD-e which co-localized with all the three OPTN variants was quantified, which revealed a significantly ($p < 0.001$) high percentage of Lm EGD-e which co-localized with GFP-OPTN, and a lower percentage of Lm EGD-e which co-localized with the ubiquitin and LC3-binding-deficient mutants of OPTN (Fig. 3.4.11 b). Because Lm*Δactα2* cannot move in the cytosol and clump together, it was not possible to quantify these bacilli. As observed in the case of SQSTM1 and NDP52, only a part of the Lm EGD-e and Lm*Δactα2* population was associated with GFP-OPTN.

a)

DAPI
Lm EGD-e
GFP-OPTN

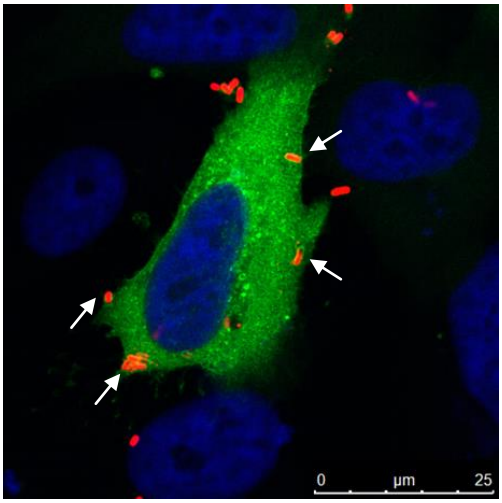

DAPI
Lm*ΔactA2*
GFP-OPTN

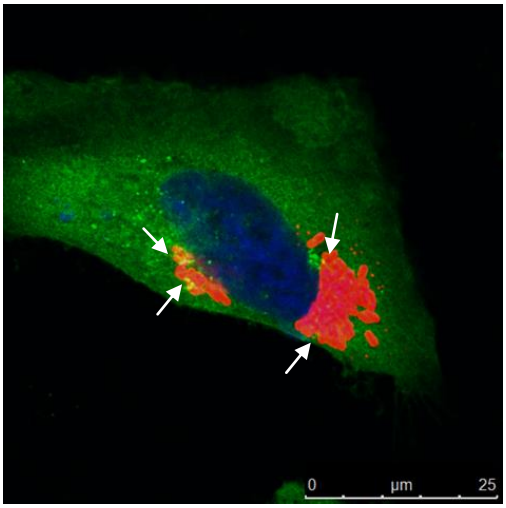

DAPI
Lm EGD-e
GFP-OPTN E478G

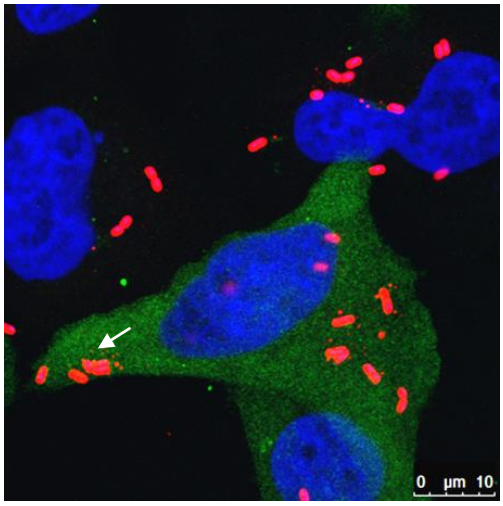

DAPI
Lm*ΔactA2*
GFP-OPTN E478G

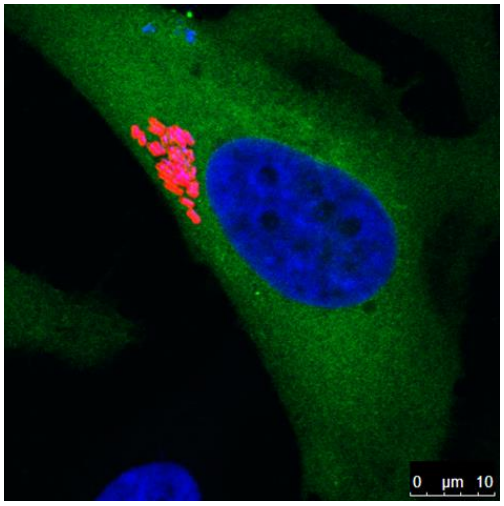

DAPI
Lm EGD-e
GFP-OPTN F178A

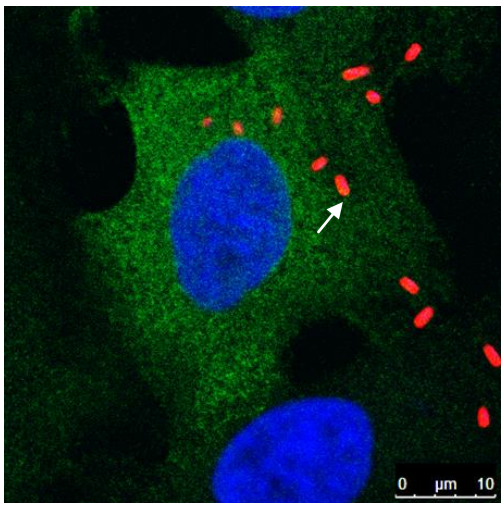

DAPI
Lm*ΔactA2*
GFP-OPTN F178A

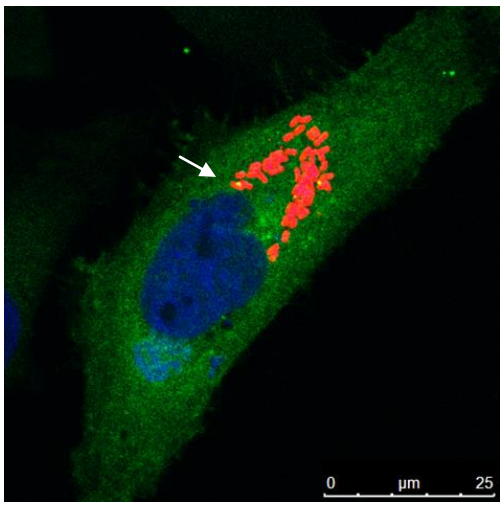

b)

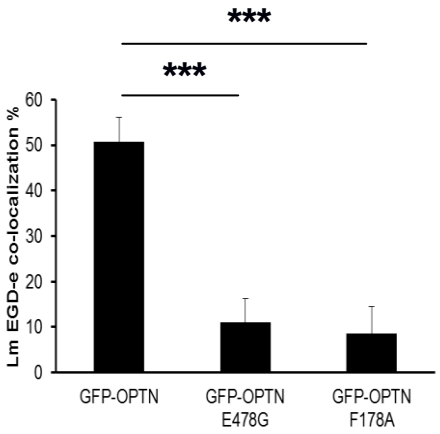

Fig. 3.4.11: OPTN co-localizes with *L. monocytogenes* and requires the LIR and UBD domains for this co-localization. a) HeLa cells were transfected with plasmids which express GFP-OPTN, GFP-OPTN E478G or GFP-OPTN F178A. They were then infected with Lm EGD-e and Lm*ΔactA2* for 4h. Gentamicin (50 µg/ml) was added 1h p. i. to eliminate the extracellular bacteria. The cells were fixed, permeabilized and stained with anti-Lm (red). The nuclei were stained with DAPI (blue). Arrows indicate co-localization of Lm with GFP-OPTN. **b)** Quantification of Lm EGD-e which co-localized with GFP-OPTN, GFP-OPTN E478G and GFP-OPTN F178A from cells represented in a). Each bar represents the mean value + SD of three independent experiments (*** $p < 0.001$).

3.5 NBR1 is an autophagy adaptor for *L. monocytogenes*

NBR1 is also a recent addition to the family of autophagy adaptors. The role of NBR1 as an autophagy adaptor for the selective autophagy of *L. monocytogenes* has not been studied. Therefore, the following experiments were conducted using *Listeria* as a model pathogen.

3.5.1 NBR1 is recruited to Lm EGD-e and Lm*ΔactA2*

NBR1 co-localizes with *F. tularensis* (Chong *et al.*, 2012) and *S. flexneri* (Mostowy *et al.*, 2011), and subsequently mediates their selective autophagy. In order to see if NBR1 also plays a role in the autophagy of *L. monocytogenes*, its co-localization with *L. monocytogenes* was examined. HeLa cells were infected with Lm EGD-e and Lm*ΔactA2* for 4h and immunofluorescence analysis was performed using an anti-NBR1 antibody. As shown in Fig. 3.5.1, both Lm EGD-e and Lm*ΔactA2* co-localized with NBR1, thereby implying that NBR1 is recruited to intracellular *L.*

monocytogenes. Additionally, only a part of the Lm EGD-e and LmΔ*actA2* population was associated with NBR1.

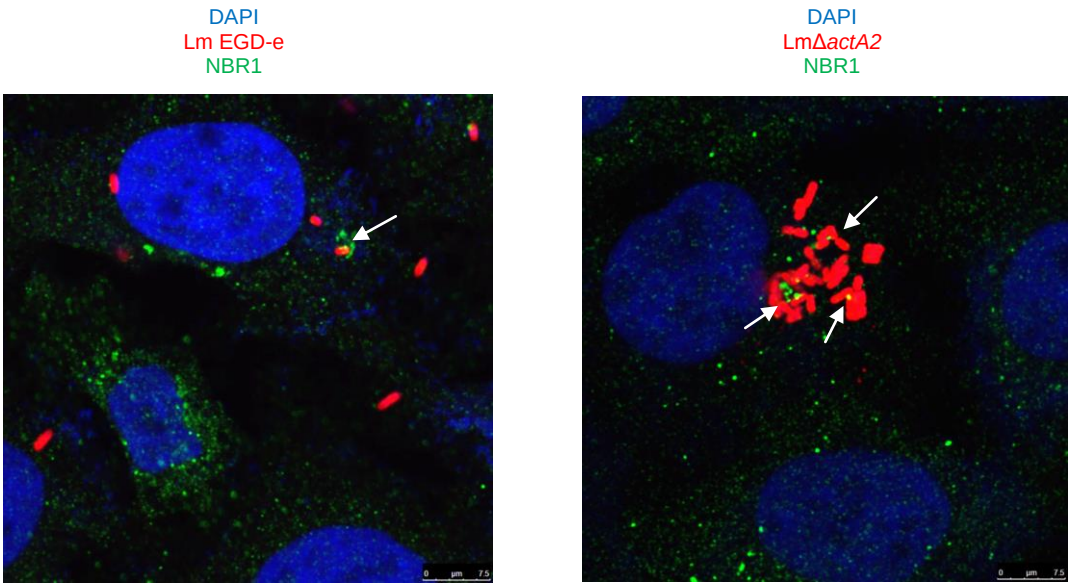

Fig. 3.5.1: NBR1 is recruited to Lm EGD-e and LmΔ*actA2*. HeLa cells were infected with Lm EGD-e and LmΔ*actA2* for 4h. Gentamicin (50 µg/ml) was added to eliminate the extracellular bacteria 1h p.i. The cells were fixed, permeabilized and stained with anti-NBR1 (green) and anti-Lm (red). Nuclei were stained with DAPI (blue). Arrows indicate co-localization of Lm with NBR1.

3.5.2 NBR1 depletion results in increased intracellular growth of Lm EGD-e and LmΔ*actA2*

It was observed that SQSTM1, NDP52 and OPTN were crucial for restraining the intracellular growth of *L. monocytogenes*. Based upon these observations, it was speculated that NBR1 may also play the same role. To test this speculation, HeLa cells transfected with siRNA against NBR1 were infected with Lm EGD-e and LmΔ*actA2* for 4h. The knockdown of NBR1 was confirmed by Western blotting (Fig. 3.5.2 a; the established knockdown of NBR1 of one experiment is shown). A 2.9-fold increase was seen in intracellular Lm EGD-e after NBR1 knockdown as compared to the control. Additionally, a 1.9-fold increase was also observed in the growth of intracellular LmΔ*actA2* in cells transfected with NBR1 siRNA, as compared to those transfected with control siRNA. It was also observed that the intracellular numbers of Lm EGD-e and LmΔ*actA2* in control siRNA-treated

cells were similar (Fig. 3.5.2 b). In order to rule out the possibility that the above difference in bacterial numbers could be caused by cell death resulting from the infection of siRNA-transfected cells, MTT assay was performed to measure the viability of HeLa cells after transfection and infection, in comparison to the viability of transfected, but uninfected cells. As shown in Fig. 3.5.2 c, over 90% viability was seen in all groups of transfected and infected cells.)

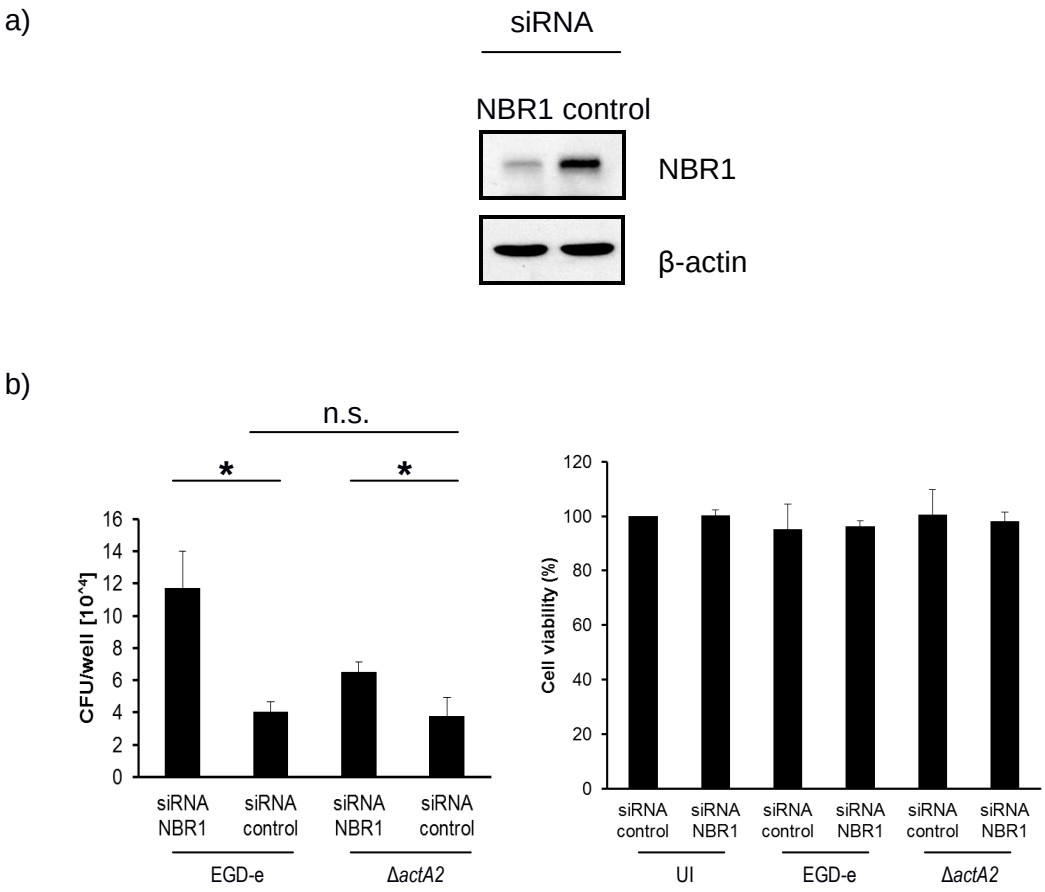

Fig. 3.5.2: NBR1 knockdown increases the intracellular growth of Lm EGD-e and Lm*ΔactA2*. a) Western blotting of HeLa cells transfected with NBR1 and control siRNA, showing NBR1 knockdown. β-actin was used as a loading control. **b)** HeLa cells were transfected with NBR1 siRNA and infected with Lm EGD-e and Lm*ΔactA2* for 4h. Gentamicin (50 µg/ml) was added 1h p. i. to eliminate the extracellular bacteria. The intracellular bacteria were plated. The results are expressed as CFU per well. Each bar represents the mean value + SD of three independent experiments performed in triplicates (* $p < 0.05$; n.s.: not significant). **c)** NBR1 was knocked down in HeLa cells and they were infected with Lm EGD-e and Lm*ΔactA2* for 4h. Gentamicin (50 µg/ml) was added 1h p. i. to eliminate the extracellular bacteria. The cells were incubated with MTT solution for 2h. The reaction was stopped by adding isopropanol containing 5% formic acid and cell viability was measured by absorbance at 562 nm. The results are expressed as percent cell viability. Each bar represents the mean value + SD of three independent experiments performed in triplicates. UI: uninfected cells.

3.6 TAX1BP1 is an autophagy adaptor for *L. monocytogenes*

There is only one study that identified TAX1BP1 as an autophagy cargo receptor (Newman *et al.*, 2012), and there is no report linking it to xenophagy.

3.6.1 TAX1BP1 is recruited to Lm EGD-e and LmΔ*actA2*

In order to investigate if TAX1BP1 might play a role in the autophagy of *L. monocytogenes*, it was first examined if TAX1BP1 associates with cytosolic *L. monocytogenes*. Towards this end, HeLa cells infected with Lm EGD-e and LmΔ*actA2* for 4h were analyzed by immunofluorescence. TAX1BP1 co-localized with both Lm EGD-e as well as LmΔ*actA2* (Fig. 3.6.1). LmΔ*actA2* clumped in the cytosol due to their non-motility, and only a part of the Lm EGD-e and LmΔ*actA2* population was associated with TAX1BP1.

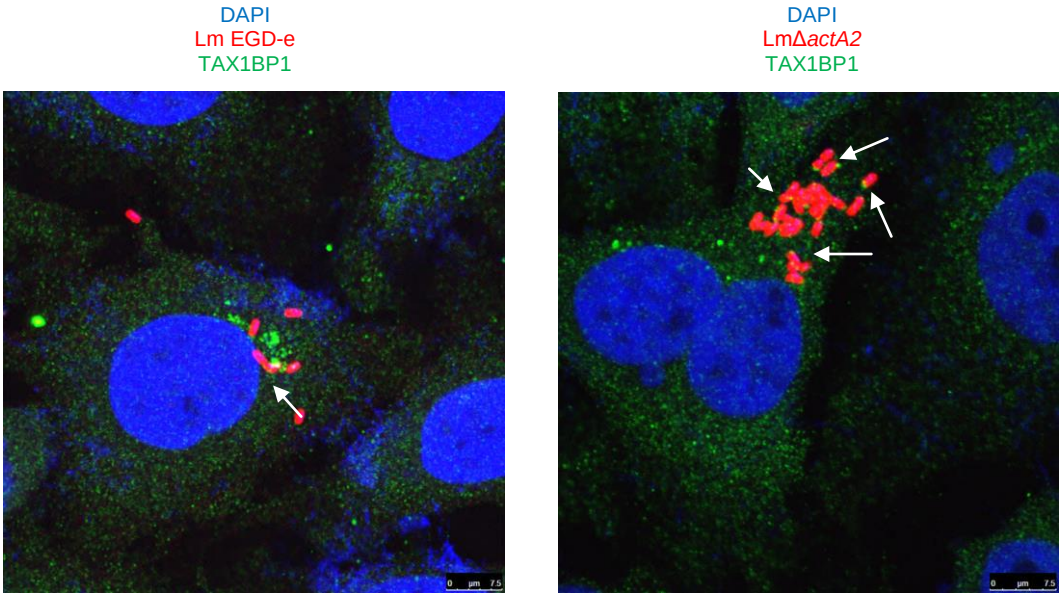

Fig. 3.6.1: TAX1BP1 is recruited to Lm EGD-e and LmΔ*actA2*. HeLa cells were infected with Lm EGD-e and LmΔ*actA2* for 4h. Gentamicin (50 µg/ml) was added 1h p. i. to eliminate the extracellular bacteria. The cells were fixed, permeabilized and stained with anti-TAX1BP1 (green) and anti-Lm (red). The nuclei were stained with DAPI (blue). Arrows indicate co-localization of Lm with TAX1BP1.

3.6.2 Depletion of TAX1BP1 leads to the increased intracellular growth of Lm EGD-e but not that of LmΔ*actA2*

An increase was observed in the intracellular growth of Lm EGD-e after the knockdown of SQSTM1, NDP52, OPTN and NBR1 in HeLa cells. To determine if the NDP52 paralog TAX1BP1 also plays a role in the intracellular growth restriction of *L. monocytogenes*, the expression of TAX1BP1 was also silenced in HeLa cells using siRNA, followed by infection with Lm EGD-e and LmΔ*actA2* for 4h. The knockdown of TAX1BP1 was confirmed by Western blotting (Fig. 3.6.2 a; the established knockdown of TAX1BP1 of one experiment is shown). As is evident in Fig. 3.6.2 b, the loss of TAX1BP1 resulted in an increase (1.8-fold) in the intracellular growth of Lm EGD-e as compared to the control, as was observed after SQSTM1, NDP52, OPTN and NBR1 knockdown. However, there was no change in the intracellular growth of LmΔ*actA2* in cells transfected with TAX1BP1 siRNA, as compared to those transfected with control siRNA. Also, no significant difference could be observed between the intracellular numbers of Lm EGD-e and LmΔ*actA2* in control siRNA-treated cells (Fig. 3.6.2 b). It could be possible that the infection of siRNA-transfected cells could have led to cell death, resulting in the above findings. Therefore, as control, MTT assay was performed to measure the viability of HeLa cells after transfection and infection, in comparison to the viability of transfected, but uninfected cells. As shown in Fig. 3.6.2 c, the above findings were not a result of the loss of cell viability.

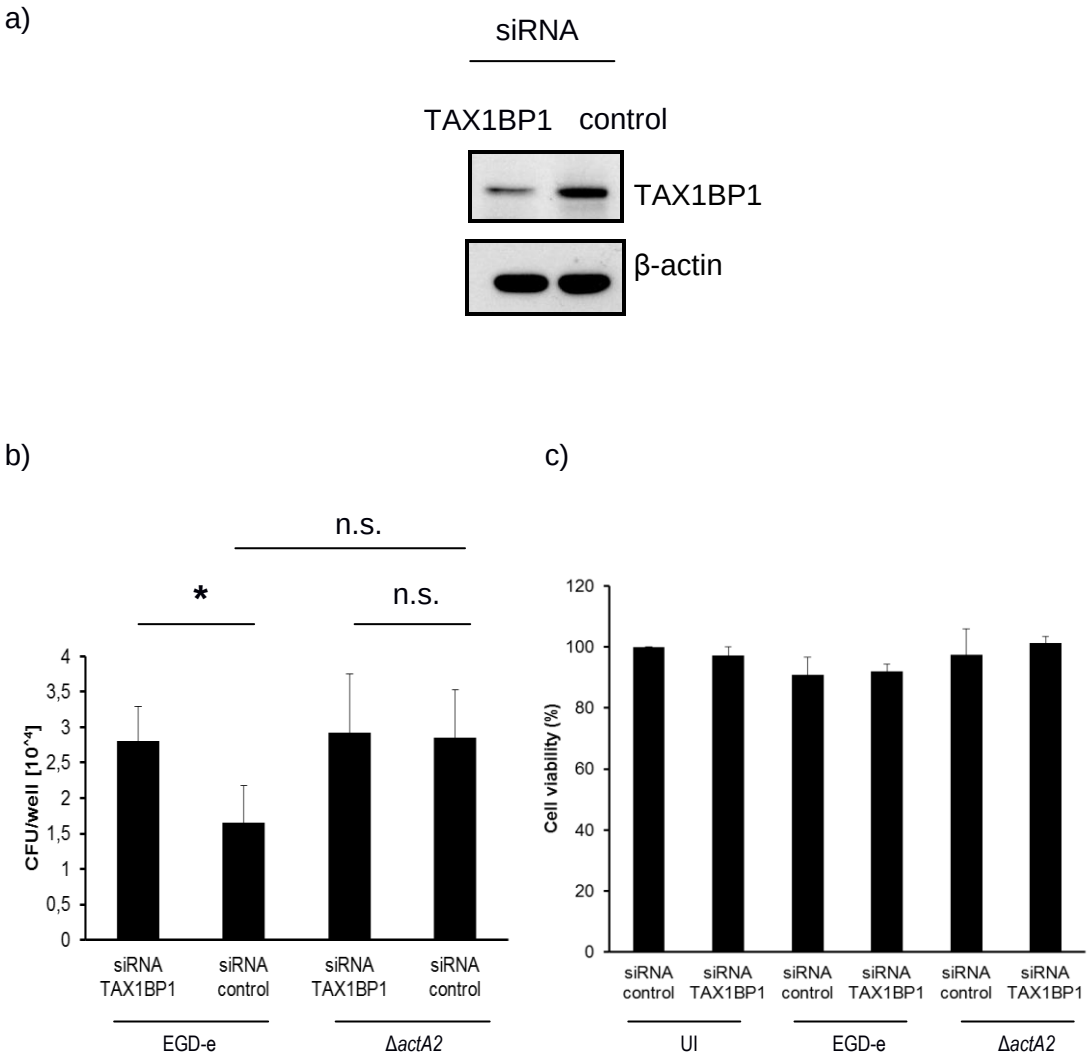

Fig.3.6.2: TAX1BP1 knockdown increases the intracellular growth of Lm EGD-e but not that of LmΔ*actA2*. a) Western blotting of HeLa cells transfected with TAX1BP1 and control siRNA, showing TAX1BP1 knockdown. β-actin was used as a loading control. **b)** HeLa cells were transfected with TAX1BP1 siRNA and infected with Lm EGD-e and LmΔ*actA2* for 4h. Gentamicin (50 µg/ml) was added 1h p. i. to eliminate the extracellular bacteria. The intracellular bacteria were plated. The results are expressed as CFU per well. Each bar represents the mean value + SD of three independent experiments performed in triplicates (* $p < 0.05$; n.s.: not significant). **c)** TAX1BP1 was knocked down in HeLa cells and they were infected with Lm EGD-e and LmΔ*actA2* for 4h. Gentamicin (50 µg/ml) was added 1h p. i. to eliminate the extracellular bacteria. The cells were incubated with MTT solution for 2h. The reaction was stopped by adding isopropanol containing 5% formic acid and the cell viability was measured by absorbance at 562 nm. The results are expressed as percent cell viability. Each bar represents the mean value + SD of three independent experiments performed in triplicates. UI: uninfected cells.

IV. Discussion

Discussion

It is now known that the autophagy adaptors SQSTM1 and NDP52 are recruited to ubiquitinated *L. monocytogenes* and mediate its autophagic degradation (Yoshikawa *et al.*, 2009; Mostowy *et al.*, 2011). The work reported herein was aimed to build upon and to add to the existing knowledge on the interaction of autophagy adaptors with *L. monocytogenes*, *in vitro*. The results reported herein, apparently for the first time, demonstrate that all the five known autophagy adaptors: SQSTM1, NDP52, OPTN, NBR1 and TAX1BP1, were involved in the autophagy-mediated growth restriction of *L. monocytogenes*, and NBR1 emerged as the most important of them all.

4.1 The effect of LC3 and ATG5 depletion on the intracellular growth of *L. monocytogenes*

LC3 is one of the most widely used markers to monitor autophagy, due to its presence on the autophagosomal membrane from the start of the autophagy process until the very end (Klionsky *et al.*, 2008). The bacteria are targeted by autophagy once exposed to the host cell cytoplasm. When HeLa cells were depleted of LC3 and ATG5 by siRNA and infected with Lm EGD-e and LmΔ*actA2*, the intracellular growth of both these bacteria was enhanced, as compared to their growth in non-depleted cells. These results are in consonance with several reported studies, which highlight the importance of the autophagy pathway in bacterial clearance during infections. Al-Younes *et al.* (2011) have reported that defective autophagy enhances the growth of *Chlamydia trachomatis*. The siRNA-mediated knockdown of ATG5 results in enhanced replication of *Legionella pneumophila* Philadelphia-1 in A/J mouse peritoneal macrophages (Matsuda *et al.*, 2009). When the mouse alveolar macrophage cell line MH-S is depleted of the autophagy related gene *beclin-1*, the number of intracellular *P. aeruginosa* is increased (Yuan *et al.*, 2012). It has also been published that the induction of autophagy by starvation, or by treatment with autophagy inducers like rapamycin leads to the clearance

of *M. tuberculosis* and *M. bovis* BCG (Gutierrez *et al.*, 2004). Several pathogens like *Staphylococcus aureus, Brucella abortus* and *Coxiella burnetii* stimulate their uptake into the autophagosomal compartment by secreting various bacterial effector proteins, and are capable of efficient growth within autophagosome-like vacuoles (Pareja and Colombo, 2013). Thus, these pathogens exploit the autophagy pathway for facilitating their own survival and growth. These results reiterate that autophagy is a crucial cellular defense mechanism to combat infection, and when it is compromised, the pathogens exploit the opportunity to establish efficient infection in the host.

4.2 The interaction of autophagy cargo receptors with *L. monocytogenes*

Immunofluorescence analysis of HeLa cells infected with Lm EGD-e and Lm*ΔactA2* showed that all the five autophagy adaptors *viz*. SQSTM1, NDP52, OPTN, NBR1 and TAX1BP1 were recruited to both these bacterial strains. Yoshikawa *et al.* (2009) have shown that a majority of the intracellular Lm*ΔactA2* population co-localizes with SQSTM1, whereas very few intracellular Lm EGD (WT) are associated with SQSTM1. Similarly, a relatively large number of Lm*ΔactA2* are found to be associated with NDP52, as compared to Lm EGD (Mostowy *et al.*, 2011). In concordance with these reported findings, the results reported in this thesis also demonstrate that only a part of the intracellular Lm EGD-e population co-localized with all the five autophagy adaptors. A probable explanation for this observation could be that because Lm EGD-e produces LLO, they may able to lyse the autophagosome and come out into the cytoplasm. Hence, the fraction of their population which might have remained within the autophagosome was positive for autophagy adaptor recruitment. However, the results in this thesis do not verify whether the bacteria which co-localized with autophagy adaptors are present in the autophagosome or in the cytoplasm. Therefore, it may also be possible that some Lm EGD-e bacteria which are able to lyse the autophagosome may be recognized again by autophagy adaptors, which

could be recruited to them in the cytoplasm. Interestingly, the immunofluorescence results of the present study showed that none of the autophagy adaptors were recruited to the entire population of intracellular Lm Δ*actA2* as well. This happening can be attributed to the likely-hood that like Lm EGD-e, a part of the intracellular Lm Δ*actA2* population could also lyse the autophagosomes by the action of LLO and come out free into the cytoplasm, so either the population which remained within the autophagosomes showed co-localization with autophagy adaptors, or the population which lysed the autophagosomes was recognized again by autophagy adaptors in the cytoplasm.

SQSTM1 was the first autophagy cargo receptor to be identified by Bjørkøy *et al.* (2005), who showed its role in the autophagic degradation of protein aggregates. SQSTM1 has been implicated in driving the autophagy of various kinds of substrates, be it protein aggregates or bacteria and viruses. With regard to *L. monocytogenes*, it has been reported that SQSTM1 delivers ubiquitinated Lm Δ*actA2* to the autophagosome by means of its interaction with LC3 (Yoshikawa *et al.*, 2009). These researchers have shown that ubiquitin and SQSTM1 positive Lm Δ*actA2* co-localize with LC3. Moreover, they have also reported that siRNA-mediated knockdown of SQSTM1 causes a significant decrease in the number of LC3 positive Lm Δ*actA2*, and in *sqstm1*$^{-/-}$ cells, the intracellular survival rate of Lm Δ*actA2* is nearly the same as that of Lm EGD-e. However, they did not report if the recruitment of SQSTM1 is involved in restricting the growth of Lm EGD-e.

In the present study, when the expression of SQSTM1 in HeLa cells was knocked down using siRNA, the intracellular growth of Lm EGD-e increased, as expected. This observation demonstrates that SQSTM1 controls *L. monocytogenes* infection by facilitating its autophagic degradation. Surprisingly, the intracellular growth of Lm Δ*actA2*, Lm Δ*actA16* and Lm Δ*actA21* declined with SQSTM1 knockdown, in contrast to the findings reported by Yoshikawa *et al.* (2009). The siRNA-mediated knockdown of SQSTM1 does not affect the levels of NBR1, OPTN and NDP52 (Helena Pillich; unpublished data from our lab). These observations suggest that

when SQSTM1 is knocked down, the levels of NBR1, OPTN and NDP52 remain unchanged, which, in turn, may mediate the autophagic degradation of Lm EGD-e, Lm Δ*actA2*, Lm Δ*actA16* and Lm Δ*actA21.* However, because Lm Δ*actA2*, Lm Δ*actA16* and Lm Δ*actA21* are relatively more ubiquitinated than Lm EGD-e, more NBR1, NDP52 and OPTN may bind to them as compared to Lm EGD-e, leading to a decline in their intracellular growth after SQSTM1 depletion. It is known that in the absence of SQSTM1, NDP52 is recruited to Lm Δ*actA* and SQSTM1 is recruited to Lm Δ*actA* in NDP52-depleted cells (Mostowy *et al.*, 2011). In SQSTM1-depleted cells, NBR1 and NDP52 have been shown to deliver *Burkholderia cenocepacia* to the autophagosome (Abdulrahman *et al.*, 2013). It has also been published that the majority of the SQSTM1-positive population of *F. tularensis* is also positive for NBR1 (Chong *et al.*, 2012). These findings signify the existence of a possible co-operation between autophagy adaptors. NBR1 has been proposed to be a likely candidate to compensate for the loss of SQSTM1 (Johansen and Lamark, 2011). Therefore, it could be possible that because of the presence of two LIRs, NBR1 could lead to more autophagic degradation of the Lm Δ*actA* strains. Further investigation in this direction is very much warranted. LIR1 and LIR2 deletion mutants of NBR1 can be used to transfect cells and the intracellular growth of Lm Δ*actA* strains can be monitored in these transfected cells to see if the absence of either one or both of the LIRs leads to increased Lm Δ*actA* growth. Additionally, high intracellular numbers of Lm Δ*actA21* were observed, in both SQSTM1-depleted and non-depleted cells. Lm Δ*actA21* is a mutant of Lm EGD-e which is non-motile and lacks the actin binding region, the Arp2/3 complex binding region and the VASP binding region (Yoshikawa *et al.*, 2009). Lm Δ*actA2* is also non-motile and lacks the entire region from aa 20–602, which includes the actin binding region, the Arp2/3 complex binding region, the VASP binding region and the C-terminal domain. Preliminary immunofluorescence data from our lab suggests that in HeLa cells, both Lm Δ*actA21* and Lm Δ*actA2* form clumps in the cytoplasm due to their inability to perform actin-mediated movement. However, the clumps formed by Lm Δ*actA2* in the cytoplasm were localized to a smaller region, whereas those formed by

Lm∆*actA21* were spread out over a wider region in the cytoplasm (Helena Pillich; unpublished data from our lab). This spreading-out of Lm∆*actA21* clumps could imply that Lm∆*actA21* may be capable of actin-independent intracellular movement. Apart from the actin-myosin system, cells also contain the tubulin-dynein system for motility. Dynein is a motor protein which causes sliding of microtubules in cilia and flagella (Gibbons and Rowe, 1965). Tubulins are proteins which constitute microtubules (Mohri, 1968). It has been published that the *S. flexneri* virulence factor VirA cleaves α-tubulin present in microtubules and thus creates a tunnel in the host cell cytoplasm, thereby facilitating bacterial movement in the cytoplasm (Yoshida *et al.*, 2006). It may be possible that like *S. flexneri*, Lm∆*actA21* may also be capable of tubulin-mediated movement in the cytoplasm. Pfeuffer *et al.* (2000) have demonstrated that stathmin, a microtubule-sequestering protein present in host cells, is recruited by *L. monocytogenes* to possibly de-stabilize microtubules and permit bacterial movement in the cytoplasm. They have also reported that Lm∆*actA2* is incapable of stathmin recruitment. Based upon this finding, it can be speculated that Lm∆*actA21* may be capable of stathmin-mediated movement in the host cell cytoplasm. Therefore, these two factors (tubulin/stathmin-mediated movement) may be responsible for the high intracellular numbers of Lm∆*actA21* observed in the results obtained in this thesis. Further investigation in this regard, i.e. monitoring the growth of Lm∆*actA21* in tubulin-depleted or stathmin-depleted cells would provide evidence to strengthen this speculation. Another probable explanation for the high intracellular numbers of Lm∆*actA21* could be that it may be capable of more invasion and intracellular growth, as compared to the other *L. monocytogenes* strains.

NDP52 or CALCOCO2 and its paralog TAX1BP1 are the two other autophagy adaptors which target ubiquitinated substrates to autophagy. Thurston *et al.* (2009) have reported that the siRNA-mediated depletion of NDP52 results in increased intracellular proliferation of *S.* Typhimurium and *S. pyogenes*. Therefore, a similar experiment was performed with Lm EGD-e and Lm∆*actA2*. It was observed that NDP52 knockdown resulted in

increased growth of Lm EGD-e, but not that of LmΔ*actA2*. This finding can be attributed to the fact that because LmΔ*actA2* cannot move in the cytosol, it is more ubiquitinated as compared to Lm EGD-e. This heavily ubiquitinated LmΔ*actA2* is probably targeted by the other autophagy adaptors simultaneously and, hence, is degraded. The findings reported by Mostowy *et al.* (2011) also support this premise. They have reported an independence in SQSTM1 and NDP52 recruitment in case of LmΔ*actA2*, as is evident by the increase in SQSTM1 positive LmΔ*actA2* after NDP52 knockdown, and *vice versa* (Mostowy *et al.*, 2011).

Galectins are cytosolic lectins which bind to glycans exposed on damaged vesicles that contain β-galactosides. Thurston *et al.* (2012) have published that galectin 8 binds to host cell glycans on damaged SCVs, recruits NDP52 and leads to the autophagic degradation of *S.* Typhimurium. siRNA-mediated knockdown of galectin 8 causes enhanced proliferation of *S.* Typhimurium (Thurston *et al.*, 2012). Moreover, it is also known that galectins 3, 8 and 9 accumulate around *L. monocytogenes* (Thurston *et al.*, 2012). LmΔ*actA* is capable of lysing the phagosome by the secretion of LLO and coming out into the host cell cytosol, but unlike Lm EGD-e, it is unable to move in the cytosol. Because LmΔ*actA* is incapable of movement in the cytosol, a part of its population could be associated with the LLO-damaged phagosomal membrane remnants. Galectins may bind to these damaged membrane remnants and recruit NDP52, which could lead to the autophagic degradation of LmΔ*actA*. Therefore, studying the intracellular growth of *L. monocytogenes*, particularly that of LmΔ*actA*, in galectin-depleted cells would also shed light on the interaction of NDP52 and galectins during *L. monocytogenes* infection. One could argue that if this was the case, the knockdown of NDP52 should have led to an increase in the intracellular growth of LmΔ*actA2*. But this was not observed, most likely because LmΔ*actA2* is heavily ubiquitinated, the ubiquitin molecules binding to it could recruit the other autophagy cargo receptors simultaneously, which could finally lead to its autophagic degradation.

IV. Discussion

Currently, there is very scant knowledge about TAX1BP1 as an autophagy cargo receptor. So far, no report has demonstrated its role in xenophagy. Because it is a paralog of NDP52, the role of TAX1BP1 in the mediation of autophagy during *L. monocytogenes* infection was analysed. The loss of TAX1BP1 resulted in increased growth of Lm EGD-e, but had no effect on the growth of Lm*Δactα2*. As observed with NDP52, this too might be a consequence of Lm*Δactα2* being targeted by the other autophagy adaptors, leading to its eventual autophagic degradation.

In concordance with published studies (Wild *et al.*, 2011), the findings reported in this thesis also showed that the overexpression of OPTN and TBK1 resulted in the phosphorylation of OPTN. Some phosphorylation was also observed in HeLa cells transfected with OPTN alone, as well as in those transfected with OPTN and the kinase-deficient TBK1. This phosphorylation can be attributed to the fact that some basal level of OPTN phosphorylation occurs normally in unstimulated cells, due to the intrinsic low level expression of OPTN and TBK1.

In this work, it could be shown that HeLa cells infected with *L. monocytogenes* showed OPTN phosphorylation. The data reported in this thesis, apparently, for the first time, provide evidence that OPTN is recruited to intracellular *L. monocytogenes*. Three independent lines of investigation revealed the role of OPTN in mediating the restriction of the intracellular growth of *L. monocytogenes*. Firstly, the knockdown of OPTN resulted in a two-fold increase in the intracellular growth of Lm EGD-e, and secondly, the inhibition of OPTN phosphorylation by treatment with a TBK1 inhibitor (BX-795) also led to an increase in the intracellular growth of *L. monocytogenes*. Thirdly, a significant decrease in intracellular Lm EGD-e growth was a consequence of the overexpression of OPTN and TBK1. These findings strongly and unambiguously support the hypothesis that OPTN plays an important role in the control of *L. monocytogenes* infection. By binding to ubiquitinated *L. monocytogenes*, OPTN directs the components of the autophagosome membrane, namely LC3, to form an enclosure around the bacterium and mediate its degradation. The decrease and increase in the

intracellular growth of *L. monocytogenes* after OPTN and TBK1 over-expression, and BX-795 treatment, respectively, are concordant with the findings reported by Wild *et al.* (2011) with regard to *S.* Typhimurium. Hence, the TBK1-mediated phosphorylation of OPTN is crucial for the enhanced autophagic degradation of *L. monocytogenes*. TBK1 also phosphorylates SQSTM1 at Ser-403 (Pilli *et al.*, 2012), and also NDP52, therefore, it cannot be ruled out that the overexpression of TBK1 or its inhibition by BX-795 may also affect the levels of SQSTM1 and NDP52, and this might also be responsible for the results obtained after the overexpression and inhibition of TBK1. This point can be addressed by knocking down SQSTM1 or NDP52, and then overexpressing TBK1 or inhibiting it by treatment with BX-795. The intracellular bacterial growth can then be monitored to see if these results are due to the phosphorylation of OPTN by TBK1 or by the phosphorylation of SQSTM1 or NDP52 by TBK1.

It is well-known that *L. monocytogenes* infection leads to increased conversion of LC3-I to LC3-II (Py *et al.*, 2007). Therefore, it was imperative to investigate if the loss of OPTN from cells affects LC3 levels after *L. monocytogenes* infection. The siRNA-mediated knockdown of OPTN in HeLa cells led to a decrease in LC3-II levels following infection with Lm EGD-e. On the basis of this result, it can be hypothesized that when OPTN bound to ubiquitinated *L. monocytogenes*, its LIR interacted with LC3. This, in turn, could mediate the autophagic degradation of *L. monocytogenes*. The phosphorylation of OPTN by TBK1 could enhance the LC3 binding by OPTN and further boost the degradation process. However, in the absence of OPTN, the autophagic degradation was compromised, which resulted in lower LC3-II to LC3-I ratios. Strategies to induce OPTN phosphorylation may, therefore, prove to be good therapeutic options to combat infection by *L. monocytogenes*. Because a decline in the ratio of LC3-II to LC3-I was observed after OPTN knockdown, it was assumed that the depletion of the other autophagy cargo receptors would also lead to similar results.

It was thought that because LmΔ*actA2*, LmΔ*actA16* and LmΔ*actA21* undergo relatively more ubiquitination and autophagy as compared to Lm EGD-e, they

may also show increased intracellular growth after OPTN knockdown. Unexpectedly, there was no difference in the intracellular growth of any of the three bacteria in OPTN-depleted cells. A possible explanation for this observation could be that the ubiquitin molecules attached to the ActA mutants act as “eat me” signals and may simultaneously recruit the other autophagy cargo receptors to them. This attachment of ubiquitin molecules to these bacteria could result in their simultaneous recognition by all cargo receptors and subsequently, their degradation. It can be deduced from these observations that autophagy adaptors may act in tandem in case of infection with LmΔ*actA*: when OPTN is absent, the other adaptors could mediate the degradation of LmΔ*actA*. Lm EGD-e, on the other hand, is capable of cytosolic movement, and is ubiquitinated to a lesser extent as compared to LmΔ*actA* (Yoshikawa *et al.*, 2009). Therefore, it may not be simultaneously degraded by all adaptors at once. As speculated previously, the high intracellular numbers of LmΔ*actA21* could be attributed either to tubulin/stathmin-mediated movement, or due to higher invasion and intracellular growth shown by it.

It could also be shown that both the UBD and LIR domains were critical for the binding of OPTN to Lm EGD-e and LmΔ*actA2*, as is evident by the lack of a significant amount of co-localization of bacteria with the OPTN E478G and OPTN F178A mutants. These results are in concordance with the findings of Wild *et al.* (2011), who have shown that OPTN binding to *S.* Typhimurium is dependent on its ubiquitin and LC3-binding domains. Moreover, it is also known that SQSTM1 binding to *L. monocytogenes* also requires its UBD and LIR domains (Yoshikawa *et al.*, 2009).

NBR1 has been identified as an autophagy cargo receptor for the selective degradation of protein inclusions by Kirkin *et al.* (2009). It has also been shown to be recruited to *F. tularensis* (Chong *et al.*, 2012) and *S. flexneri* (Mostowy *et al.*, 2011). Apparently, so far, there is no reported study which describes the interaction of NBR1 with *L. monocytogenes*. In the present study, an increase in the intracellular growth of both Lm EGD-e as well as LmΔ*actA2* was observed in cells which lack NBR1. NBR1 was found to be

the only autophagy adaptor which regulated the selective degradation of both Lm EGD-e and Lm Δ*actA2*. Moreover, the increase in the intracellular growth of Lm EGD-e (2.9-fold) and Lm Δ*actA2* (1.9-fold) in NBR1-depleted cells was more than that observed with the knockdown of any of the other autophagy adaptors. Therefore, it can be proposed that among all the known autophagy adaptors, NBR1 may play the most important role in mediating the degradation of *L. monocytogenes*. The presence of two distinct LIRs in NBR1 has been revealed, one between aa 727–738, and another between aa 542–636 (Kirkin *et al.*, 2009). The GST pull-down experiments using members of the LC3/GABARAP families have shown that both these LIRs are capable of interacting with ATG8, although it is the former which mainly interacts with ATG8-like proteins. Therefore, the increase in the intracellular growth of Lm Δ*actA2* after NBR1 knockdown jells well with this observation by Kirkin *et al.* (2009). It might be that due to the presence of two LIRs, NBR1 could mediate more autophagic degradation of Lm EGD-e and Lm Δ*actA2* as compared to any other autophagy adaptor. The structure of the ubiquitin-binding domain of NBR1 has been recently published (Walinda *et al.*, 2014). The authors report that due to the structural differences between the UBDs of NBR1 and SQSTM1, NBR1 has a much higher affinity to bind ubiquitin as compared to SQSTM1. On the basis of this stand-point, it can be speculated that because of higher affinity for ubiquitin, NBR1 may bind to Lm EGD-e and Lm Δ*actA2* (which is relatively more ubiquitinated than Lm EGD-e) more efficiently as compared to the other autophagy adaptors, and hence it may lead to more autophagic degradation of these bacteria. This, in all probability, is one good reason as to why the maximum increase in the intracellular growth of Lm EGD-e and Lm Δ*actA2* was observed after NBR1 knockdown.

Mostowy *et al.* (2011) have reported that in NBR1-depleted HeLa cells, the recruitment of SQSTM1 and NDP52 to *S. flexneri* is reduced. Their observation can also stand to be a good explanation for our herein reported observation of the increase in the intracellular growth of both Lm EGD-e and Lm Δ*actA2*, after the knockdown of NBR1. It could be possible that because the depletion of NBR1 could also lead to a reduction of SQSTM1 and NDP52

levels, an increase in the intracellular growth of LmΔ*actA2* was evident. Another probable explanation for our observations could be that the LLO-damaged phagosomal membrane enclosing LmΔ*actA* is also ubiquitinated. In addition to binding to ubiquitinated LmΔ*actA*, NBR1 could also bind to the ubiquitinated LLO-damaged phagosomal membrane which encloses LmΔ*actA*, and consequently link it to the autophagosomal membrane. This phenomenon could result in NBR1 being the main autophagy cargo receptor for *L. monocytogenes*, as is evident by the observed increase in the intracellular growth of both Lm EGD-e and LmΔ*actA*. As per current knowledge, apparently, there is no report on the interaction of NBR1 with damaged membrane remnants. Future investigations in this regard may provide much needed support for this hypothesis; it will be discussed further in the outlook section of this thesis. Fig. 4.1 depicts a proposed model for the binding of autophagy cargo receptors to *L. monocytogenes*, based upon the findings reported in this study.

Thus, the binding of autophagy cargo receptors to *L. monocytogenes* mediates its degradation by selective autophagy. The employment of five distinct autophagy cargo receptors to *L. monocytogenes* might be a significant survival strategy by the cell to ensure maximal targeting of cytosol-exposed *L. monocytogenes*. However, just like *L. monocytogenes* has evolved strategies to evade autophagy, whether or not it has also adopted some mechanisms to evade recognition by autophagy cargo receptors, or to exploit the binding of autophagy cargo receptors for its own intracellular survival and growth, remains an open question.

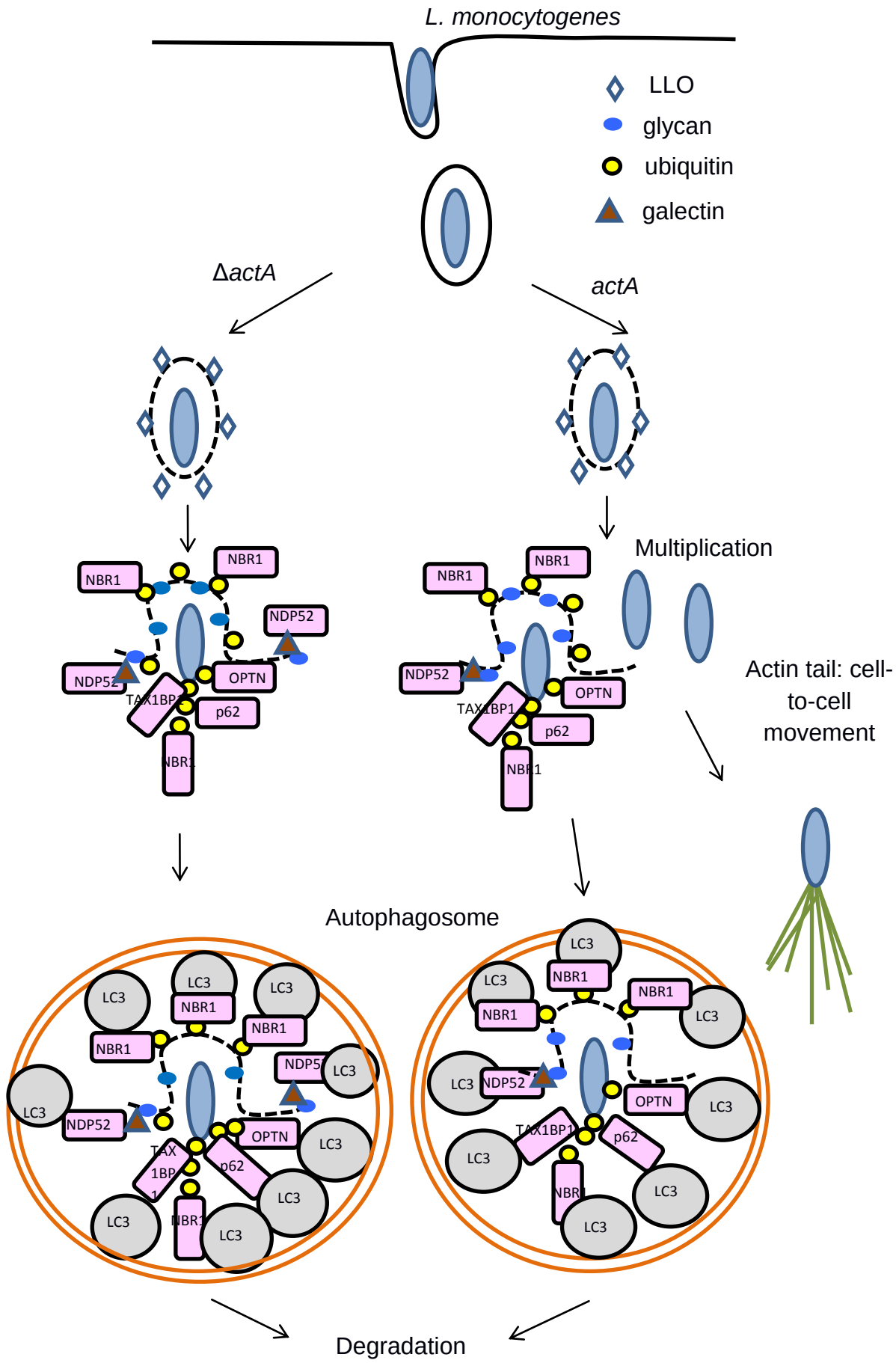
L. monocytogenes
LLO
glycan
ubiquitin
galectin
ΔactA
actA
Multiplication
Actin tail: cell-to-cell movement
Autophagosome
Degradation
NBR1
NDP52
OPTN
p62
TAX1BP1
LC3

Fig. 4.1: Model for the binding of autophagy cargo receptors to *L. monocytogenes*. Intracellular *L. monocytogenes* is trapped within a phagosomal vacuole. It expresses the *hly* gene which leads to the lysis of the phagosomal vacuole by LLO. *L. monocytogenes* may still be associated with phagosomal membrane remnants and glycans present in the vacuole are recognized by galectins. This leads to the ubiquitination of *L. monocytogenes* and the recruitment of autophagy cargo receptors. *L. monocytogenes* which expresses *actA* polymerizes actin and forms an actin tail at one end of the bacilli. A population of these bacilli is targeted by autophagy cargo receptors which link it to the autophagosomal membrane and lead to its degradation. LLO-damaged phagosomal membrane remnants may also get ubiquitinated and NBR1 may link them to the autophagosomal membrane. Another population of *actA*-expressing *L. monocytogenes* moves to the neighbouring cell. On the other hand, the autophagy cargo receptors binding ubiquitinated *L. monocytogenes* which lack *actA* link it to the autophagosomal membrane. This results in the autophagic degradation of LmΔ*actA*.

An interesting observation which was observed in the present study was that the intracellular numbers of Lm EGD-e and LmΔ*actA2* were similar in HeLa cells transfected with control siRNA. This is in contrast to the findings reported by Yoshikawa *et al.* (2009), who have shown that the intracellular survival of LmΔ*actA2* is lower than that of Lm EGD-e in MDCK cells and MEFs. A plausible explanation for this contradiction could be that as observed in immunofluorescence analysis, a part of the population of Lm EGD-e and LmΔ*actA2* could be able to lyse the autophagosome by the action of LLO and escape out into the cytoplasm and, hence the entire bacterial population would not be degraded by autophagy, which, in turn, could result in similar rates of intracellular survival of Lm EGD-e and LmΔ*actA2*. Another reason for this contradiction could be the difference in cell lines used: MDCK cells and MEFs were used in the report by Yoshikawa *et al.* (2009), while HeLa cells have been used in the present study. Moreover, in the present study, it was also observed that even though SQSTM1, NDP52, OPTN and TAX1BP1 were recruited to LmΔ*actA2*, depletion of either one of these adaptors did not result in an increase in the intracellular growth of LmΔ*actA2*. A probable reason for this could be that because LmΔ*actA2* is heavily ubiquitinated, when either one of these adaptors is knocked down, the remaining adaptors may mediate the autophagic degradation of LmΔ*actA2*.

Another important finding seen in the present study was the difference in the intracellular growth ratio of Lm EGD-e after the knockdown of each of the

autophagy adaptors as compared to the control. Knockdown of SQSTM1 led to a 2-fold increase in Lm EGD-e growth, knockdown of NDP52 led to a 1.4-fold increase, knockdown of OPTN resulted in a 2.2-fold increase, depletion of TAX1BP1 resulted in a 1.8-fold increase and the depletion of NBR1 led to a 2.9-fold increase in the intracellular growth of Lm EGD-e. Thus, from these differences, it can be deduced that *L. monocytogenes* may be targeted by autophagy adaptors at different time-points during infection. A strategy for further investigation in this regard is discussed in the outlook section of this thesis.

4.3 *In vivo* and clinical relevance

The results reported in this thesis, have been generated by conducting experiments, *in vitro*. It should be emphasized here that the study of a group of autophagy cargo receptors using an isolated population of HeLa cells, *in vitro*, may just be gross oversimplification of the events occurring *in vivo*, as essentially various other autophagy-related events may also occur during infections. Therefore, the results reported herein have their own limitations, and there is need to sublimate them to *in vivo* situations, and finally to translational studies to make them clinically useful.

There are various experimental animal model systems for the study of the *L. monocytogenes* infection, the most widely used being mice (Marco *et al.*, 1997), *Drosophila melanogaster* (Mansfield *et al.*, 2003), *Galleria mellonella* (Mukherjee *et al.*, 2010) and zebrafish (Levraud *et al.*, 2009). *L. monocytogenes* infection of SQSTM1, NDP52, OPTN, NBR1 and TAX1BP1 knock-out mice can be expected to be the most relevant and useful model to monitor intracellular bacterial growth and host survival, in order to determine whether the *in vitro* findings reported herein hold true *in vivo*, or not. More pointedly, it has recently been reported that the morpholino-based knockdown of SQSTM1 reduces zebrafish survival in response to *S. flexneri* infection (Mostowy *et al.*, 2013). Because *S. flexneri* and *L. monocytogenes* are both facultative intracellular pathogens targeted by autophagy, it may just

be possible that this result holds true for *L. monocytogenes* as well. Therefore, efforts should be made to adopt a similar strategy by using morpholinos to selectively knock down a few or all the autophagy cargo receptors in *Galleria*, *Drosophila* or zebrafish, infect them with *L. monocytogenes*, and then compare the course of infection and survival rate in both the sufficient and the deficient organisms.

The results obtained in this thesis have the potential to be translated into clinical settings. The induction of autophagy is known to control infection (Van Limbergen *et al.*, 2009). There have been previous attempts to employ commonly used autophagy inducers like rapamycin for therapeutic applications, however, numerous side effects have jeopardized this strategy. Rapamycin has been shown to repress the translation of many proteins, and also lead to immunosuppression (Van Limbergen *et al.*, 2009). Moreover, rapamycin is thought to induce non-selective autophagy, and as per current knowledge, there is no report showing a change in the intracellular level of autophagy cargo receptors after rapamycin treatment. Therefore, both experimental and clinical researches need to be done on strategies to up-regulate the recruitment of autophagy receptors to *L. monocytogenes* and other intracellular bacteria, which can be used as either stand-alone or an adjunct to currently used anti-bacterial therapies for the treatment of various bacterial infections.

V. Outlook

Outlook

The most important finding reported in this dissertation is the involvement of all the five known autophagy cargo receptors, i.e. SQSTM1, OPTN, NBR1, NDP52 and TAX1BP1 in the autophagy of *L. monocytogenes, in vitro*.

In this study, it was observed that OPTN depletion had no effect on the intracellular growth of LmΔ*actA2*. siRNA-based experiments with SQSTM1, NDP52 and TAX1BP1 also had similar outcomes, wherein only the intracellular growth of Lm EGD-e increased, whereas that of LmΔ*actA2* was either unaffected or decreased (as with SQSTM1). However, NBR1 had the distinction of being the only autophagy cargo receptor whose absence led to increased intracellular growth of both Lm EGD-e and LmΔ*actA2*. Further investigations, especially at molecular level, are needed to be undertaken in order to elucidate the mechanism of the binding of autophagy adaptors to *L. monocytogenes*. Immunofluorescence analysis can elaborate whether all the autophagy cargo receptors bind to the same domain of *L. monocytogenes*, or to different ones. Monitoring the intracellular growth of *L. monocytogenes* after galectin knockdown will reveal the importance of galectin-NDP52 interaction during *L. monocytogenes* infection. Immunofluorescence studies can also demonstrate if there are differences in galectin binding between LmΔ*actA* mutants.

Dupont *et al.* (2009) have reported that damaged vacuole remnants of *L. monocytogenes* are ubiquitinated and labelled with SQSTM1 and LC3. Because SQSTM1 and NBR1 are paralogs, it is highly probable that NBR1 may also bind to damaged membrane remnants. Immunofluorescence microscopy can be used to check for co-localization between NBR1 and galectin 3 (a widely used marker for membrane remnants) in cells infected with *L. monocytogenes*.

The results obtained in this study suggest a possible co-operation among autophagy adaptors in mediating the degradation of LmΔ*actA2*, as is evident by the lack of increase in the intracellular growth of LmΔ*actA2* after SQSTM1, OPTN, NDP52 and TAX1BP1 knockdown. Silencing of two or

more of these autophagy adaptors together will confirm this suggestion. If the knockdown of two or more autophagy adaptors together results in an increase in the intracellular growth of LmΔ*actA2*, it would mean that the autophagy adaptors act in tandem to mediate the autophagy of LmΔ*actA2*.

The differences observed in the intracellular growth ratio of Lm EGD-e after the knockdown of each of the autophagy cargo receptors, as compared to control cells, indicate that *L. monocytogenes* might be targeted by cargo receptors at different time-points of infection. In order to see which cargo receptor binds at which stage of infection, time-lapse microscopy can be used to observe the recruitment of cargo receptors to *L. monocytogenes* at various time-points following infection.

Infection with *L. monocytogenes* induces the unfolded protein response (UPR), and activates all the three branches of UPR, namely the ATF6, PERK and IRE1 pathways (Pillich *et al.*, 2012). Activation of the UPR also leads to autophagy (Yorimitsu *et al.*, 2006). It will be intriguing to investigate if the silencing of UPR pathways affects the recruitment of autophagy adaptors to *L. monocytogenes*; immunofluorescence microscopy can be used towards this end. Alternatively, cells depleted of autophagy adaptors can be infected with *L. monocytogenes*, and the activation of the UPR can be monitored by Western blotting or real time PCR. These studies will demonstrate if cellular defence mechanisms are interdependent in combatting infection.

It is already known that *L. monocytogenes* is sensitive to interferon-γ-mediated killing (Khor *et al.*, 1986). Interferon-γ is known to induce both autophagy (Gutierrez *et al.*, 2004) and caspase-11 activation (Kano *et al.*, 1999). Therefore, examination of caspase 11 levels following infection with Lm EGD-e and LmΔ*actA* would also shed some light on the differences in the induction of host cell defences against the two bacterial strains.

VI. Summary

Summary

The data presented in this study shed light on the involvement of all the known five autophagy cargo receptors (also known as autophagy adaptors) i.e. SQSTM1, NDP52, OPTN, NBR1 and TAX1BP1, in mediating the restriction of the intracellular growth of *L. monocytogenes*. The involvement of the three autophagy adaptors: OPTN, NBR1 and TAX1BP1, previously unknown to link *L. monocytogenes* to the autophagosomal membrane, has been identified. The phosphorylation of OPTN by TBK1 was essential for the growth restriction of *L. monocytogenes*. NBR1 seems to be the most important autophagy cargo receptor for *L. monocytogenes*, as it was the only one to restrict the growth of both Lm EGD-e and Lm Δ*actA2*. NBR1 knockdown also resulted in the highest increase in the intracellular growth of Lm EGD-e (2.9-fold) and Lm Δ*actA2* (1.9-fold), as compared to the other cargo receptors. With the exception of NBR1, the absence of all the other autophagy cargo receptors: OPTN, SQSTM1, NDP52 and TAX1BP1, only led to increased intracellular loads of Lm EGD-e, but not those of Lm Δ*actA2*. Because of its inability to move within the host cell cytosol after its escape from the phagosomal compartment, Lm Δ*actA* is much more ubiquitinated than Lm EGD-e. This may lead to the simultaneous binding of several autophagy cargo receptors to Lm Δ*actA*, thereby linking it to the autophagosomal membrane for its subsequent degradation. Lm EGD-e, on the other hand, is capable of intracellular movement by means of the ActA protein. It is, therefore, susceptible to autophagy at different stages, like at the time of multiplication in the cytoplasm, or while entering from one cell to the other, and all the five known autophagy adaptors are capable of recruiting it to the autophagosome. A part of the population of Lm EGD-e that is free in the cytoplasm is targeted by autophagy, while another part of this population forms an actin tail and moves from one cell to the other.

VII. Zusammenfassung

Zusammenfassung

Die Daten in dieser Studie geben Aufschluss über die Beteiligung aller fünf bekannten Autophagie-Cargo-Rezeptoren (auch als Autophagie-Rezeptoren bezeichnet), d.h. SQSTM1, NDP52, OPTN, NBR1 und TAX1BP1, bei der Einschränkung des intrazellulären Wachstums von *L. monocytogenes*. Die Mitwirkung der drei Autophagie-Rezeptoren OPTN, NBR1 und TAX1BP1 bei der Bindung von *L. monocytogenes* an die Autophagosomen-Membran wurde hier erstmals beschrieben. Die Phosphorylierung von OPTN durch TBK1 ist hierbei von entscheidender Bedeutung für die Wachstumsrestriktion von *L. monocytogenes*. NBR1 übernimmt wahrscheinlich die Hauptfunktion als Autophagie-Rezeptor für *L. monocytogenes*, da er sowohl das Wachstum von Lm EGD-e als auch von LmΔ*actA2* einschränkt. Der knock-down von NBR1 mit siRNA führte zur höchsten Zunahme des intrazellulären Wachstums von Lm EGD-e (2,9-fach) und LmΔ*actA2* (1,9-fach) im Vergleich zum knock-down aller anderen Autophagie-Rezeptoren. Im Gegensatz zu NBR1 führte der knock-down aller anderen Autophagie-Rezeptoren nur zu einer Zunahme des Wachstums von Lm EGD-e, aber nicht von LmΔ*actA2*. Da sich LmΔ*actA2* nach seiner Freisetzung aus dem Phagosom nicht bewegen kann, ist es im Vergleich zu Lm EGD-e viel stärker ubiquitiniert. Das erlaubt die gleichzeitige Bindung mehrerer Autophagie-Rezeptoren an LmΔ*actA2* mit anschließender Kopplung an die Autophagosomen-Membran und bakteriellen Abbau. Im Gegensatz zu LmΔ*actA2* kann sich Lm EGD-e mit Hilfe des ActA Proteins intrazellulär bewegen. Es ist deshalb zu verschiedenen Zeitpunkten anfällig für Autophagie: bei der Vermehrung im Zytoplasma oder beim Befall der nächsten Wirtszelle. Alle fünf Autophagie-Rezeptoren können die ubiquitinierten Bakterien an das Autophagosom koppeln. Ein freibeweglicher Anteil von Lm EGD-e wird im Zytoplasma gezielt durch Autophagie beseitigt, während andere Lm EGD-e Bakterien einen Aktin-Schwanz bilden und die nächste Zelle infizieren.

VIII. List of abbreviations

List of abbreviations

α	alpha
aa	amino acid
A	Ampere
APS	ammonium peroxidisulphate
Arp	actin-related protein
ATG	autophagy-related gene
β	beta
BCA	Bicinchoninic acid
BHI	brain heart infusion
BSA	bovine serum albumin
°C	degree Celsius
CFU	colony-forming unit
CHAPS	3-[(3-cholamidopropyl) dimethylammonio]-1-propanesulfonate
cm	centimeter
ddH_2O	double distilled water
DAPI	4',6-diamidino-2-phenylindole
DNA	deoxyribonucleic acid
DMEM	Dulbecco's modified Eagle medium
DMSO	dimethylsulphoxide
E	glutamic acid
ECL	enhanced chemiluminescence

VIII. List of abbreviations

ER	endoplasmic reticulum
E. coli	*Escherichia coli*
et al.	et alii
F	phenylalanine
FBS	foetal bovine serum
g	gram
GABARAP	gamma-aminobutyric acid receptor-associated protein
h	hour
HBSS	Hank's balanced salt solution
HeLa	human epithelial cell line derived from cells taken from Henrietta Lacks
HEPES	4-(2-hydroxyethyl)-1-piperazineethane-sulfonic acid
HRP	horseradish peroxidase
IF	immunofluorescence
IgG	Immunoglobulin G
Inl	internalin
K	kilo [10^3]; also lysine
kDa	kilodalton
Lm	*Listeria monocytogenes*
l	litre
LB	Luria Bertani
LC3	microtubule-associated protein 1 light chain 3

VIII. List of abbreviations

LIR	LC3-interacting region
LLO	listeriolysin O
µ	micro [10^{-6}]
m	milli [10^{-3}]
M	molar
min	minute(s)
MDCK	Madine-Darby canine kidney cells
MEF	mouse embryonic fibroblast
MOI	multiplicity-of-infection
mQH_2O	Millipore filtered water
mRNA	messenger RNA
MTT	3-(4,5-dimethylthiazol-2-yl)-2,5-diphenyltetra-zolium bromide
MVP	major vault protein
n	nano [10^{-9}]
Nap1	nucleosome assembly protein 1
NBR1	neighbor of BRCA1 gene 1
NDP52	nuclear dot protein 52
OD	optical density
OPTN	optineurin
PAGE	polyacrylamide gel electrophoresis
PB1	Phox and Bem1p
PBS	phosphate-buffered saline

VIII. List of abbreviations

PKC	protein kinase C
Plc	phospholipase
PMSF	phenylmethanesulfonylfluoride
PVDF	polyvinylidenefluoride
rcf	relative centrifugal force
RIPA	radioimmunoprecipitation assay
RNA	ribonucleic acid
rpm	revolutions per minute
RT	room temperature
SCV	*Salmonella*-containing vacuole
SDS	sodium dodecyl sulphate
s	second(s)
Ser	serine
Sintbad	similar to Nap1 TBK1 adaptor
siRNA	small interfering RNA
SKICH	skeletal muscle and kidney-enriched inositol phosphate carboxyl homology
S. Typhimurium	*Salmonella enterica* serovar Typhimurium
SQSTM1	sequestosome 1
TANK	TRAF family member-associated NFκB activator
TAX1BP1	TAX1 binding protein 1
TBK1	TANK-binding kinase 1
TBS	tris-buffered saline

VIII. List of abbreviations

TEMED	tetramethylethylenediamine
Tris	tris (hydroxymethyl) aminomethane
Tween-20	polyoxyethylene (20) sorbitan monolaurate
UBD	ubiquitin-binding domain
V	volt
VASP	vasodilator-stimulated phosphoprotein
(v/v)	volume per volume
(w/v)	weight per volume
WB	Western blot
WT	wild type

IX. List of figures and tables

9.1 List of figures

IX. List of figures and tables

IX. List of figures and tables

9.2 List of tables

X. References

References

Abdulrahman, B. A., Khweek, A. A., Akhter, A., Caution, K., Tazi, M., Hassan, H., Zhang, Y., *et al.* 2013. “Depletion of the Ubiquitin-Binding Adaptor Molecule SQSTM1/p62 from Macrophages Harboring Cftr ΔF508 Mutation Improves the Delivery of *Burkholderia cenocepacia* to the Autophagic Machinery.” *The Journal of Biological Chemistry* 288 (3) (January 18): 2049-58.

Al-Khodor, S., Marshall-Batty, K., Nair, V., Ding, L., Greenberg, D. E., and Fraser, I. D. 2014. “*Burkholderia cenocepacia* J2315 Escapes to the Cytosol and Actively Subverts Autophagy in Human Macrophages.” *Cellular Microbiology* 16 (3) (March): 378-95.

Alouf, J. E. and Geoffroy, C. 1991. "The Family of the Antigenically-Related, Cholesterol-Binding ('Sulfhydryl-Activated') Cytolytic Toxins." *Sourcebook of Bacterial Protein Toxins, Academic Press, London, U. K.*:147-186.

Al-Younes, H. M., Al-Zeer, M. A., Khalil, H., Gussmann, J., Karlas, A., Machuy, N., Brinkmann, V., Braun, P. R., and Meyer, T. F. 2011. “Autophagy-Independent Function of MAP-LC3 during Intracellular Propagation of *Chlamydia trachomatis*.” *Autophagy* 7 (8) (August): 814-828.

Anand, P. K., Tait, S. W., Lamkanfi, M., Amer, A. O., Nunez, G., Pagès, G., Pouysségur, J., *et al.* 2011. "TLR2 and RIP2 Pathways Mediate Autophagy of *Listeria monocytogenes* via Extracellular Signal-Regulated Kinase (ERK) Activation." *The Journal of Biological Chemistry* 286 (50) (December 16): 42981-91.

Birmingham, C. L., Canadien, V., Gouin, E., Troy, E. B., Yoshimori, T., Cossart, P., Higgins, D. E., and Brumell, J. H. 2007. “*Listeria monocytogenes* Evades Killing by Autophagy during Colonization of Host Cells.” *Autophagy* 3 (5) (September-October): 442-51.

Birmingham, C. L., Canadien, V., Kaniuk, N. A., Steinberg, B. E., Higgins, D. E., and Brumell, J. H. 2008. "Listeriolysin O Allows *Listeria monocytogenes* Replication in Macrophage Vacuoles." *Nature* 451 (7176) (January 17): 350-4.

Birmingham, C. L., Smith, A. C., Bakowski, M. A., Yoshimori, T., and Brumell, J. H. 2006. “Autophagy Controls *Salmonella* Infection in Response to Damage to the *Salmonella*-Containing Vacuole.” *The Journal of Biological Chemistry* 281 (16) (April 21): 11374-83.

Bjørkøy, G., Lamark, T., Brech, A., Outzen, H., Perander, M., Overvatn, A., Stenmark, H., and Johansen, T. 2005. “p62/SQSTM1 Forms Protein Aggregates Degraded by Autophagy and Has a Protective Effect on

Huntingtin-Induced Cell Death." *The Journal of Cell Biology* 171 (4) (November 21): 603-14.

Boyle, K. B., and Randow, F. 2013. "The Role of 'Eat-Me' Signals and Autophagy Cargo Receptors in Innate Immunity." *Current Opinion in Microbiology* 16 (3) (June): 339-48.

Bubert, A., Sokolovic, Z., Chun, S. K., Papatheodorou, L., Simm, A., and Goebel, W. 1999. "Differential Expression of *Listeria monocytogenes* Virulence Genes in Mammalian Host Cells." *Molecular and General Genetics: MGG* 261 (2) (March): 323-36.

Burman, C., and Ktistakis, N. T. 2010. "Autophagosome Formation in Mammalian Cells." *Seminars in Immunopathology* 32 (4) (December): 397-413.

Cemma, M., Kim, P. K., and Brumell, J. H. 2011. "The Ubiquitin-binding Adaptor Proteins p62/SQSTM1 and NDP52 are Recruited Independently to Bacteria-Associated Microdomains to Target *Salmonella* to the Autophagy Pathway." *Autophagy* 7(3) (March): 341-5.

Chakraborty, T., Ebel, F., Domann, E., Niebuhr, K., Gerstel, B., Pistor, S., Temm-Grove, C. J., *et al.* 1995. "A Focal Adhesion Factor Directly Linking Intracellularly Motile *Listeria monocytogenes* and *Listeria ivanovii* to the Actin-based Cytoskeleton of Mammalian Cells." *The EMBO Journal* 14 (7) (April 3): 1314-21.

Chong, A., Wehrly, T. D., Child, R., Hansen, B., Hwang, S., Virgin, H. W., and Celli, J. 2012. "Cytosolic Clearance of Replication-Deficient Mutants Reveals *Francisella tularensis* Interactions with the Autophagic Pathway." *Autophagy* 8 (9) (September): 1342-56.

Collins, M. D., Wallbanks, S., Lane, D. J., Shah, J., Nietupski, R., Smida, J., Dorsch, M., and Stackebrandt, E. 1991. "Phylogenetic Analysis of the genus *Listeria* Based on Reverse Transcriptase Sequencing of 16S rRNA." *International Journal of Systemic Bacteriology* 41 (2) (April): 240-6.

Cossart, P., and Mengaud, J. 1989. "*Listeria monocytogenes*. A Model System for the Molecular Study of Intracellular Parasitism." *Molecular Biology & Medicine* 6 (5) (October): 463-74.

Dabiri, G. A., Sanger, J. M., Portnoy, D. A., and Southwick, F. S. 1990. "*Listeria monocytogenes* Moves Rapidly through the Host-Cell Cytoplasm by Inducing Directional Actin Assembly." *Proceedings of the National Academy of Sciences of the United States of America* 87 (16) (August): 6068-72.

Decatur, A. L., and Portnoy, D. A. 2000. "A PEST-like sequence in Listeriolysin O Essential for *Listeria monocytogenes* Pathogenicity." *Science (New York, N. Y.)* 290 (5493) (November 3):992-5.

X. References

de Reuck, A. V. S., and Cameron, M. P. 1963. Ciba Foundation Symposium on Lysosomes. London: *J. A. Churchill Ltd.*

De Valck, D., Jin, D. Y., Heyninck, K., Van de Craen, M., Contreras, R., Fiers, W., Jeang, K. T., and Beyaert, R. 1999. "The Zinc Finger Protein A20 Interacts with a Novel Anti-Apoptotic Protein Which Is Cleaved by Specific Caspases." *Oncogene* 18 (29) (July 22): 4182-90.

Deretic, V., Saitoh, T., and Akira, S. 2013. "Autophagy in Infection, Inflammation and Immunity." *Nature Reviews Immunology* 13 (10) (October): 722-37.

Dortet, L., Mostowy, S., Samba-Louaka, A., Gouin, E., Nahori, M. A., Wiemer, E. A., Dussurget, O., and Cossart, P. 2011. "Recruitment of the Major Vault Protein by InlK: A *Listeria monocytogenes* Strategy to Avoid Autophagy." *PLoS Pathogens* 7 (8) (August): e1002168.

Dramsi, S., Dehoux, P.,Lebrun, M., Goossens, P. L., and Cossart, P. 1997. '' Identification of Four New Members of the Internalin Multigene Family of *Listeria monocytogenes* EGD.'' *Infection and Immunity* 65 (5) (May): 1615-25.

Dupont, N., Lacas-Gervais, S., Bertout, J., Paz, I., Freche, B., Van Nhieu, G. T., van der Goot, F. G., Sansonetti, P. J., and Lafont, F. 2009. "*Shigella* Phagocytic Vacuolar Membrane Remnants Participate in the Cellular Response to Pathogen Invasion and Are Regulated by Autophagy." *Cell Host & Microbe* 6 (2) (August 20): 137-49.

Farber, J. M. and Losos, J. Z. 1988. "*Listeria monocytogenes*: A Foodborne Pathogen." *Canadian Medical Association Journal* 138 (5) (March 1): 413-418.

Fujita, N., Morita, E., Itoh, T., Tanaka, A., Nakaoka, M., Osada, Y., Umemoto, T., *et al.* 2013. "Recruitment of the Autophagic Machinery to Endosomes during Infection Is Mediated by Ubiquitin." *The Journal of Cell Biology* 203 (1) (October 14): 115-28.

Gaillard, J. L., Berche, P., Frehel, C., Gouin, E., and Cossart, P. 1991. "Entry of *L. monocytogenes* into Cells Is Mediated by Internalin, a Repeat Protein Reminiscent of Surface Antigens from Gram-Positive Cocci." *Cell* 65 (7) (June 28): 1127-41.

Gal, J., Ström, A. L., Kwinter, D. M., Kilty, R., Zhang, J., Shi, P., *et al.* 2009. ''Sequestosome 1/p62 Links Familial ALS Mutant SOD1 to LC3 *via* an Ubiquitin-Independent Mechanism.'' *Journal of Neurochemistry* 111 (4) (November): 1062-73.

X. References

Geetha, T. and Wooten, M. W. 2002. "Structure and Functional Properties of the Ubiquitin Binding Protein p62." *FEBS Letters* 512 (1-3) (February 13): 19-24.

Geoffroy, C., Gaillard, J. L., Alouf, J. E., and Berche, P. 1987. "Purification, Characterization, and Toxicity of the Sulfhydryl-Activated Hemolysin Listeriolysin O from *Listeria monocytogenes*." *Infection and Immunity* 55 (7) (July): 1641-46.

Geoffroy, C., Raveneau, J., Beretti, J. L., Lecroisey, A., Vázquez-Boland, J. A., Alouf, J. E., and Berche, P. 1991. "Purification and Characterization of an Extracellular 29-kilodalton Phospholipase C from *Listeria monocytogenes*." *Infection and Immunity* 59 (7) (July): 2382-8.

Ghai, R. 2006. "*Transcriptional Response of Murine Bone Marrow Macrophages to Listeriolysin, the Pore-Forming Toxin of Listeria monocytogenes.*" Ph.D. Thesis. Justus Liebig University: Germany.

Gibbons, I. R. and Rowe, A. J. 1965. "Dynein: A Protein with Adenosine Triphosphatase Activity from Cilia." *Science (New York, N. Y.)* 149 (3682) (July 23): 424-6.

Glaser, P., Franqeul, L., Buchreiser, C., Rusniok, C., Amend, A., Baquero, F., Berche, P. *et al.* 2001. "Comparative Genomics of *Listeria* species." *Science (New York. N. Y.)* 294 (5543) (October 26): 849-52.

Goto, A., Yano, T., Terashima, J., Iwashita, S., Oshima, Y., and Kurata, S. 2010. "Cooperative Regulation of the Induction of the Novel Antibacterial Listericin by Peptidoglycan Recognition Protein LE and the JAK-STAT Pathway." *The Journal of Biological Chemistry* 285 (21) (May 21): 15731-8.

Greiffenberg, L., Goebel, W., Kim, K. S., Weiglein, I., Bubert, A., Engelbrecht, F., Stins, M. and Kuhn, M. 1998. "Interaction of *Listeria monocytogenes* with Human Brain Microvascular Endothelial Cells: InlB-dependent Invasion, Long-term Intracellular Growth, and Spread from Macrophages to Endothelial Cells." *Infection and Immunity* 66 (11) (November): 5260-7.

Gutierrez, M. G., Master, S. S., Singh, S. B., Taylor, G. A., Colombo, M. I., and Deretic, V. 2004. "Autophagy Is a Defense Mechanism Inhibiting BCG and *Mycobacterium tuberculosis* Survival in Infected Macrophages." *Cell* 119 (6) (December 17): 753-66.

Ivanov, S., and Roy, C. R. 2009. "NDP52: The Missing Link between Ubiquitinated Bacteria and Autophagy." *Nature Immunology* 10 (11) (November): 1137-39.

X. References

Jo, E. K., Yuk, J. M., Shin, D. M., and Sasakawa, C. 2013. “Roles of Autophagy in Elimination of Intracellular Bacterial Pathogens.” *Frontiers in Immunology* 4 (May 6): 97.

Johansen, T., and Lamark, T. 2011. “Selective Autophagy Mediated by Autophagic Adaptor Proteins.” *Autophagy* 7 (3) (March): 279-96.

Kajava, A. V. 1998. "Structural Diversity of Leucine-rich Repeat Proteins." *Journal of Molecular Biology* 277 (3) (April 3): 519-27.

Kano, A., Haruyama, T., Akaike, T., and Watanabe, Y. 1999. "IRF-1 is an Essential Mediator in IFN-gamma-induced Cell Cycle Arrest and Apoptosis of Primary Cultured Hepatocytes." *Biochemical and Biophysical Research Communications* 257 (3) (April 21): 672-7.

Khor, M., Lowrie, D. B., and Mitchison, D. A. 1986. “Effects of Recombinant Interferon-Gamma and Chemotherapy with Isoniazid and Rifampicin on Infections of Mouse Peritoneal Macrophages with *Listeria monocytogenes* and *Mycobacterium microti in vitro*.” *British Journal of Experimental Pathology* 67 (5) (October): 707-17.

Khweek, A. A., Caution, K., Akhter, A., Abdulrahman, B. A., Tazi, M., Hassan, H., Majumdar, N., *et al.* 2013. “A Bacterial Protein Promotes the Recognition of the *Legionella pneumophila* Vacuole by Autophagy.” *European Journal of Immunology* 43 (5) (May): 1333-44.

Kirkin, V., Lamark, T., Sou, Y. S., Bjørkøy, G., Nunn, J. L., Bruun, J. A., Shvets, E., *et al.* 2009. “A Role for NBR1 in Autophagosomal Degradation of Ubiquitinated Substrates.” *Molecular Cell* 33 (4) (February 27): 505-16.

Klionsky, D. J. 2008. "Autophagy Revisited: a Conversation with Christian de Duve." *Autophagy* 4 (6) (August): 740-3.

Klionsky, D. J., Abeliovich, H., Agostinis, P., Agrawal, D. K., Aliev, G., Askew, D. S., Baba, M., *et al.* 2008. “Guidelines for the Use and Interpretation of Assays for Monitoring Autophagy in Higher Eukaryotes.” *Autophagy* 4 (2) (February): 151-175.

Kocks, C., Gouin, E., Tabouret, M., Berche, P., Ohayon, H., and Cossart, P. 1992. “*L. monocytogenes*-Induced Actin Assembly Requires the *actA* Gene Product, a Surface Protein.” *Cell* 68 (3) (February 7): 521-31.

Korac, J., Schaeffer, V., Kovacevic, I., Clement, A. M., Jungblut, B., Behl, C., Terzic, J., and Dikic, I. 2013. “Ubiquitin-Independent Function of Optineurin in Autophagic Clearance of Protein Aggregates.” *Journal of Cell Science* 126 (Pt 2) (January 15): 580-92.

Köster, S., van Pee, K., Hudel, M., Leustik, M., Rhinow, D., Kühlbrandt, W., Chakraborty, T., and Yildiz, Ö. 2014. "Crystal Structure of Listeriolysin

O Reveals Molecular Details of Oligomerization and Pore Formation." *Nature Communications* 5:3690 (April 22).

Laemmli, U.K. 1970. “Cleavage of Structural Proteins during the Assembly of the Head of Bacteriophage T4.” *Nature* 227 (5259) (August 15): 680-685.

Lamark, T., Kirkin, V., Dikic, I., and Johansen, T. 2009. “NBR1 and p62 as Cargo Receptors for Selective Autophagy of Ubiquitinated Targets.” *Cell Cycle (Georgetown, Tex.)* 8 (13) (July 1): 1986-90.

Levraud, J. P., Disson, O., Kissa, K., Bonne, I., Cossart, P., Herbomel, P., and Lecuit, M. 2009. “Real-Time Observation of *Listeria monocytogenes*-Phagocyte Interactions in Living Zebrafish Larvae.” *Infection and Immunity* 77 (9) (September): 3651-60.

Li, Y., Kang, J., and Horwitz, M. S. 1998. “Interaction of an Adenovirus E3 14.7-Kilodalton Protein with a Novel Tumor Necrosis Factor Alpha-Inducible Cellular Protein Containing Leucine Zipper Domains.” *Molecular and Cellular Biology* 18 (3) (March): 1601-10.

Mansfield, B. E., Dionne, M. S., Schneider, D. S., and Freitag, N. E. 2003. “Exploration of Host-Pathogen Interactions Using *Listeria monocytogenes* and *Drosophila melanogaster*.” *Cellular Microbiology* 5 (12) (December): 901-11.

Marco, A. J., Altimira, J., Prats, N., López, S., Dominguez, L., Domingo, M., and Briones, V. 1997. “Penetration of *Listeria monocytogenes* in Mice Infected by the Oral Route.” *Microbial Pathogenesis* 23 (5) (November): 255-63.

Marquis, H., Doshi, V., and Portnoy, D. A. 1995. "The broad-range Phospholipase C and a Metalloprotease Mediate Listeriolysin O-Independent Escape of *Listeria monocytogenes* from a Primary Vacuole in Human Epithelial Cells." *Infection and Immunity* 63 (11) (November): 4531-4.

Matsuda, F., Fujii, J., and Yoshida, S. 2009. “Autophagy Induced by 2-Deoxy-D-Glucose Suppresses Intracellular Multiplication of *Legionella pneumophila* in A/J Mouse Macrophages.” *Autophagy* 5 (4) (May): 484-493.

Mohri, H. 1968. "Amino-acid Composition of "Tubulin" Constituting Microtubules of Sperm Flagella." *Nature* 217 (5133) (March 16): 1053-4.

Mostowy, S., Boucontet, L., Mazon Moya, M. J., Sirianni, A., Boudinot, P., Hollinshead, M., Cossart, P., Herbomel, P., Levraud, J. P., and Colucci-Guyon, E. 2013. “The Zebrafish as a New Model for the *in vivo* Study of *Shigella flexneri* Interaction with Phagocytes and Bacterial Autophagy.” *PLoS Pathogens* 9 (9): e1003588.

X. References

Mostowy, S., Sancho-Shimizu, V., Hamon, M. A., Simeone, R., Brosch, R., Johansen, T., and Cossart, P. 2011. “p62 and NDP52 Proteins Target Intracytosolic *Shigella* and *Listeria* to Different Autophagy Pathways.” *The Journal of Biological Chemistry* 286 (30) (July 29): 26987-95.

Mukherjee, K., Altincicek, B., Hain, T., Domann, E., Vilcinskas, A., and Chakraborty, T. 2010. “*Galleria mellonella* as a Model System for Studying *Listeria* Pathogenesis.” *Applied and Environmental Microbiology* 76 (1) (January): 310-7.

Murray, E. G. D., Webb, R. E., and Swann, M. B. R. 1926. "A Disease of Rabbits Characterized by a Large Mononuclear Leucocytosis, Caused by a Hitherto Undescribed Bacillus Bacterium *monocytogenes* (n. sp.)." *The Journal of Pathology and Bacteriology* 29: 407-439.

Newman, A. C., Scholefield, C. L., Kemp, A. J., Newman, M., McIver, E. G., Kamal, A., and Wilkinson, S. 2012. “TBK1 Kinase Addiction in Lung Cancer Cells Is Mediated via Autophagy of Tax1bp1/Ndp52 and Non-Canonical NF-κB Signalling.” *PloS One* 7 (11): e50672.

Osawa, T., Mizuno, Y., Fujita, Y., Takatama, M., Nakazato, Y., and Okamoto, K. 2011. “Optineurin in Neurodegenerative Diseases.” *Neuropathology : Official Journal of the Japanese Society of Neuropathology* 31 (6) (December): 569-74.

Pareja, M. E., and Colombo, M. I. 2013. “Autophagic Clearance of Bacterial Pathogens: Molecular Recognition of Intracellular Microorganisms.” *Frontiers in Cellular and Infection Microbiology* 3 (September 30) 3: 54.

Pfeuffer, T., Goebel, W., Laubinger, J., Bachmann, M., and Kuhn, M. 2000. "LaXp180, a Mammalian ActA-Binding Protein, Identified with the Yeast two-hybrid System, co-localizes with Intracellular *Listeria monocytogenes*." *Cellular Microbiology* 2 (2) (April): 101-14.

Pilli, M., Arko-Mensah, J., Ponpuak, M., Roberts, E., Master, S., Mandell, M. A., Dupont, N., *et al.* 2012. “TBK-1 Promotes Autophagy-Mediated Antimicrobial Defense by Controlling Autophagosome Maturation.” *Immunity* 37 (2) (August 24): 223-34.

Pillich, H., Loose, M., Zimmer, K. P., and Chakraborty, T. 2012. “Activation of the Unfolded Protein Response by *Listeria monocytogenes*.” *Cellular Microbiology* 14 (6) (June): 949-64.

Py, B. F., Lipinski, M. M., and Yuan, J. 2007. “Autophagy Limits *Listeria monocytogenes* Intracellular Growth in the Early Phase of Primary Infection.” *Autophagy* 3(2) (March-April): 117-125.

Rezaie, T., Child, A., Hitchings, R., Brice, G., Miller, L., Coca-Prados, M., Héon, E., *et al.* 2002. “Adult-Onset Primary Open-Angle Glaucoma Caused

by Mutations in Optineurin." *Science (New York, N.Y.)* 295 (5557) (February 8): 1077-9.

Ramaswamy, V., Crescence, V. M., Rejitha, J. S., Lekshmi, M. U., Dharsana, K. S., Prasad, S. P., and Vijila, H. M. 2007. "*Listeria*-Review of Epidemiology and Pathogenesis." *Journal of Microbiology, Immunology and Infection* 40 (1) (February): 4-13.

Rogov, V., Dötsch, V., Johansen, T., and Kirkin, V. 2014. "Interactions between Autophagy Receptors and Ubiquitin-like Proteins Form the Molecular Basis for Selective Autophagy." *Molecular Cell* 53 (2) (January 23): 167-78.

Sahlender, D. A., Roberts, R. C., Arden, S. D., Spudich, G., Taylor, M. J., Luzio, J. P., Kendrick-Jones, J., and Buss, F. 2005. "Optineurin Links Myosin VI to the Golgi Complex and Is Involved in Golgi Organization and Exocytosis." *The Journal of Cell Biology* 169 (2) (April 25): 285-95.

Sallen, B., Rajoharison, A., Desvarenne, S., Quinn, F., and Mabilat, C. 1996. "Comparative Analysis of 16S and 23S rRNA Sequences of *Listeria* species." *International Journal of Systematic Bacteriology* 46 (3) (July): 669-74.

Seto, S., Tsujimura, K., and Koide, Y. 2012. "Coronin-1a Inhibits Autophagosome Formation around *Mycobacterium tuberculosis*-Containing Phagosomes and Assists Mycobacterial Survival in Macrophages." *Cellular Microbiology* 14 (5) (May): 710-27.

Smith, G. A., Marquis, H., Jones, S., Johnston, N. C., Portnoy, D. A., and Goldfine, H. 1995. "The Two Distinct Phospholipases C of *Listeria monocytogenes* Have Overlapping Roles in Escape From a Vacuole and Cell-to-Cell Spread." *Infection and Immunity* 63 (11) (November):4231-7.

Tanida, I. 2011. "Autophagy Basics." *Microbiology and Immunology* 55 (1) (January): 1-11.

Tattoli, I., Sorbara, M. T., Yang, C., Tooze, S. A., Philpott, D. J., and Girardin, S. E. 2013. "*Listeria* Phospholipases Subvert Host Autophagic Defenses by Stalling Pre-autophagosomal Structures." *The EMBO Journal* 32 (23) (November 27): 3066-78.

Thurston, T. L., Ryzhakov, G., Bloor, S., von Muhlinen, N., and Randow, F. 2009. "The TBK1 Adaptor and Autophagy Receptor NDP52 Restricts the Proliferation of Ubiquitin-Coated Bacteria." *Nature Immunology* 10 (11) (November): 1215-21.

Thurston, T. L., Wandel, M. P., von Muhlinen, N., Foeglein, A., and Randow, F. 2012. "Galectin 8 Targets Damaged Vesicles for Autophagy to

Defend Cells against Bacterial Invasion." *Nature* 482 (7385) (January 15): 414-8.

Towbin, H., Staehelin, T., and Gordon, J. 1979. "Electrophoretic Transfer of Proteins from Polyacrylamide Gels to Nitrocellulose Sheets: Procedure and Some Applications." *Proceedings of the National Academy of Sciences of the United States of America* 76 (9) (September): 4350-4.

Van Limbergen, J., Stevens, C., Nimmo, E. R., Wilson, D. C., and Satsangi, J. 2009. "Autophagy: From Basic Science to Clinical Application." *Mucosal Immunology* 2 (4) (July): 315-30.

van Wijk, S. J., Fiskin, E., Putyrski, M., Pampaloni, F., Hou, J., Wild, P., Kensche, T., Grecco, H. E., Bastiaens, P., and Dikic, I. 2012. "Fluorescence-Based Sensors to Monitor Localization and Functions of Linear and K63-Linked Ubiquitin Chains in Cells." *Molecular Cell* 47 (5) (September 14): 797-809.

Vázquez-Boland, J. A., Kocks, C., Dramsi, S., Ohayon, H., Geoffroy, C., Mengaud, J., and Cossart, P. 1992. "Nucleotide Sequence of the Lecithinase Operon of *Listeria monocytogenes* and Possible Role of Lecithinase in Cell-to-Cell Spread." *Infection and Immunity* 60 (1) (January): 219-30.

Vázquez-Boland, J. A., Kuhn, M., Berche, P., Chakraborty, T., Domínguez-Bernal, G., Goebel, W., González-Zorn, B., Wehland, J., and Kreft, J. 2001. "*Listeria* Pathogenesis and Molecular Virulence Determinants." *Clinical Microbiology Reviews* 14 (3) (July): 584-640.

Verstrepen, L., Verhelst, K., Carpentier, I., and Beyaert, R. 2011. "TAX1BP1, a Ubiquitin-Binding Adaptor Protein in Innate Immunity and Beyond." *Trends in Biochemical Sciences* 36 (7) (July): 347-54.

von Muhlinen, N., Akutsu, M., Ravenhill, B. J., Foeglein, Á., Bloor, S., Rutherford, T. J., Freund, S. M., Komander, D., and Randow, F. 2012. "LC3C, Bound Selectively by a Noncanonical LIR Motif in NDP52, Is Required for Antibacterial Autophagy." *Molecular Cell* 48 (3) (November 9): 329-42.

Walinda, E., Morimoto, D., Sugase, K., Konuma, T., Tochio, H., and Shirakawa, M. 2014. "Solution Structure of the Ubiquitin-Associated (UBA) Domain of Human Autophagy Receptor NBR1 and Its Interaction with Ubiquitin and Polyubiquitin." *The Journal of Biological Chemistry* 289 (20) (May 16): 13890-902.

Wild, P., Farhan, H., McEwan, D. G., Wagner, S., Rogov, V. V., Brady, N. R., Richter, B., *et al.* 2011. "Phosphorylation of the Autophagy Receptor Optineurin Restricts *Salmonella* Growth." *Science (New York, N.Y.)* 333 (6039) (July 8): 228-33.

X. References

Yano, T., Mita, S., Ohmori, H., Oshima, Y., Fujimoto, Y., Ueda, R., Takada, H., *et al.* 2008. "Autophagic Control of *Listeria* Through Intracellular Innate Immune Recognition in *Drosophila*." *Nature Immunology* 9 (8) (August): 908-16.

Ying, H., and Yue, B. Y. 2012. "Cellular and Molecular Biology of Optineurin." *International Review of Cell and Molecular Biology* 294: 223-58.

Yorimitsu, T., Nair, U., Yang, Z., and Klionsky, D. J. 2006. "Endoplasmic Reticulum Stress Triggers Autophagy." *The Journal of Biological Chemistry* 281 (40) (October 6): 30299-304.

Yoshida, S., Handa, Y., Suzuki, T., Ogawa, M., Suzuki, M., Tamai, A., Abe, A., *et al.* 2006. "Microtubule-Severing Activity of *Shigella* is Pivotal for Intercellular Spreading." *Science (New York, N. Y.)* 314 (5801) (November 10): 985-9.

Yoshikawa, Y., Ogawa, M., Hain, T., Yoshida, M., Fukumatsu, M., Kim, M., Mimuro, H., *et al.* 2009. "*Listeria monocytogenes* ActA-Mediated Escape from Autophagic Recognition." *Nature Cell Biology* 11 (10) (October): 1233-40.

Yuan, K., Huang, C., Fox, J., Laturnus, D., Carlson, E., Zhang, B., Yin, Q., Gao, H., and Wu, M. 2012. "Autophagy Plays an Essential Role in the Clearance of *Pseudomonas aeruginosa* by Alveolar Macrophages." *Journal of Cell Science* 125 (Pt 2) (January 15): 507-15.

Zatloukal, K., Stumptner, C., Fuchsbichler, A., Heid, H., Schnoelzer, M., Kenner, L., Kleinert, R., Prinz, M., Aguzzi, A., and Denk, H. 2002. "p62 Is a Common Component of Cytoplasmic Inclusions in Protein Aggregation Diseases." *The American Journal of Pathology* 160 (1) (January): 255-63.

Zheng, Y. T., Shahnazari, S., Brech, A., Lamark, T., Johansen, T., and Brumell, J. H. 2009. "The Adaptor Protein p62/SQSTM1 Targets Invading Bacteria to the Autophagy Pathway." *Journal of Immunology (Baltimore, Md. : 1950)* 183 (9) (November 1): 5909-16.

XI. Declaration

Declaration

I declare that I have completed this dissertation single-handedly without the unauthorized help of a second party and only with the assistance acknowledged therein. I have appropriately acknowledged and referenced all text passages that are derived literally from or are based on the content of published or unpublished work of others, and all information that relates to verbal communications. I have abided by the principles of good scientific conduct laid down in the charter of the Justus Liebig University of Giessen in carrying out the investigations described in the dissertation.

Place, date	Sign

XII. Acknowledgements

Acknowledgements

First and foremost, I would like to express my sincere gratitude to my guide Prof. Dr. Trinad Chakraborty, Director, Institute of Medical Microbiology, for giving me the opportunity to work on this dissertation. This thesis would not have been possible without his invaluable expertise, guidance and support.

My special thanks and gratitude go to Prof. Dr. Michael Martin, my second supervisor, for his keen interest, valuable suggestions, constructive criticisms, tremendous encouragement, and insightful comments on the work reported in this dissertation.

Words cannot express my thanks to Dr. Helena Pillich for her excellent mentorship during the entire course of my Ph. D. I am grateful to her for performing the siRNA transfections, as well as for teaching me various techniques. Her constant encouragement and constructive criticism motivated me to perform better every time.

I am grateful to Dr. Krishnaraj Rajalingam, Institute of Biochemistry II, Johann Wolfgang Goethe University, Frankfurt, for giving me the opportunity to use the confocal microscope, and Mr. Arun Murali for his help with the confocal analysis. I also thank Prof. Dr. Ivan Dikic and Dr. Philipp Wild for providing the phospho-OPTN antibody and the OPTN plasmids.

I acknowledge my appreciation to Dr. Katrin Gentil for critically reading this thesis and for her valuable suggestions.

I especially thank Ms. Sylvia Krämer for providing an endless supply of BHI and LB agar plates, and Mrs. Nelli Schklarenko for helping me with bacterial transformations.

This academic and research journey would not have been possible without the support of my colleagues Dr. Martin Leustik, Ms. Maria Loose, Ms. Lea Herges and Ms. Judith Schmiedel, who provided me a friendly working atmosphere, and indulged in helpful and stimulating discussions.

XII. Acknowledgements

Lastly, I am highly indebted to my parents for their encouragement at each and every stage of my personal and academic life. Their constant belief in me inspired me to bring out my best.

(MADHU SINGH)

Der Lebenslauf wurde aus der elektronischen Version der Arbeit entfernt.

The curriculum vitae was removed from the electronic version of the paper.